

The Institute of Paper Chemistry

Appleton, Wisconsin

Doctor's Dissertation

The Viscosity of Fiber Suspensions

William Roy Blakeney

June, 1965

THE VISCOSITY OF FIBER SUSPENSIONS

A thesis submitted by

William Roy Blakeney
B.S. (Ch.E.) 1960, Clemson College
M.S. 1962, Lawrence College

in partial fulfillment of the requirements
of The Institute of Paper Chemistry
for the degree of Doctor of Philosophy
from Lawrence University,
Appleton, Wisconsin

June, 1965

TABLE OF CONTENTS

	Page
SUMMARY	1
INTRODUCTION	3
THEORETICAL	7
PAST EXPERIMENTAL WORK	12
Work of Eirich, <u>et al.</u>	12
Work of Nawab and Mason	13
Work of Myers	18
Comparison of Nawab's and Myers' Experimental Data	21
The Problem	21
ANALYSIS OF THE PROBLEM	23
CHOICE OF VISCOMETER AND SUSPENSION	28
Choice of Viscometer	28
General Description of Myers' Viscometer	28
Description of Cylinders	28
Description of Electrical System	30
Cleaning and Control of Air to Air Bearing	30
Choice of Suspension	33
EXPERIMENTAL PROCEDURES	38
Fiber Preparation and Characterization	38
Cutting Procedure	38
Straight Fibers	38
Curved Fibers	38
Measurement of Fiber Lengths	39
Measurement of Fiber Diameters	39
Operation of the Viscometer	39
Calibration of the Viscometer	41

Performance of the Viscometer	42
Determination of Inner Cylinder End Effects	45
Procedure for Making a Viscosity-Concentration Study	47
General Procedure	47
Detailed Procedures	47
Preparation of Fibers	47
Preparation of Suspension	50
Determination of Apparent Viscosity	50
Procedure for Changing Concentration	50
Determination of Volume Concentration	50
Determination of Changes in the Viscosity of the Suspending Medium	51
Calculation of Relative Viscosities	51
Fiber Orientation Determinations	52
Apparatus	52
Photographic Procedure	54
Analysis of the Photographs	56
RESULTS AND DISCUSSION	57
Discussion of the Torque-Angular Velocity Relationship	57
The Effect of Concentration on the Orientations of the Particles	59
The Relative Viscosity-Concentration Relationship	64
Discussion of the Relative Viscosity-Concentration Relationship at Low Concentrations	66
Discussion of the Relative Viscosity-Concentration Relationship at High Concentrations	68
The Effect of the Wall on the Relative Viscosity	71
The Effect of Fiber Curvature on the Relative Viscosity of a Fiber Suspension	78

Discussion of Past Experimental Work in Relation to This Work	87
The Behavior of Flocculated Suspensions	90
General Behavior	91
The Effect of Concentration on the Relative Viscosity	93
CONCLUSIONS	99
SUGGESTIONS FOR FUTURE WORK	101
NOMENCLATURE	102
ACKNOWLEDGMENTS	105
LITERATURE CITED	106
APPENDIX I. BURGERS' DERIVATION OF AN EQUATION FOR THE VISCOSITY OF A SUSPENSION OF RIGID RODS	109
APPENDIX II. EXPERIMENTAL DATA	120
APPENDIX III. DETERMINATION OF THE ORIENTATIONS OF THE FIBERS IN A FLOWING SUSPENSION FROM PHOTOGRAPHS	125
APPENDIX IV. THE VISCOSITY OF SUCROSE AND GLYCEROL SOLUTIONS	127
APPENDIX V. GENERAL COMMENTS CONCERNING THE USE OF MYERS' VISCOMETER	128

SUMMARY

Past experimental studies of the viscosity of suspensions of rigid rods have yielded results which are inconsistent within themselves and in disagreement with theoretically predicted behavior. Analysis of the past experimental work in the light of theory indicated that several important variables affecting the viscosity of suspensions of rigid rods were not completely understood. These variables are concentration, the presence of the viscometer walls, and curvature of the rods.

This study was undertaken for three reasons: (1) to determine the magnitude of the effect of the above variables on the viscosity, (2) to compare theoretical results with experimental results obtained under conditions more closely approximating the conditions assumed in the theory, and (3) to determine the reasons for the inconsistencies in the past experimental data.

The choice of the conditions under which the experiments were made was governed primarily by the conditions assumed in the theory. It was found that straight, nylon fibers, of length-to-diameter ratio ≈ 20 , suspended in a tetrachloroethane-paraffin oil solution, met theoretical conditions as closely as possible. Viscosity measurements were made in the concentric cylinder viscometer designed by Myers (16, 19). Using this system, the effect of concentration on the apparent viscosity could be determined.

The magnitude of the effect of fiber curvature was evaluated by making viscosity measurements on fibers of known curvature keeping all other variables constant.

Wall effects were studied by varying the annulus width of the viscometer.

It was found that at volume concentrations below 0.0042, relative viscosities obtained experimentally were within 10% of those predicted by theory provided measured values of the orientations of the particles were used in the calculations.

As the volume concentration increased above 0.0042, there was a rapid increase in viscosity followed by a slight decrease and a second increase. The rise and dip in the viscosity were found to be due partially to changes in the orientations of the rods and partially to fiber-fiber interactions.

The investigation of the effect of the wall on the viscosity of straight, rigid rods indicated that the effect was negligible even at fiber diameter and fiber length to annulus width ratios of 0.0176 and 0.358, respectively.

Viscosity measurements on suspensions of curved fibers showed that a very slight curvature has a pronounced effect on the viscosity. A relationship between fiber curvature and the ratio of the experimental to the theoretical intrinsic viscosity was obtained. It was found that above a certain degree of curvature, the above ratio is dependent only on the degree of curvature and not on the actual length-to-diameter ratio of the fibers.

An analysis of the results of past studies in view of the findings of this study indicated that the most probable reasons for the disagreement within the past studies and between the past studies and theory were: (1) the concentration ranges covered were too high and, (2) in most cases, the fibers used were curved.

Some viscosity data were obtained using flocculated suspensions. It was found that the suspensions were non-Newtonian. The viscosity obtained at any given concentration was higher than that obtained using well-dispersed suspensions. The difference depended on the degree of flocculation.

INTRODUCTION

The hydrodynamic treatment of the movement of macroscopic particles with respect to a viscous fluid was begun over a century ago by Stokes (1). Stokes solved his general hydrodynamic equation describing the motion of a fluid for the slow translation of a sphere in an infinite fluid of constant density and viscosity. The general hydrodynamic equation derived by Stokes was first developed by Navier (2) and has since become known as the Navier-Stokes equation.

Oseen (3), partially incorporating fluid inertial effects, solved the Navier-Stokes equation for the translation of a sphere and obtained an improvement over Stokes' solution. Oseen then solved for the limiting case of the effect of an arbitrary point force on the velocity components of a fluid. The resulting equations have been used as the starting point for several later works in this field. Later, Overbeck (4) analyzed the more general case of an ellipsoid in creeping motion. Using Oseen's method, Lamb (5), and later Burgers (6), solved the special cases of the translation of infinitely long, and long but finite cylinders, respectively. No further theoretical development in this area was accomplished until the recent works of Tchen (7) and Brenner (8). Tchen, also using Oseen's method, predicted the translation of curved ellipsoids. Brenner, by accounting for back flow due to a particle in translation, proposed general solutions for boundary effects. Many of these theoretical predictions have been experimentally verified; however, there remain important discrepancies.

The more complex problem of particle rotations in a linear velocity gradient has also received much attention in theoretical hydrodynamics. This phenomenon has been treated in studies of the effect of suspended macroscopic particles on the apparent viscosity of a fluid.

The first theoretical contribution in this area was Einstein's (9) equation for the viscosity of a suspension of rigid spheres. Jeffery (10) then extended Einstein's work to the more general case of ellipsoids. Burgers, again using Oseen's solution for the effect of a point force, obtained an equation for the viscosity of suspensions of rigid rods. In his solution, Burgers did not take into account flow around the ends of the rods or the effect of the thickness of the rods on rotation. Therefore, his solution was approximate as compared to the rigorous solutions of Einstein and Jeffery.

All of the above theoretical studies on the viscosity of suspensions were based on the assumptions of no influence of one particle on another, no inertial effects, and no wall effects. The apparent contradiction between Burgers' use of Oseen's solution and the assumption of no inertial effects is explained in the text.

Experimental studies on the viscosity of suspensions of rigid, macroscopic spheres using concentric cylinder viscometers have verified Einstein's theory (11, 12). Also, Jeffery's equations describing the rotation of ellipsoids in a linear velocity gradient have been shown to be correct (13). Since Jeffery's viscosity equation reduces to that of Einstein, it has also been assumed to be correct.

Experimental viscosity measurements on suspensions of cylindrical fibers began with the work of Eirich, et al. (14) before Burgers' theory was published. Later, Nawab and Mason (15) and more recently Myers (16) made similar studies. None of the results obtained in the experimental studies agreed with Burgers' theory.

Nawab and Mason suggested that curvature of the fibers used in their study could have accounted for some of the difference between theoretical and experimental results.

Myers suggested that some of his work may have been influenced by wall effects.

No measurements of the magnitude of the effect of the wall or fiber curvature on the viscosity were made, however, and the concensus of opinion among these workers was that the primary reason for the lack of agreement between theoretical and experimental results was due to failure of the theory.

No theoretical studies have been made on the effect of fiber curvature on viscosity. However, Tchen (7) has shown theoretically that a large fiber curvature has a significant effect on the translation of a fiber in a fluid. Also, Forgacs and Mason (17) showed experimentally that a slight curvature has a large effect on the rotational behavior of fibers in a linear velocity gradient. Therefore, one would also expect some effect on the viscosity of a fiber suspension due to fiber curvature.

Wall effects due to a discontinuity of the suspension at the wall have been predicted by Vand (18) for suspensions of spheres. Also, Brenner's work indicates that there may be a wall effect in measurements of the viscosity of suspensions. However, the presence of wall effects in concentric cylinder viscometers has not been conclusively demonstrated by experimentation.

Although not mentioned by Nawab and Mason, or Myers as a possible reason for lack of agreement between theoretical and experimental results, the concentration of the fibers used in all of the past studies was relatively large leading to the possibility of significant fiber-fiber interactions.

Since the magnitude of the effect of concentration, fiber curvature, and wall effects, on the viscosity of fiber suspensions was not fully understood, it was felt that premature conclusions had been reached as to the accuracy of Burgers' theory. Therefore, the object of this study was (1) to determine the magnitude of the effect of these variables on the viscosity of suspensions of rigid rods so that a better evaluation of Burgers' theory could be made, and (2) to obtain a better understanding of the effect of these variables on the apparent viscosity.

THEORETICAL

In this section a very brief outline of Burgers' (6) derivation of an equation for the viscosity of suspensions of rigid rods is given. Only the major steps in the derivation plus those points which will be considered in some detail later in the dissertation are presented. A more complete derivation is given in Appendix I.

Burgers was concerned with the effect of rigid rods suspended in a liquid under conditions of flow described by the equations: $\frac{v_x}{x} = \frac{G}{O} \frac{y}{y}$, $\frac{v_y}{y} = 0$, $\frac{v_z}{z} = 0$ on the viscosity of the suspension.

The following assumptions are made in the derivation:

1. There are no inertial effects.
2. The particles are straight, rigid cylinders large enough so that there will be no effect due to Brownian motion.
3. There is no slip of the liquid at the particle surface. Slip, in this case, "implies an infinitely greater resistance to the sliding of one portion of the liquid past another than to the sliding of the fluid over a solid" (20).
4. There is no effect on any one particle due to the presence of any other.
5. There is no wall effect.

Burgers found that the forces which develop in a fluid due to the presence of the rods could be expressed in the form of a doublet* of strength $\underline{M} = 2\underline{F}e$. To determine the magnitude of \underline{M} in terms of the dimensions and orientations of the particles, Burgers used Oseen's (21) solution of the Navier-Stokes equation

*Two forces of opposite and equal magnitude, \underline{F} , acting at points a distance $2e$ from one another along a straight line constitutes a doublet of strength $\underline{M} = 2\underline{F}e$.

for the effect of an arbitrary force on the velocity of a fluid. Although Oseen's solution partially takes into account fluid inertial effects, Burgers made simplifying assumptions which eliminated these effects from consideration. In determining the magnitude of \underline{M} , effects due to the ends of the rods were neglected.

Knowing the magnitude of the doublets formed, Burgers determined the effect of these doublets on the shear rate of the liquid and therefore on the viscosity of the suspension. In this step, Burgers neglected effects due to the thickness of the rods. The results of these calculations, given in terms of the relative viscosity of the suspension, are as follows:

$$\mu_r = 1 + \alpha_o c \quad (1)$$

$$\alpha_o = \left\{ (L/d)^2 / [6(\ln 2L/d - 1.80)] \right\} \sin^4 \theta \cdot \sin^2 2\phi \quad (2)$$

where

\underline{c} = volume concentration = $\underline{n} \pi (\underline{d}^2/4) \underline{L}$

\underline{L} = length of the rod

\underline{d} = diameter of the rod

ϕ and θ = spherical co-ordinates (defined by Fig. 1) describing the orientation of the rods

\underline{n} = number of rods per unit volume.

Burgers' analysis of the motion of the particles led to the result that after an infinite period of time, all the particles would become aligned in the direction of flow and remain there. This was known from actual observations not to be true. The reason that Burgers' equations failed to predict the continuous rotation of the particles was that, throughout the derivation, effects due to the thickness of the particles were neglected. This result prevented an averaging of the factor $\sin^4 \theta \sin^2 2\phi$. Thus, Burgers turned to Jeffery's (10) equations for the

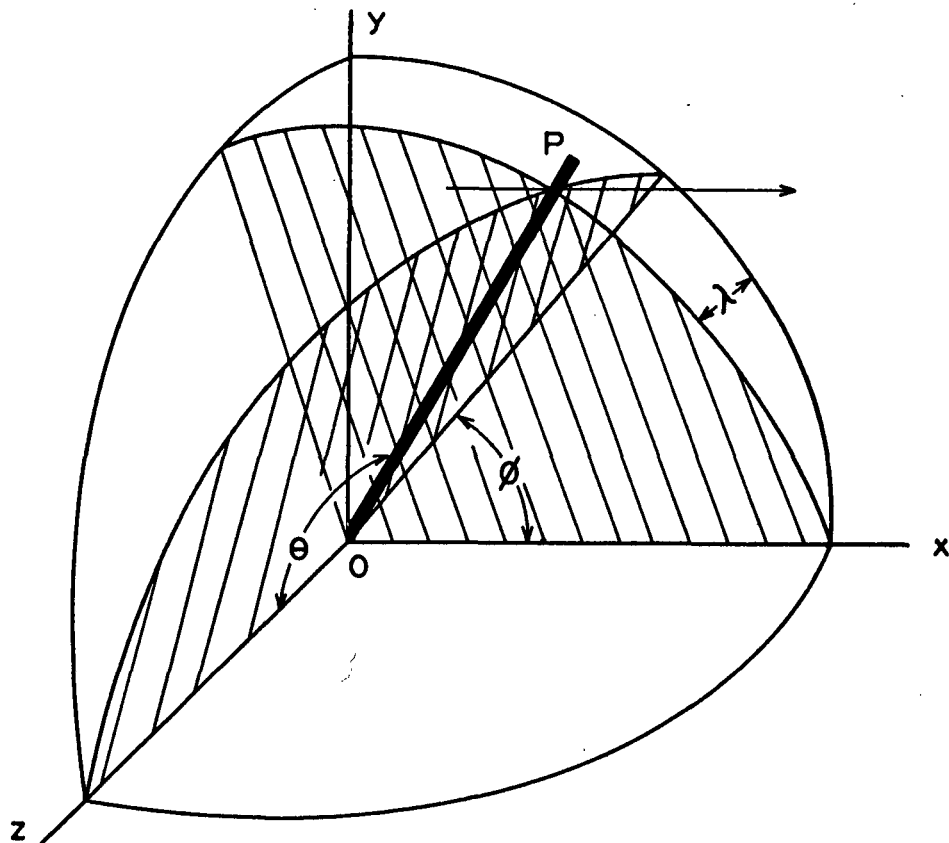


Figure 1. Rigid Rod in a Velocity Gradient

motion of ellipsoids in a linear velocity gradient to obtain an expression for $\overline{\sin^4 \theta \sin^2 2\phi}$.

Note that, in doing this, Burgers is assuming that ellipsoids and cylinders will behave the same in rotation. Assuming Jeffery's equation for the motion of ellipsoids to be correct, Mason, et al. (22-24) showed that cylinders have a period of rotation which is less than that of an ellipsoid with the same length-to-diameter ratio. This will be discussed in more detail later.

In Jeffery's derivation, the thickness of the particles is taken into account. Jeffery's equations for the angular velocities of ellipsoids are as follows:

$$d\phi/dt = G_0(a^2 \sin^2 \phi + b^2 \cos^2 \phi)/(a^2 + b^2) \quad (3)$$

where $\underline{a} = L/2$ and $\underline{b} = d/2$, and

$$d\theta/dt = G_0(a^2 - b^2)\sin\theta\cos\theta\sin\phi\cos\phi/(a^2 + b^2) \quad (4)$$

If $\underline{t} = 0$ when $\phi = 0$, integration of Equation (3) gives:

$$\tan \phi = b/a \tan G_0 \underline{a} \underline{b} \underline{t} / (a^2 + b^2) \quad (5)$$

Dividing Equation (4) by Equation (3) and integrating gives:

$$\tan \theta = K \underline{a} / \sqrt{a^2 \sin^2 \phi + b^2 \cos^2 \phi} \quad (6)$$

where \underline{K} is a constant of integration, referred to as the "orbit constant." When \underline{K} equals infinity, the particle will rotate in the \underline{xy} -plane. When \underline{K} equals zero, the particle will be oriented vertically and spin about its axis.

When the particle thickness is taken into account, the theory predicts that the particles will never stop rotating in a velocity gradient.

Using Equations (5) and (6), Jeffery solved for the mean value of the orientation factor and found that:

$$\overline{\sin^4 \theta \sin^2 \phi} = \frac{2a^2 b^2}{(a^2 - b^2)^2} \left[\frac{K^2(a^2 + b^2) + 2b^2}{\sqrt{(K^2 a^2 + b^2)(K^2 b^2 + b^2)}} - 2 \right] \quad (7).$$

If only particles with $\underline{a}/\underline{b} \gg 1$ are considered, the following approximation can be used:

$$\overline{\sin^4 \theta \sin^2 \phi} \approx (2b/a)(K/\sqrt{K^2 + 1}) \quad (8).$$

Now if θ_0 and ϕ_0 are the values of the angles θ and ϕ for the position from which the particles started, then from Equation (6),

$$K = \tan \theta_0 \sqrt{\sin^2 \phi_0 + (b^2/a^2) \cos^2 \phi_0} \quad (9)$$

and neglecting $b^2/a^2 \cos^2 \phi_0$, then:

$$K \cong \left| \tan \theta_0 \sin \phi_0 \right| = \left| \cot \lambda_0 \right| \quad (10)$$

where λ is defined by Fig. 1.

Thus, by combining Equations (8) and (10),

$$\overline{\sin^4 \theta \sin^2 2\phi} = (2b/a) \left| \cos \lambda_0 \right| = (2d/L) \left| \cos \lambda_0 \right| \quad (11).$$

This is still the mean value of the orientation factor for one definite orbit. In order to find the average for all orbits, Burgers, following Eisen-schitz (25), assumed that the values of λ_0 would be evenly distributed over the surface of a sphere. For this case, $\left| \overline{\cos \lambda_0} \right|$ becomes $2/\pi$ and

$$\overline{\sin^4 \theta \sin^2 2\phi} = 4d/(L\pi) \quad (12).$$

For the limiting case of $K = \text{infinity}$ in Equation (8), i.e., orientation in the xy-plane,

$$\overline{\sin^4 \theta \sin^2 2\phi} = 2d/L \quad (13).$$

Now substituting the values found for $\overline{\sin^4 \theta \sin^2 2\phi}$ into Equation (2), the following results are obtained:

Random orientation,

$$\alpha_{OR} = (2L/d)/[3\pi(\ln 2L/d - 1.80)] \quad (14).$$

Orientation in the xy-plane,

$$\alpha_{oxy} = (L/d)/[3(\ln 2L/d - 1.80)] \quad (15).$$

PAST EXPERIMENTAL WORK

WORK OF EIRICH, ET AL.

The first work on the viscosity of suspensions of rods was done by Eirich, et al. (14). The rods used were prepared from filaments of silk and rayon.

Eirich used a concentric cylinder viscometer having a rotating annular cup. A torque sensing cylinder was placed in this annulus thus forming a double annulus viscometer. The dimensions of the viscometer were as follows:

Rotating cylinders

Diameter of outer cylinder	41.5 mm.
Diameter of inner cylinder	29.4 mm.

Torque sensing cylinder

Diameter	35.0 mm.
Wall thickness	1.4 mm.
Height	30.5 mm.

Eirich's viscosity measurements were made over an angular velocity range from 100 to 250 rad./sec.

The viscosity studies on the silk fibers were carried out in a medium of tetrachloroethane and olive oil which had a viscosity of approximately 6 centipoises. For studies with the rayon fibers, a mixture of bromoform and olive oil with a viscosity of approximately 15 centipoises was used.

It will be shown in the Analysis of the Problem that the angular velocities used by Eirich were much too high for stable flow in the viscometer annulus. Therefore, the actual results which Eirich obtained for intrinsic viscosities of his suspensions will not be given.

WORK OF NAWAB AND MASON

The first significant contribution to the understanding of the viscosity behavior of suspensions of rods was made by Nawab and Mason (15).

This work was done using rayon fibers suspended in castor oil (viscosity \approx 25 poises). The physical properties of the fibers are listed in Table I.

TABLE I
PHYSICAL PROPERTIES OF FIBERS USED BY NAWAB AND MASON

Rayon fibers, 3.5 microns in diameter

Sample	Fiber Lengths, mm.	Length-to-Diameter Ratio	Modulus of Elasticity, dynes/sq. cm.	Appearance of Fibers During and After Shearing
A	0.15	43.2	26.4×10^{10}	All particles straight
B	0.26	75.3	26.4×10^{10}	
C	0.40	113	26.4×10^{10}	Some particles curved, all rigid
D	0.61	173	26.4×10^{10}	Large fraction curved, slight springiness
E	0.84	240	26.4×10^{10}	Large fraction curved, increased springiness
F	1.25	356	26.4×10^{10}	Large fraction curved, springy and flexible rotations. Aggregation

Viscosity measurements were made in a coaxial cylinder viscometer with rotating bob and fixed cup using shear rates from 9.9 to 93.3 sec.⁻¹. Annulus widths of 3.3 mm. and 12.3 mm. were used in the studies on Samples A, B, and C to determine whether or not there was any wall effect. None was found. The largest fibers and the smallest annulus width resulted in L/D and d/D ratios of 0.12 and 0.00106 where D is the annulus width.

Nawab and Mason questioned the validity of the results obtained by Eirich, et al. because of the possibility that they may have been affected by wall effects, polydispersity, and aggregation. However, no mention was made of the fact that Eirich's measurements were made in the regime of unstable flow.

Nawab and Mason, in considering their experimental results as compared to the results predicted by Burgers' theory, stated that Equation (1) should be corrected by a factor β as follows:

$$\mu_r = 1 + \beta \alpha_0 c \quad (16)$$

where $\beta = (\underline{L/d})/(\underline{L/d})_e$, and where $(\underline{L/d})_e$ is the "equivalent ellipsoidal" axis ratio of a rod. This "equivalent ellipsoidal" axis ratio was arrived at by Mason, et al. (22-24) as follows.

Jeffery (10) has shown that the period of rotation of an ellipsoid is defined by:

$$\begin{aligned} TG &= 2\pi (L/d + d/L) \quad (17) \\ &= 2\pi L/d \text{ for large values of } \underline{L/d}, \end{aligned}$$

where \underline{T} = period of rotation, sec., and

\underline{G} = velocity gradient, sec.⁻¹.

Mason, et al. measured the period of rotation for cylinders in a known velocity gradient, calculated the "equivalent ellipsoidal" axis ratio $(\underline{L/d})_e$, and compared these values with the known $\underline{L/d}$ values for the cylinders. The results of the measurements are presented in Fig. 2.

An empirical correlation of the results presented in Fig. 2 is given by Equation (18).

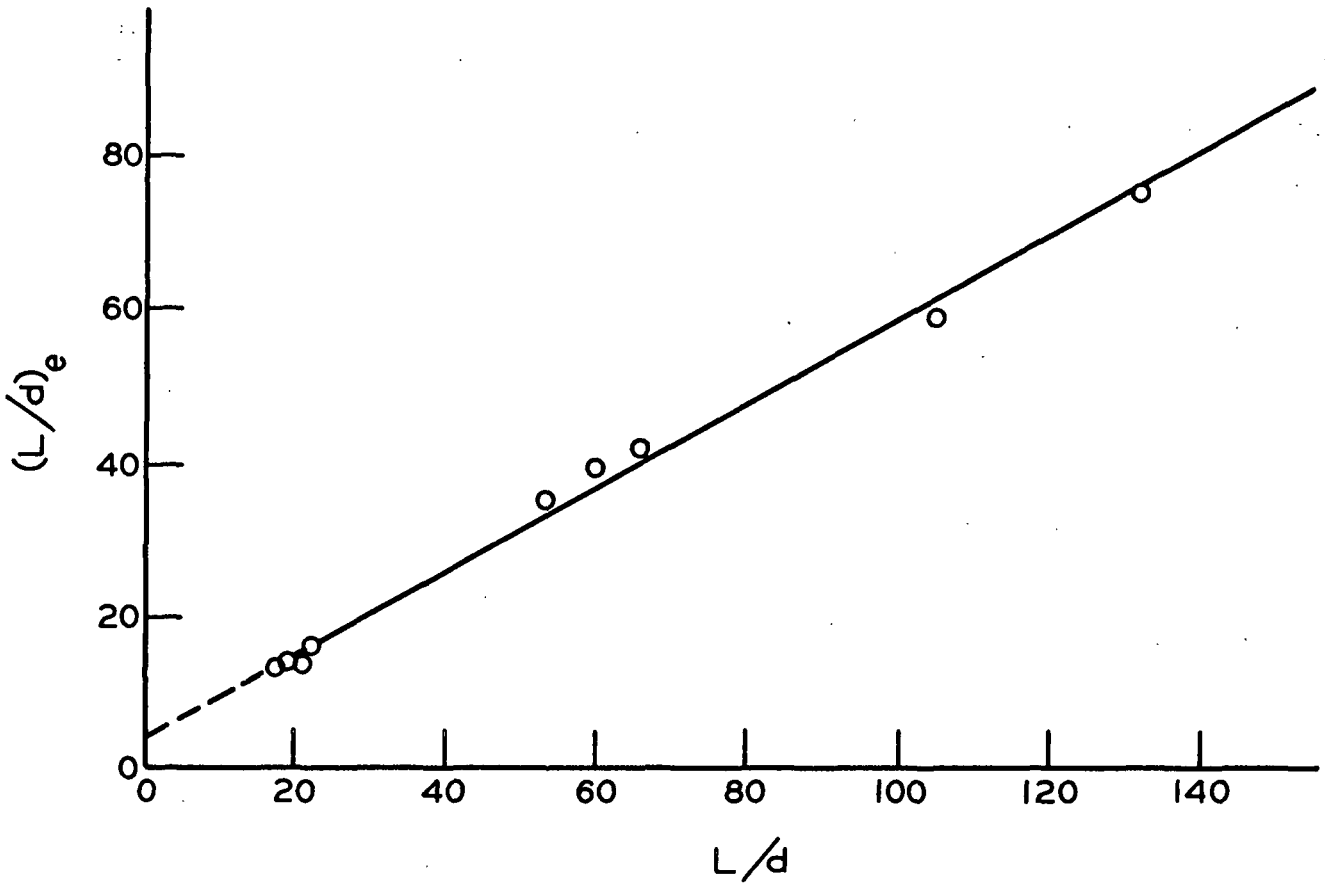


Figure 2. Relationship Between the Actual and "Equivalent Ellipsoidal" Axis Ratios

$$(L/d)_e = 3.72 + 0.547(L/d) \quad (18)$$

for $15 < \underline{L/d} < 140$.

The lower limit has been placed on Equation (18) since Goldsmith and Mason (26) have shown that as the rods become disks, $(\underline{L/d})_e$ increases with decreasing $\underline{L/d}$. The upper limit was used because no measurements have been made at larger $\underline{L/d}$ ratios to confirm the linearity of the relationship.

Nawab and Mason state that Burgers assumed that $(\underline{L}/\underline{d})_e/(\underline{L}/\underline{d}) = 1$ when he used Jeffery's equations for the behavior of ellipsoids to calculate $\sin^4 \theta \sin^2 2\phi$. This is equivalent to saying that $(\underline{L}/\underline{d})_e$ should be used in Equation (11) since this equation was derived for ellipsoids.

Table II is a comparison of the results obtained by Nawab and Mason with those from Burgers' theory both uncorrected and corrected using the β factor.

TABLE II
COMPARISON OF EXPERIMENTAL AND THEORETICAL
INTRINSIC VISCOSITIES

Sample	Equation (14)		Equation (15)		Measured α_o
	α_{oR}	$\beta\alpha_{oR}$	α_{oxy}	$\beta\alpha_{oxy}$	
A	3.5	5.8	--	9.1	8.2
B	4.9	--	--	--	15.2
C	6.6	14.2	--	22.2	18.5
D	9.0	23.3	--	36.7	44
E	11.7	36.6	--	57.5	76

Nawab and Mason pointed out that the approximate agreement between the measured α_o and $\beta\alpha_{oxy}$ is fortuitous since it is known from measured distributions of ϕ and λ (23) that the particles are not all aligned in the xy -plane. Mason and Manley (23) calculated the specific viscosity, $\mu'_{sp} = \mu_r - 1$, for suspensions of cylinders using measured values of \underline{K} and Equation (19) and compared this value with μ_{sp} calculated from Equations (1) and (14). The results are given in Table III.

$$\mu'_{sp} = \mu_r - 1 = \frac{\pi L^3 n}{12L/d(\ln 2L/d - 1.80)} \int_0^{\infty} \frac{K p(K)}{\sqrt{K^2 + 1}} dK \quad (19)$$

where $\underline{p}(\underline{K})\underline{dK}$ = fraction of particles with values of the orbit constant, \underline{K} between \underline{K} and $\underline{K} + \underline{dK}$.

TABLE III
COMPARISON OF SPECIFIC VISCOSITIES CALCULATED FOR
RANDOM AND MEASURED ORIENTATIONS

$\underline{L}/\underline{d}$	$\mu'_{\underline{sp}}/\mu_{\underline{sp}}$
20.4	0.55
68.4	0.50
115.5	0.55

From Table III it can be seen that by using measured values for the orientation of the particles, the values for $\mu_{\underline{sp}}$ and therefore α_0 should be about half that predicted from the assumption of random orientation. Therefore, Nawab and Mason's experimental values for α_0 (see Table II) are more than four times greater than those predicted by Burgers' theory when measured values for orientations of the particles are used.

Nawab and Mason suggested that one of the reasons for the large difference between theoretical and experimental results could be that the fibers used in Runs B, C, D, and E were curved and in C, D, and E were also flexible (see Table I). In a later publication, Forgacs and Mason (17) showed that a very slight fiber curvature has a tremendous effect on the period of rotation and therefore on $(\underline{L}/\underline{d})_e$ and β . The results of this study are given in Fig. 3.

In the light of the above considerations, Nawab and Mason state that "the importance of determining values of β , and in this connection (viscosity studies) of working with perfectly straight particles is evident."

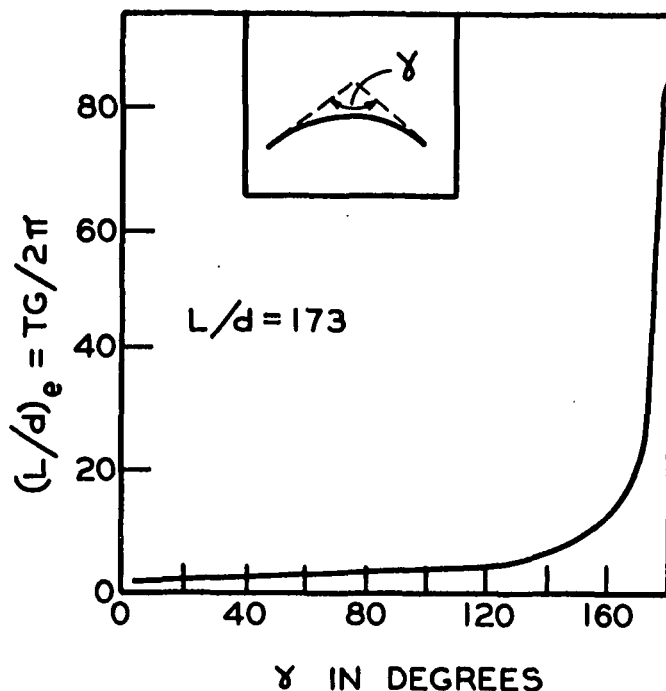


Figure 3. The Effect of Curvature on $(L/d)_e$ for the Rotation of Rigid Fibers in the xy -Plane

Nawab and Mason conclude their discussion with the following remarks.

"While the experimental work described here is incomplete in many respects and requires extension, it served to demonstrate the inadequacy of existing theories of reduced and intrinsic viscosity of rigid rods."

WORK OF MYERS

Myers (9) studied the viscosity of suspensions of nylon fibers of axis ratios varying from 20 to 160 and diameters of 16.79, 44.85, and 75.5 microns. The volume concentration range varied from 0.00019 to 0.0278. The apparatus used was a concentric cylinder viscometer designed by Myers (16, 19) to allow measurements at low shear rates of the order of 0.5 sec.^{-1} .

Myers compared his results with Burgers' theory and found little agreement as can be seen from Fig. 4.

Myers showed that the studies made using the 16.79μ diameter fibers were within the range of $\underline{d/D}$ and $\underline{L/D}$, i.e., 0.00106 and 0.12, used by Nawab and Mason (15), in which wall effects were found to be of no account and thus assumed that wall effects were not present in his measurements using these particular fibers. However, measurements using larger fibers did not fit these criteria.

Myers suggested that the relationship between α_0 and $\underline{L/d}$ given in parameters of $\underline{d/D}$ came about due to the increasing wall effect with increasing fiber diameter (see Fig. 4). The maximum values of $\underline{d/D}$ and $\underline{L/D}$ in Myers' study were 0.00333 and 0.268, respectively.

Myers criticized Nawab and Mason's (15) correction of Burgers' equations using the factor β . He stated that this is an oversimplification of the true reason for the difference between observed and theoretical results. In support of his statement, Myers pointed out that Burgers' equation for the drag on a cylinder in slow translation perpendicular to its axis underpredicts experimental values (27). Since, according to Myers, the strength of the doublet formed on cylinders in a linear velocity gradient was arrived at by the same mathematical procedure as that used to determine the drag force on a cylinder translating perpendicular to its axis, then there is little reason to believe that Burgers' viscosity equation can be corrected merely by correcting the orientation factor.

However, Burgers used an approximation (6, 28) in his calculation of the resistance of a cylinder which was not used in his calculation of the strength of the doublet. Burgers also pointed out that his estimation of the resistance

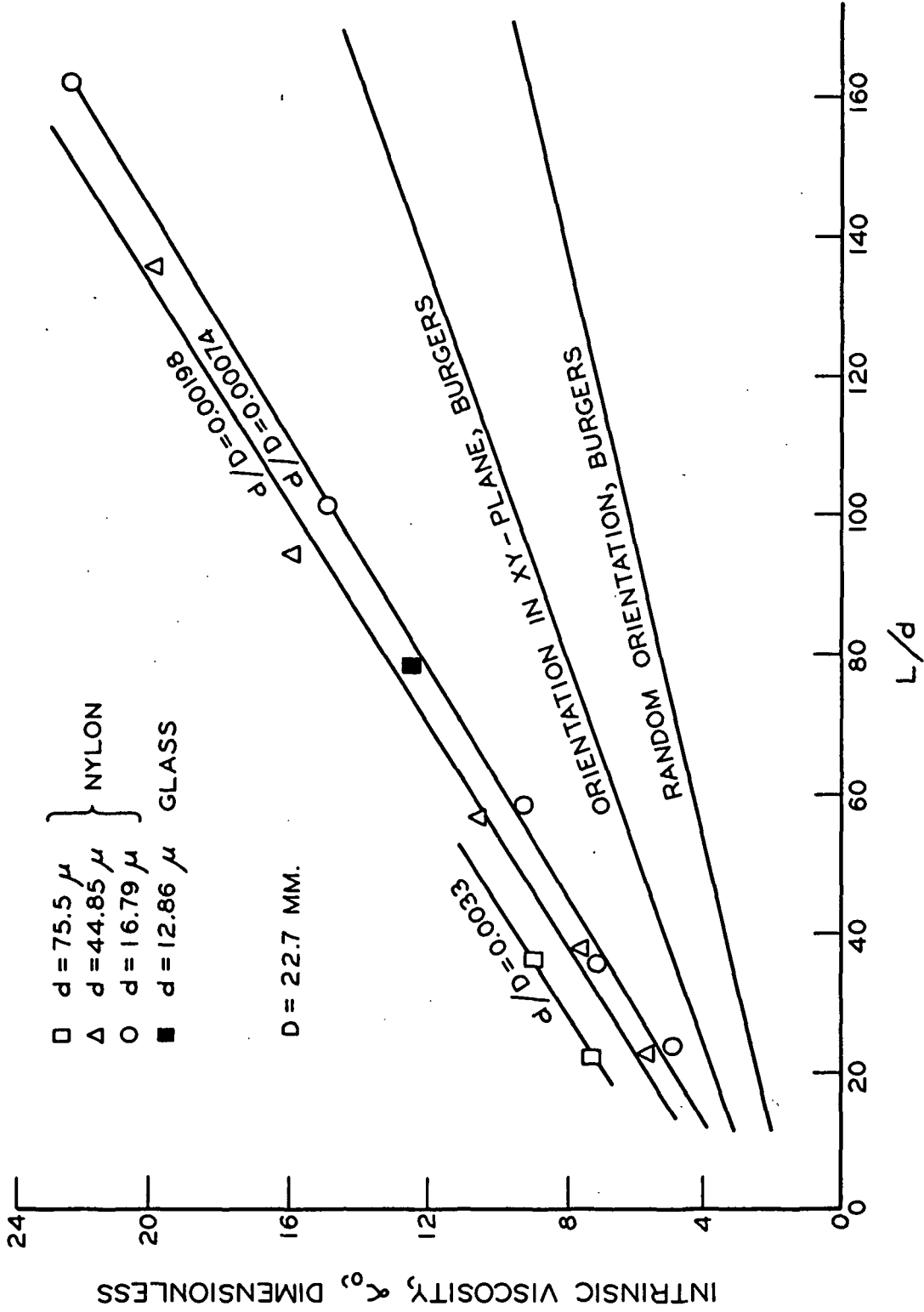


Figure 4. Myers' Intrinsic Viscosity Data Versus L/d

of a cylinder in translation was expected to be low due to the approximation made.

Therefore, it cannot be said, a priori, that Burgers' viscosity equation is incorrect.

COMPARISON OF NAWAB'S AND MYERS' EXPERIMENTAL DATA

Figure 5 gives a comparison of Nawab and Mason's (15), and Myers' (16) experimental data. As can be seen, there is little agreement between the two studies. Both studies did show that the intrinsic viscosity, α_0 , increased with increasing L/d .

THE PROBLEM

As was shown in Fig. 5, Nawab's and Myers' experimental studies were not in agreement. Also, as was pointed out in the section on Past Experimental Work, none of the experimental results have agreed with theoretically predicted results.

Therefore, the problem was to determine the reasons for the differences in the experimental results and why there has been no agreement between experimental results and theoretically predicted results.

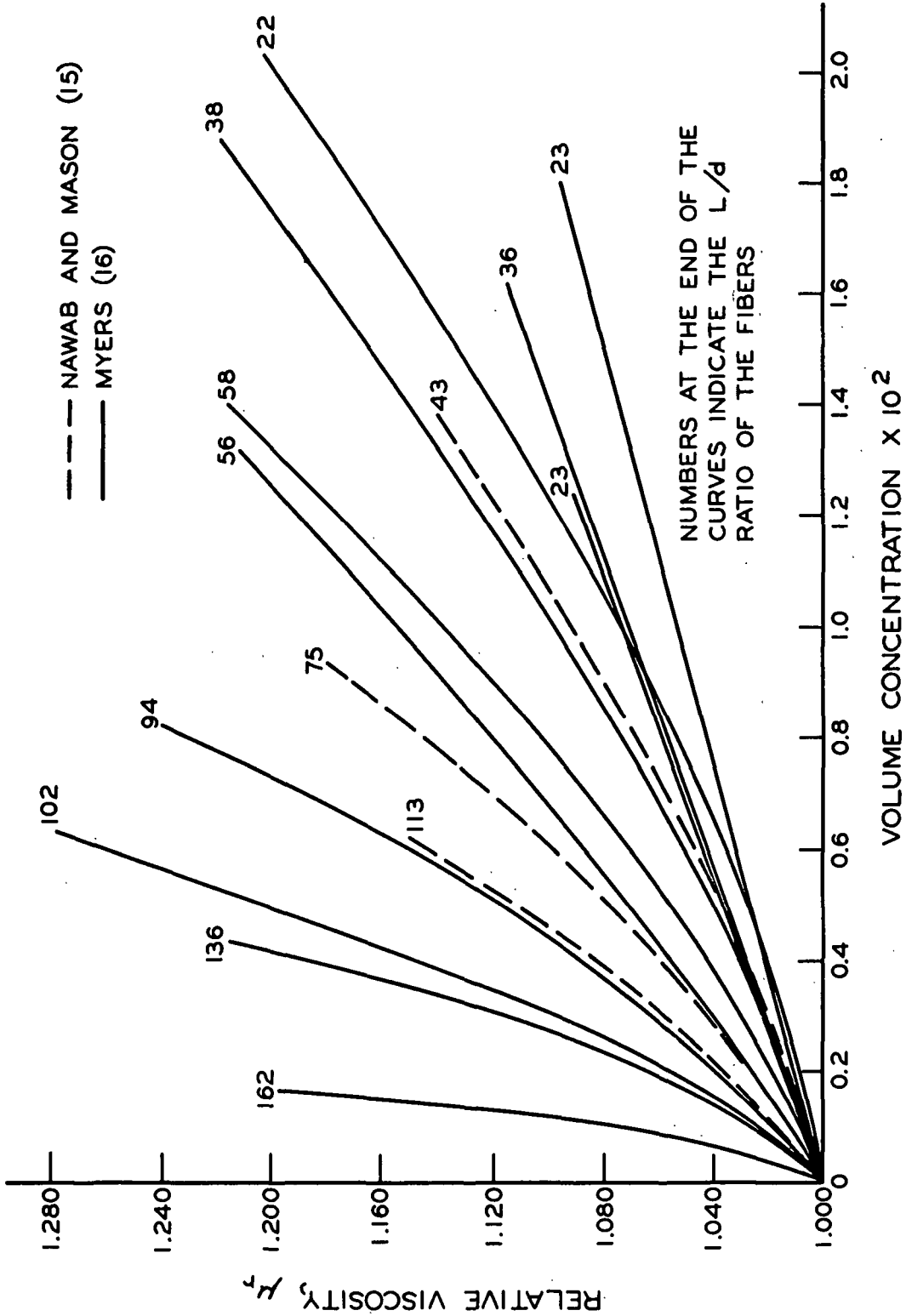


Figure 5. Comparison of the Data of Nawab and Mason, and Myers

ANALYSIS OF THE PROBLEM

In analyzing the problem it will be most enlightening to consider the differences in the experimental methods compared with conditions assumed in Burgers' theory.

The following questions will be asked and answered for each experimental work being considered.

1. Were there inertial effects?
2. Were the fibers flexible?
3. Were the fibers curved or crooked?
4. Was there fiber-fiber interaction?
5. Were there wall effects?

The answers to these questions are given in Table IV. Where a yes or no answer cannot be given or where clarification of the answer is needed, the situation will be discussed later in the text.

TABLE IV
COMPARISON OF PAST EXPERIMENTAL METHODS

Question Number	Eirich, <u>et al.</u>	Nawab and Mason	Myers
1	Yes ^a	No ^a	No ^a
2	--	See Table I	No ^a
3	Yes	See Table I	Yes in all but two cases
4	Yes	Yes ^a	Yes ^a
5	--	No	? ^a

^aExplanation of these answers follows in Questions 1, 2, 4, and 5.

QUESTION 1

There are two types of inertial effects which are important in the systems considered here, the first associated with the liquid itself and the second associated with the flow of the liquid around the particles.

Taylor (29) showed that the streaming laminar flow in a concentric cylinder viscometer with the inner cylinder rotating and the outer cylinder stationary becomes unstable when the angular velocity of the inner cylinder reaches a certain critical value, ω_c , given by the following equation:

$$\omega_c = \sqrt{\frac{1/2 (r_1 + r_2) \mu^2 \pi^4 f}{r_1^2 D^3 \rho^2 (0.0571 f^2 - 0.00056)}} \quad (20)$$

where

$$f = 1 - 0.652 \frac{D}{r_1}$$

r_1 = radius of inner cylinder, cm.

r_2 = radius of outer cylinder, cm.

μ = viscosity of the liquid, g./cm. - sec.

D = annulus width, cm.

ρ = density, g./cc.

Using Equation (20) it can be shown that, for stable laminar flow, Eirich should have worked at angular velocities below 9.6 rad./sec. However, as stated previously, Eirich actually worked at angular velocities ranging between 100 and 250 rad./sec. Therefore, it can be seen that Eirich's work was done using unstable flow. For this reason, Eirich's work will not be considered any further.

However, Nawab and Mason, and Myers, all worked at angular velocities below ω_c for their particular cases and therefore inertial effects connected with the liquid were unimportant.

Consider now the possibility of inertial effects due to the flow of the liquid over the fibers. There is no basis for comparison as to whether or not inertial effects are important for the flow of the liquid along the axis of the fiber. Therefore, some other basis must be used.

Myers (16) suggested that if it can be shown that inertial effects are not important for the extreme case of a fiber held stationary in a liquid moving at the maximum velocity used in a given study then it should be acceptable to assume that inertial effects were not important in the actual viscosity measurements. If this is done for the studies of Nawab and Mason, and Myers using as a criterion for the absence of inertial effects that the Reynolds number, Re , based on the diameter of the fiber, is less than one (30), it is found that for Nawab and Mason's study, $Re \approx 0.05$ and for Myers, $Re \approx 0.25$. Therefore, inertial effects were not important in this case either.

QUESTION 2

To determine whether or not the fibers used in past studies were flexible under the conditions of shear used in the viscosity measurements, Equation (21) was used.

$$(G\mu)_{\text{critical}} = \frac{E_b (\ln 2L/d - 1.75)}{2(L/d)^4} \quad (21)$$

where E_b = modulus of elasticity in bending, dynes/sq. cm.

This equation, which predicts the shear rate necessary to buckle a rod, was derived by Forgacs and Mason (31) using Burgers' equation for the forces acting on a thin rod in a linear velocity gradient. Equation (21) was also shown to be approximately correct using dacron, rayon, and nylon fibers suspended in a linear velocity gradient.

Except for the fiber samples listed in Table I which were known to be flexible or bent due to the velocity gradient, using Equation (21), the other samples used by Nawab and Mason, and Myers can be shown to be rigid.

QUESTION 4

The frequency of interaction was probably much greater in Nawab and Mason's work than in Myers' work due to the higher shear rates used.

Also, all of the concentrations used by Nawab and Mason, and the vast majority of those used by Myers, were relatively high for the particular L/d ratios used and, therefore, fiber-fiber interaction would be expected to be appreciable.

It should be noted, however, that all of the concentrations used in these studies were well below those necessary for the formation of a continuous fiber network (32).

QUESTION 5

As was pointed out earlier, Myers hypothesized that the presence of wall effects caused the behavior shown in Fig. 4. However, this was not proved absolutely.

Consider now the over-all picture represented by Table IV. For strictest agreement with the assumed conditions in Burgers' theory, all questions should

be answered No. As can be readily seen, none of the studies quoted were performed under conditions which agreed with those assumed in Burgers' theory. The differences were: most of the fibers used were curved, in all cases there was considerable fiber-fiber interaction, and, in Myers' study there may have been wall effects.

The questions that remain to be answered are, what are the magnitude of these effects on the viscosity of suspensions of rigid rods and, if the conditions assumed in Burgers' theory are more closely met, will there be better agreement between theoretical and experimental results?

In order to answer these questions, the following study of the viscosity of fiber suspensions was made.

CHOICE OF VISCOMETER AND SUSPENSION

CHOICE OF VISCOMETER

In order to satisfy the condition of a linear velocity gradient, it was necessary to make the viscosity measurements in a concentric cylinder viscometer. The viscometer designed by Myers met all of the requirements. Although a thorough discussion of this viscometer has been given by Myers (16, 19), a description will be given here since an understanding of the viscometer is necessary in order to follow the experimental procedures.

GENERAL DESCRIPTION OF MYERS' VISCOMETER

The viscometer consisted of a stationary outer cylinder and a rotating inner cylinder. The inner cylinder was suspended from an air bearing by a nylon cord. The air bearing was driven by a rotating magnetic field produced by 6 electromagnets driven at a constant angular velocity of 1070 r.p.m. The driver was an 1800 r.p.m. synchronous motor connected to the electromagnets by a pulley system.

A diagram of the viscometer is given in Fig. 6.

Note that the upper part of the viscometer was separated from the lower part by an air gap. This was done to prevent vibrations from the drive from disturbing the air bearing. Note also that the air bearing was covered by a Plexiglas shield to prevent air currents produced by the drive from affecting the performance of the air bearing.

DESCRIPTION OF CYLINDERS

The inner cylinder was a hollow brass cylinder, 15.28-cm. long, 4.98-cm. in diameter and closed at the top and bottom.

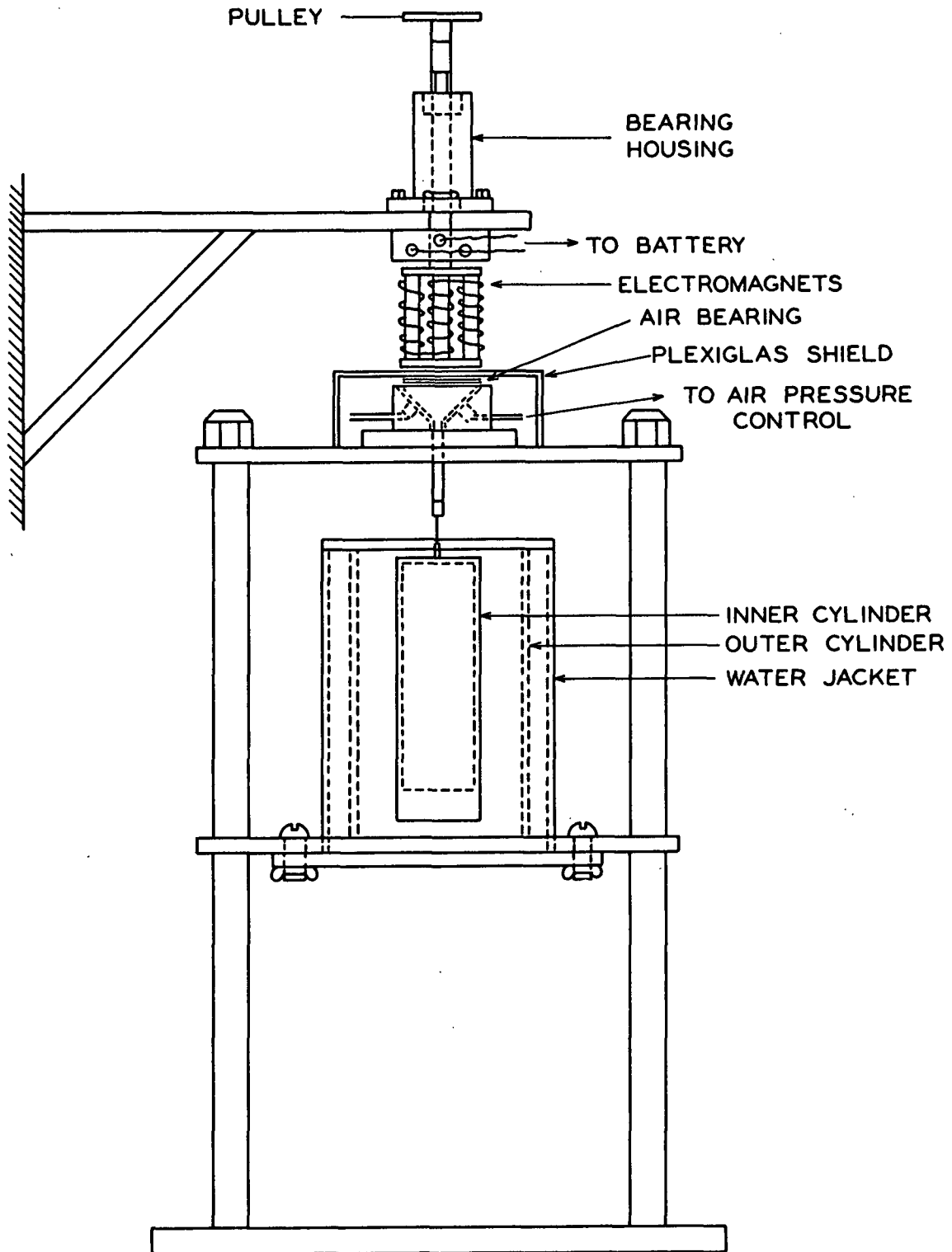


Figure 6. Myers' Concentric Cylinder Viscometer

Two outer cylinders were used. Both were made from glass tubing and were 18.5-cm. long. A 5.47-cm. diameter outer cylinder was used for calibration purposes and wall effect studies. A 9.53-cm. diameter outer cylinder was used for the remainder of the study.

Both outer cylinders were surrounded by water jackets. Water from a constant temperature water bath was circulated through the jacket controlling the temperature in the annulus to within 0.05°C.

A diagram of a water-jacketed cylinder is given in Fig. 7.

DESCRIPTION OF ELECTRICAL SYSTEM

The torque delivered by the magnetic drive was varied by changing the current to the electromagnets. The current was supplied by a 6-volt storage battery and varied by means of a rheostat. A 0-2 ampere d.c. ammeter which could be read to the nearest 0.002 ampere was in series with the battery and electromagnets to measure the current to the electromagnets.

Before each viscosity measurement, an alternating current was passed through the coils of the electromagnets to destroy any permanent magnetism which may have set up in the cores due to passage of the direct current. This was done by starting the flow of alternating current through the coils at 3 amperes and slowly decreasing the current to zero by means of a variable voltage autotransformer.

A diagram of the electrical system is given in Fig. 8.

CLEANING AND CONTROL OF AIR TO AIR BEARING

The air supply for the air bearing came from a laboratory air line. The air was fed through a pressure regulator which held the pressure constant at

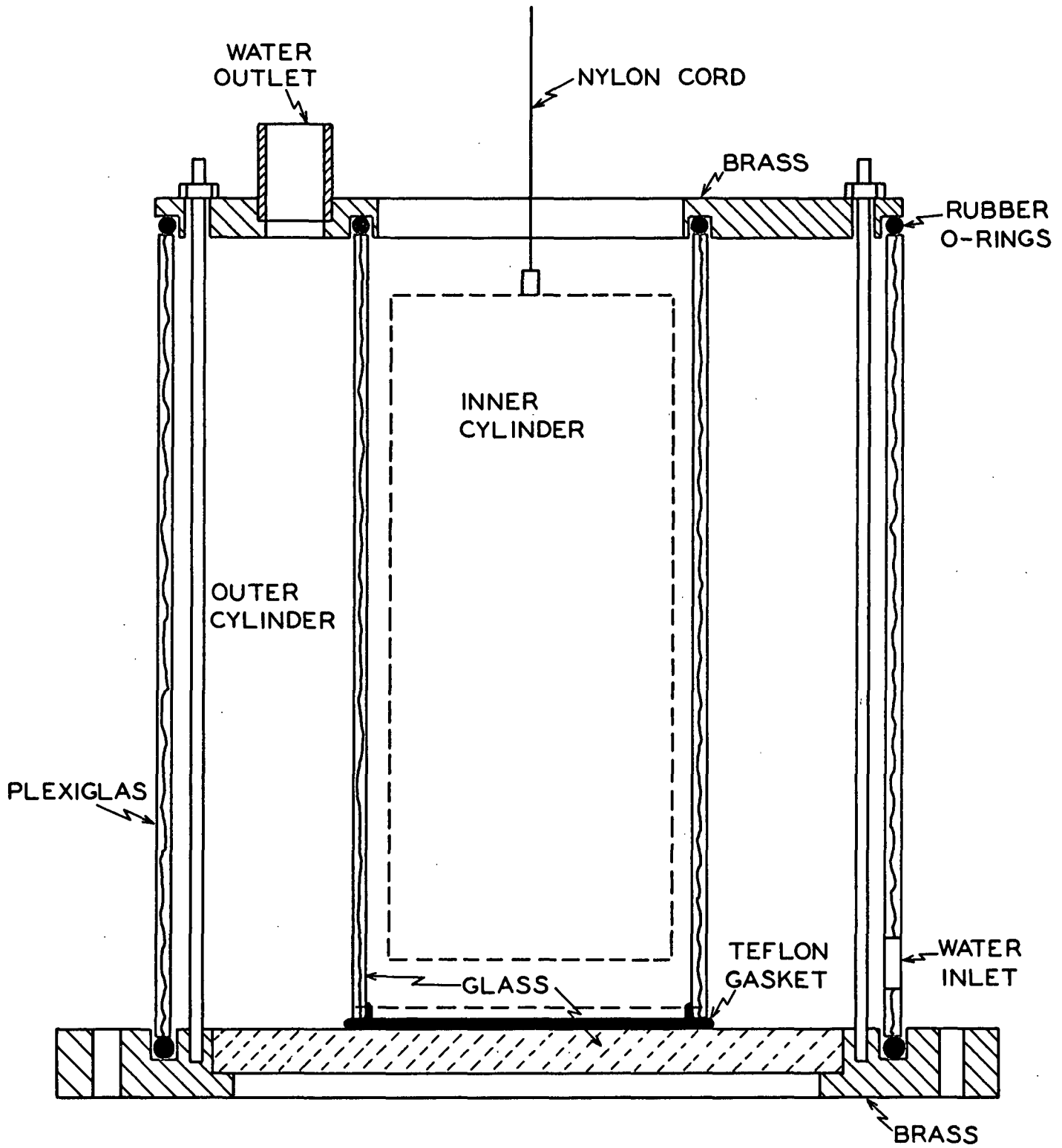


Figure 7. Water-Jacketed Cylinders

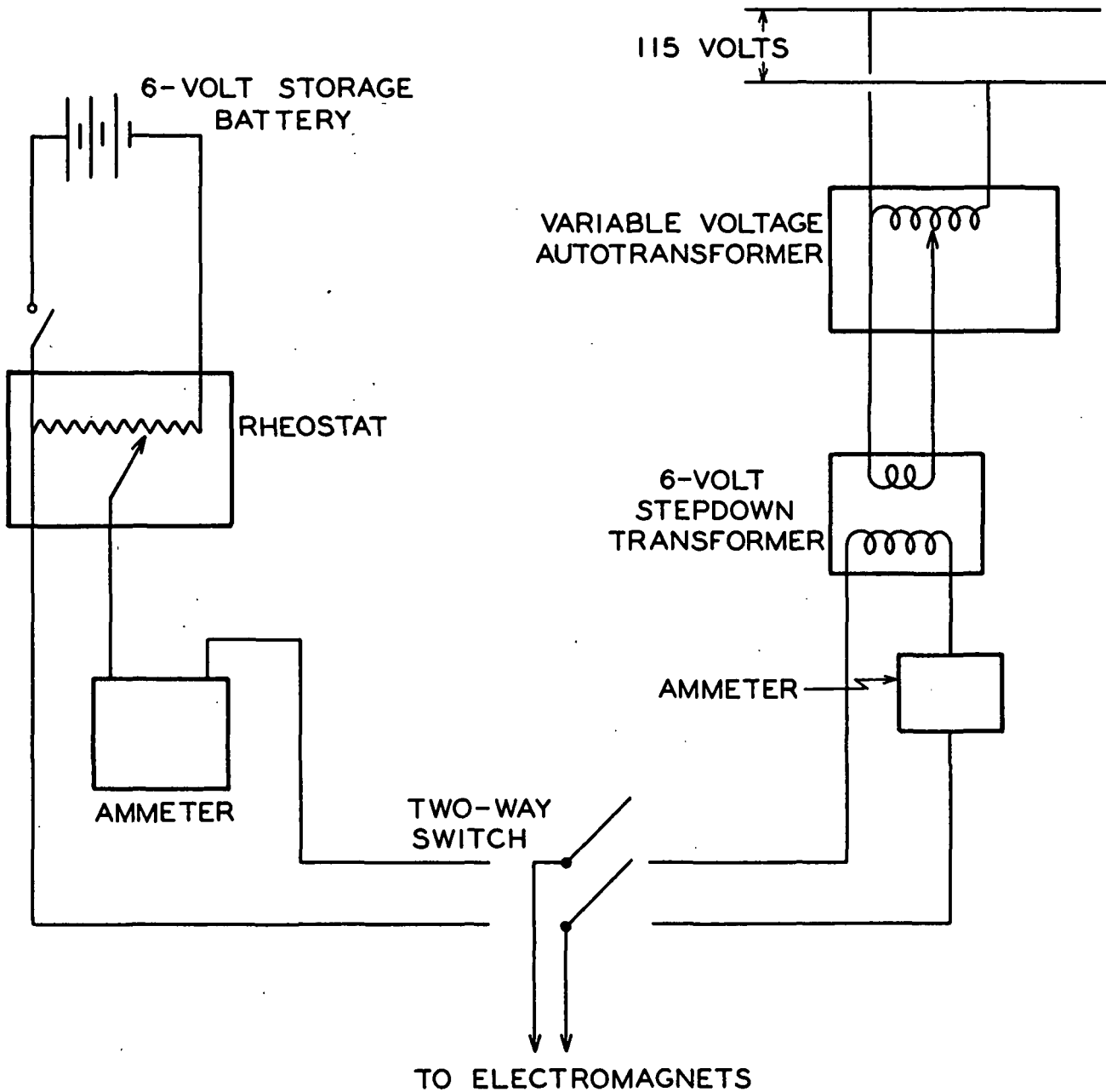


Figure 8. Diagram of Electrical System

30 p.s.i.g., a screen to remove large particles, and a filter to remove small particles and water. A second pressure regulator was used as a final control of the air to the air bearing. A U-tube manometer, using tetrabromoethane, was placed between the second pressure regulator and the air bearing so that any pressure changes could be detected.

CHOICE OF SUSPENSION

The choice of the suspension to be studied was governed by several factors. First, the assumptions made in the theoretical section had to be met as closely as possible. Second, there could be no physical or chemical effect of the suspending medium on the fibers. Third, the suspension used had to be well dispersed. These criteria were met in the following ways.

Inertial effects were eliminated by working at Reynolds numbers, based on the diameter of the fibers, of much less than one. The Reynolds number was calculated in the same manner as discussed in the analysis of the problem.

Straight, rigid cylinders were obtained by cutting nylon filament of circular cross section to the desired length.

For convenience in future discussions, fiber-fiber interaction will be broken down into two types, hydrodynamic interaction and mechanical interaction. Hydrodynamic interaction will mean the effect of one fiber's flow field on any other. Mechanical interaction will mean physical contact between the fibers.

In order to minimize fiber-fiber interactions of both types, Mason's (33) "critical concentration" for free rotation of the fibers was used as a guide.

To estimate this "critical concentration," Mason allowed a volume to each fiber equal to a sphere of diameter equal to the length of the fiber. Therefore,

for free rotation:

$$V_E n = (4\pi/3)(L/2)^3 n = 1 \quad (22)$$

where

V_E = the effective volume occupied by one fiber

n = the number of fibers per unit volume

Substitution for n in terms of concentration which now becomes the "critical concentration," c_o gives

$$(4\pi/3)(L/2)^3 c_o / (\pi L d^2 / 4) = 1 \quad (23)$$

or
$$2/3(L/d)^2 c_o = 1 \quad (24).$$

Therefore,

$$c_o = 1.5/(L/d)^2 \quad (25).$$

If Equations (1) and (14) are combined and c_o from Equation (25) is substituted for c , it is found that:

$$\mu_r \text{ at } c_o = 1 + 1/[\pi (L/d)(\ln 2L/d - 1.80)] \quad (26)$$

Therefore, to obtain the highest possible relative viscosities and still remain below the "critical concentration," fibers of small L/d ratio should be used. However, there are also limitations to the smallness of the L/d ratio. First, Burgers' derivation requires that L/d be much greater than one. Second, if the L/d ratio of the fibers is too small, the effect of the ends of the fibers might become important.

If α_o from Equation (14) is plotted versus L/d the relationship given in Fig. 9 results. It can be seen that below an L/d of approximately 10, Burgers'

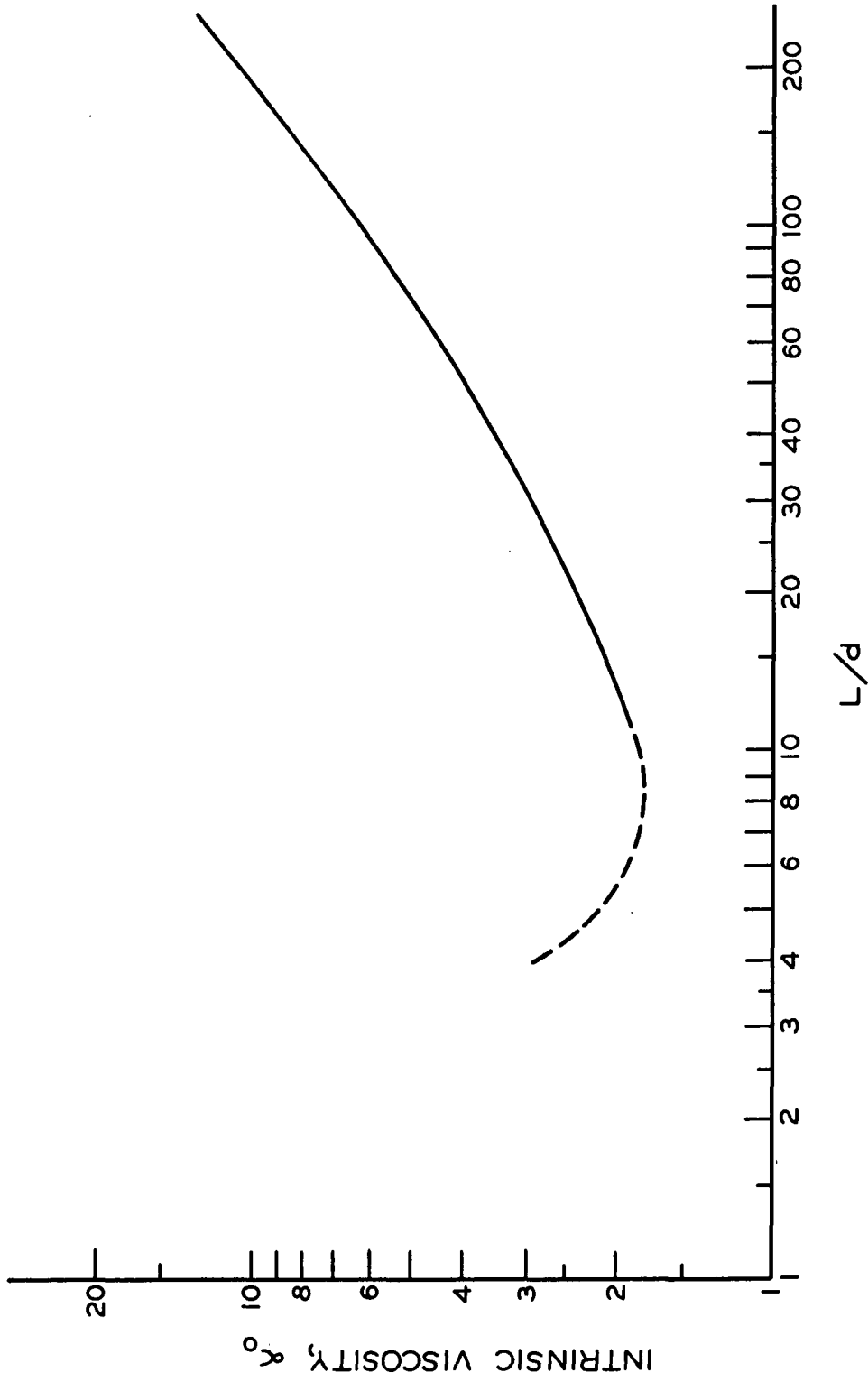


Figure 9. Relationship Between α_0 and L/d as Given By Equation (14)

theory begins to predict an increase in α_0 with decreasing L/d . Therefore, for this study, fibers with $L/d > 10$ were needed to stay in the region where Burgers' theory applies.

In a study of the translation of cylinders through a liquid, Han (27) showed that the ratio of the experimentally determined drag force to that predicted theoretically by Burgers (6), who neglected fiber end effects, was constant until the L/d ratio of the fibers was smaller than 10. The deviation of this ratio from a constant was attributed to fiber end effects. This was used as a guide to the elimination of fiber end effects in this study.

Therefore, in order to make this study in the range of L/d where Burgers' theory applies, prevent fiber end effects from being appreciable, and yet to use an L/d ratio small enough to obtain a measurable relative viscosity below the "critical concentration," it was decided to work with fibers with an L/d ratio of approximately 20.

Wall effects were eliminated from considerations in the initial part of this study by using a viscometer annulus width large enough to give L/D and d/D ratios small enough to be in the range that Nawab and Mason (15) showed wall effects to be absent.

Studies made at E. I. du Pont de Nemours and Company (34) showed that nylon shortened only 3% in tetrachloroethane (TCE) after 1000 hr. at 70°F. and only 2% in paraffin oil (PO) after 10 hr. at 210°F.

Myers (16) stated that no swelling or shrinkage of his nylon fibers could be detected after soaking in a mixture of TCE and PO for 24 hr. at 23°C. Myers also found that nylon fibers remained well dispersed in a mixture of TCE and PO.

Since TCE and PO have different densities, one greater and one less than that of nylon, the density of the solution could be adjusted to prevent floating or settling of the fibers.

For the above reasons, a mixture of TCE and PO was chosen as the suspending medium for the nylon fibers.

EXPERIMENTAL PROCEDURES

FIBER PREPARATION AND CHARACTERIZATION

The nylon fibers used in this study were cut from Du Pont nylon yarn.

CUTTING PROCEDURE

Straight Fibers

The straight fibers were prepared from the nylon yarn by the following procedure.

The yarn was wound on a circular wheel two feet in diameter so that the strands were nearly parallel. The fiber bundle thus obtained was cut from the wheel, and laid into a trough formed by a piece of steel channel closed at both ends. At each end, bolts, through the sides of the channel, held the fibers below the top of the trough. The ends of the fiber bundles hung over the ends of the trough and weights were attached to keep the fibers straight. Fischer Tissuemat Wax (m.p. 54-56°C.) was then poured over the fibers filling the trough. After the wax had hardened, the block of wax containing the fiber bundle was removed from the trough and cut into several smaller blocks. The desired fiber lengths were then cut using a microtome. The majority of the wax was removed by melting the wax and filtering the suspension. The remaining wax was removed by extracting the fibers with pentane in a Soxhlet for 8 hours.

Curved Fibers

The curved fibers used were cut from the same nylon yarn used for the straight fibers. The fibers became curved due to the cutting procedure. The procedure was as follows. The nylon yarn was wound on the wheel as before. The fiber bundle was glued to chipboard and removed from the wheel. A cutter,

made from razor blades held in a parallel array by threaded drill rods and nuts, and spaced by washers or shim stock, was forced through the fiber bundle using a hydraulic press.

This was the same procedure used by Myers (16) to cut all but his shortest fibers.

MEASUREMENT OF FIBER LENGTHS

Fiber lengths were determined by projecting the images of the fibers on to the screen of the fiber length measuring apparatus (35) developed by the Finnish Pulp and Paper Research Institute. This magnified the fiber lengths 50 times. The images on the screen were then measured with a scale to the nearest millimeter. At least 100 fibers were measured and the average length determined.

MEASUREMENT OF FIBER DIAMETERS

Fiber diameter measurements were made using a microscope with a 43X objective lens and a Dyson image-splitting eye-piece (36). The resulting total magnification was 1700X. Approximately 30 fibers were measured to obtain an average diameter.

OPERATION OF THE VISCOMETER

In order to determine the torque-angular velocity relationship for a solution or suspension, the following operational procedure was followed.

1. The outer cylinder, containing the solution to be measured, was centered on the base of the viscometer by means of the two bolts shown in Fig. 6.

2. Water from the constant temperature bath was started to circulate through the water jacket and the solution was allowed to come to the desired temperature.

3. The air pressure to the air bearing was adjusted to an amount just necessary to "float" the bearing. This pressure was determined by passing an electric current through the male and female portions of the bearing while the air pressure was being increased from zero. When the current ceased to flow, indicated by an ammeter in the circuit, the male portion of the bearing was "floating." Experience showed that it was necessary to increase the air pressure by 2 cm. of tetrabromoethane over the amount just necessary to support the bearing for proper performance of the viscometer.

4. The electromagnets were demagnetized using the procedure described on p. 30.

5. The motor driving the electromagnets was started.

6. A small direct current was supplied to the electromagnets which delivered a low torque to the inner cylinder.

7. The inner cylinder was allowed to come to an equilibrium angular velocity and the time per revolution was measured to the nearest 0.1 sec. with a stopwatch. Measurements were made for several revolutions and the results averaged.

One revolution was determined from the passage of a light beam, reflected off a mirror on the shaft of the air bearing, past a given spot.

8. The average time per revolution and the current to the electromagnets were recorded.

9. The current to the electromagnets was increased and steps 7-8 were repeated until the desired range of torques had been covered.

During the operation of the viscometer, periodic checks were made of the angular velocity of the magnetic drive, and the spacing between the magnetic

drive and the air bearing. The angular velocity of the magnetic drive was measured using a stroboscope, and the air gap spacing was measured using a feeler gage. A change in either of these quantities required correction of the change and recalibration of the viscometer.

CALIBRATION OF THE VISCOMETER

The viscometer was calibrated using the small (4.98 cm. diameter) cup and a known viscosity sucrose solution (approximately 33% by weight).

The solution was prepared using reagent-grade sucrose and distilled water and was deaerated for approximately 15 minutes.

The concentration of the solution was determined by weighing a sample of the solution, evaporation of the solution to dryness in a vacuum oven at 50°C., and weighing the residue. The viscosity of the solution was determined from tables given by Bates (37).

Having prepared the sucrose solution, calibration of the viscometer was then accomplished by determining the angular velocity of the inner cylinder for several different currents to the magnetic drive over the range from 0-2 amperes. The torque delivered by the magnetic drive was then determined using Equation (27).

$$T' = 4\pi \mu h \omega_b / (1/r_1^2 - 1/r_2^2) \quad (27)$$

where

T' = torque, dyne-cm.

h = inner cylinder length, cm.

ω_b = angular velocity of inner cylinder, rad./sec.

r_1 = radius of inner cylinder, cm.

r_2 = radius of outer cylinder, cm.

Thus, by plotting torque versus current, a calibration curve such as that shown in Fig. 10 was obtained.

The calibration of the viscometer was checked periodically as a matter of course. Also, if there was reason to believe that the calibration had changed, the viscometer was recalibrated.

PERFORMANCE OF THE VISCOMETER

Values for the torque delivered by the magnetic drive were determined from the current to the drive using a calibration curve such as the one shown in Fig. 10. The angular velocity was determined from the time per revolution of the inner cylinder.

Figure 11 gives an example of the reproducibility of the viscometer.

The solution being tested was a TCE-PO solution (sp. gr. ≈ 1.14). The apparent viscosities (T/ω) obtained for Runs 1, 2, and 3 were 102.3, 102.3, and 102.6 dyne-cm.-sec., respectively. The slopes were figured by least squares with a prescribed intercept of zero. The data for these runs are given in Appendix II, Table X.

Below torques of approximately 10 dyne-cm., the data deviated from linearity indicating a loss in precision. For this reason, the data taken in this study were obtained at torques above 10 dyne-cm.

Note that at high angular velocities, the torque-angular velocity relationship in Fig. 11 becomes curved. This was due to instability of the flow in the annulus, i.e., the formation of Taylor vortices (29).

Only the data in the linear portion of the curves were used in calculation of apparent viscosities.

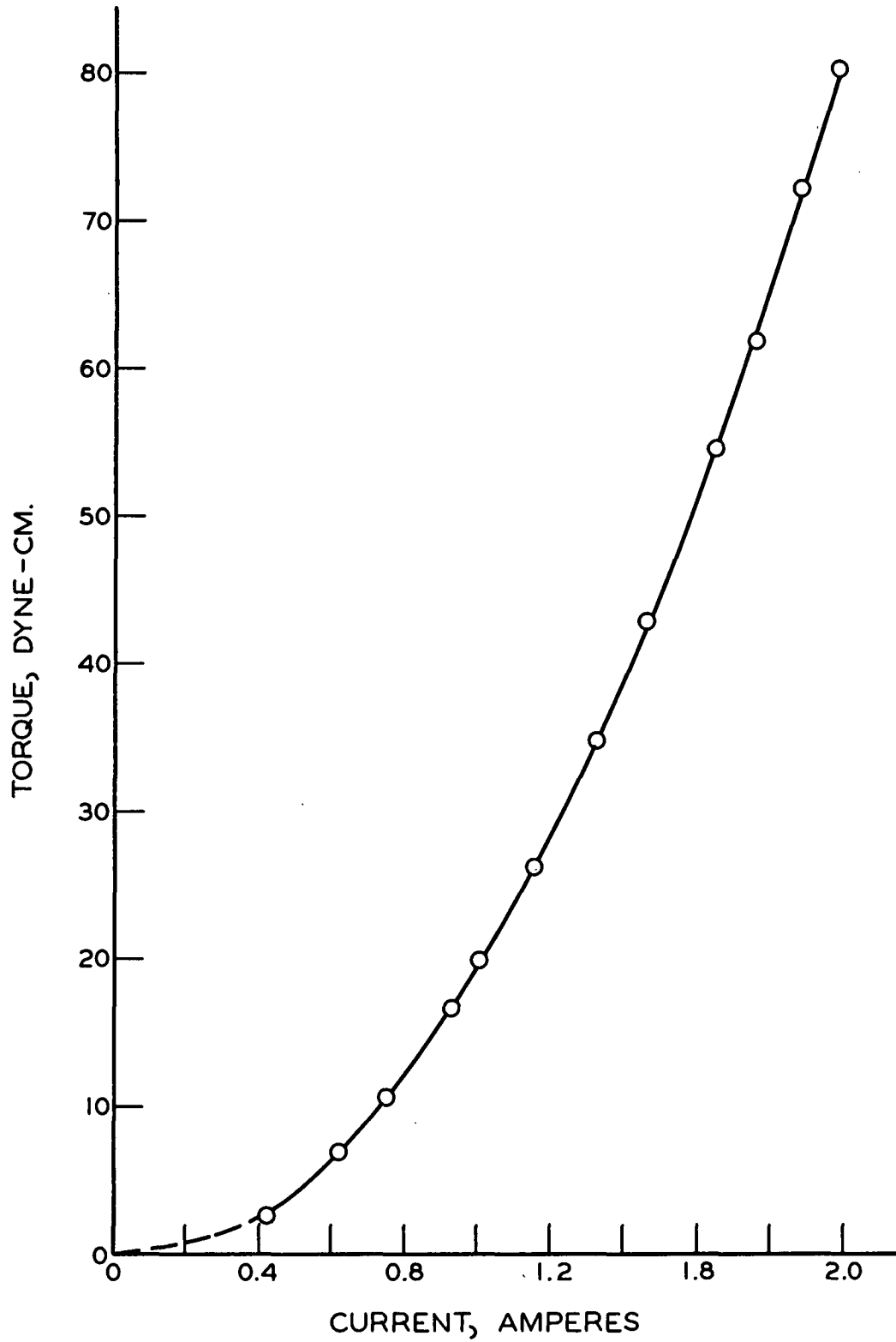


Figure 10. Calibration Curve

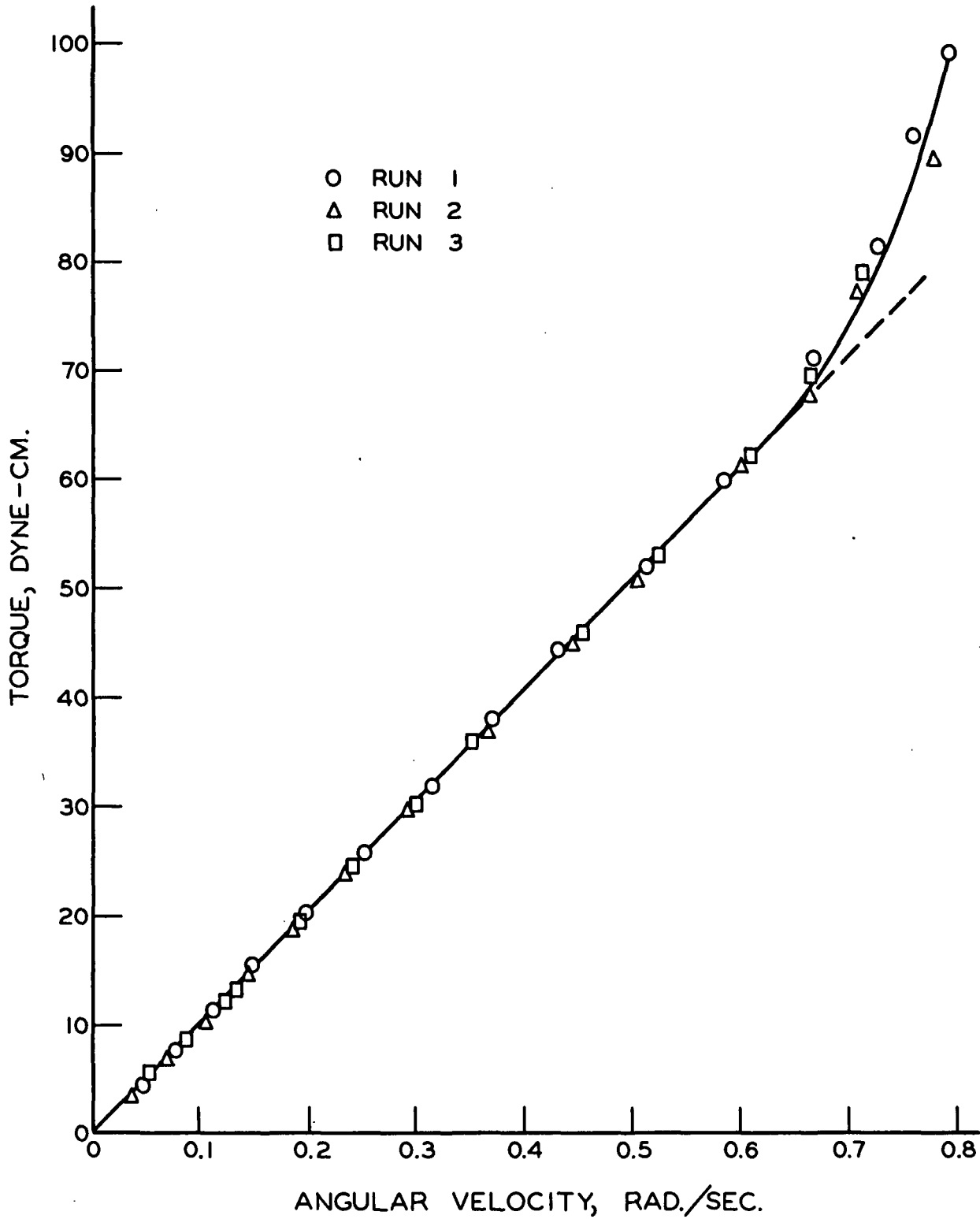


Figure 11. Reproducibility Measurements on a TCE-PO Solution

Figure 12 gives an example of the reproducibility of the measurements using nylon fiber suspension. The fibers being used in these particular runs were 16.9 μ in diameter with an L/d ratio of 19.2.

The following apparent viscosities were found for these runs: Runs 4A and B, 97.3, 97.0; Runs 5A and B, 108.1, 108.0 dyne-cm.-sec. The data for these runs are given in Appendix II, Table XI.

In general, the precision of the measurements was found to be within $\pm 0.25\%$.

DETERMINATION OF INNER CYLINDER END EFFECTS

Before the relative viscosity of a solution or suspension could be determined using the large (9.53 cm. diameter) cup, the effect of the ends of the inner cylinder had to be known.

End corrections were determined for both the top and bottom ends of the inner cylinder.

The procedure for the correction of the effect of the bottom end of the inner cylinder has been discussed by Oka (38) and used by Lindsley and Fischer (39), and Myers (16) in their work with concentric cylinder viscometers. This procedure is as follows. The liquid level in the cup was varied and the apparent viscosity at each liquid level was plotted against the height of the liquid on the inner cylinder. A line through all points except the one obtained with the inner cylinder submerged was extrapolated to zero height. The intercept was the end correction for the bottom end of the inner cylinder for this one particular liquid.

The correction for the effect of the top of the inner cylinder was found by subtracting the apparent viscosity obtained with the liquid level just at

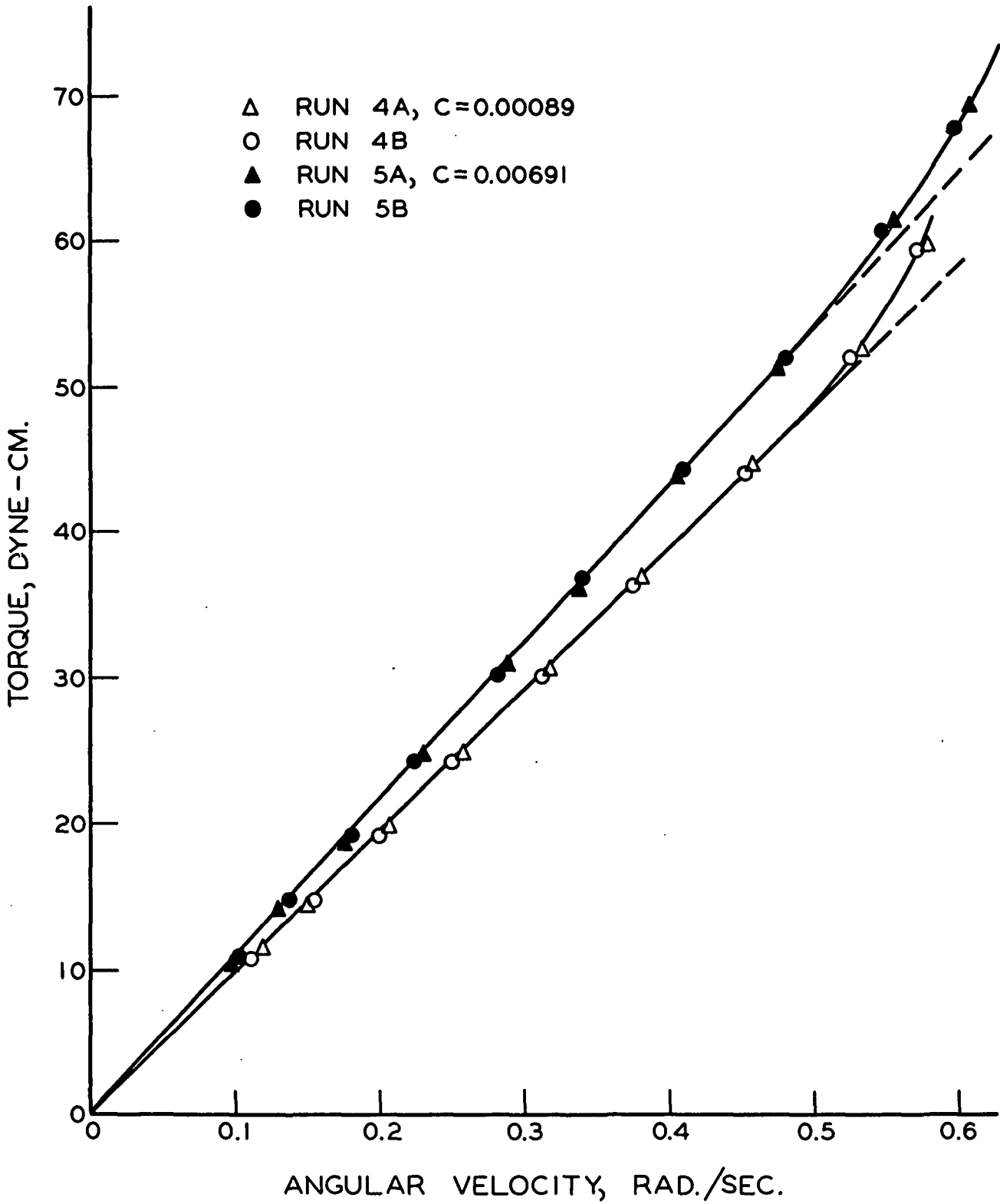


Figure 12. Torque-Angular Velocity Relationships for Fiber Suspensions

the top of the cylinder from that obtained with the cylinder submerged 4 mm. below the surface.

Determinations of the end corrections were made using several liquids of different viscosities. The relationships found are given in Fig. 13.

The top end correction was then plotted versus the apparent viscosity of the liquid obtained with the inner cylinder submerged and the bottom end correction was plotted versus the apparent viscosity obtained with the liquid level just at the top of the inner cylinder. The end correction curves determined in the above manner are shown in Fig. 14.

Since Myers (16) showed that the end correction depended only on the apparent viscosity of a solution or suspension and not on the presence or absence of fibers, only pure solutions were used to make the end corrections in this study.

PROCEDURE FOR MAKING A VISCOSITY-CONCENTRATION STUDY

GENERAL PROCEDURE

A suspension of the highest concentration desired to be studied was prepared and the apparent viscosity was determined. The concentration was then reduced and the apparent viscosity determined. This procedure was followed until the desired concentration range had been covered.

DETAILED PROCEDURES

Preparation of Fibers

Before each series of viscosity-concentration runs was made, the fibers to be used were washed thoroughly with carbon tetrachloride and dried overnight in a vacuum oven at 50°C.

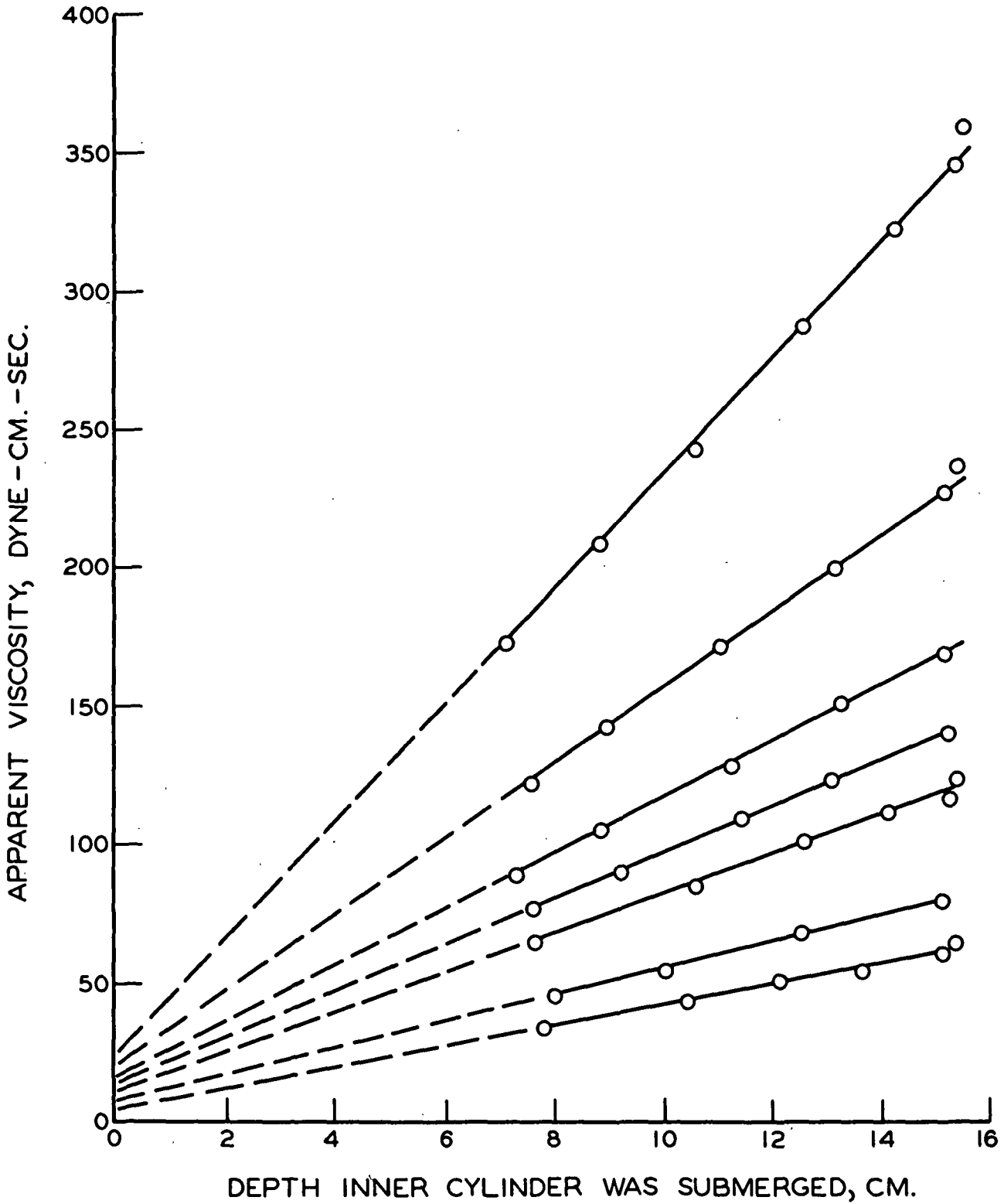


Figure 13. Determination of the Corrections for the Ends of the Inner Cylinder

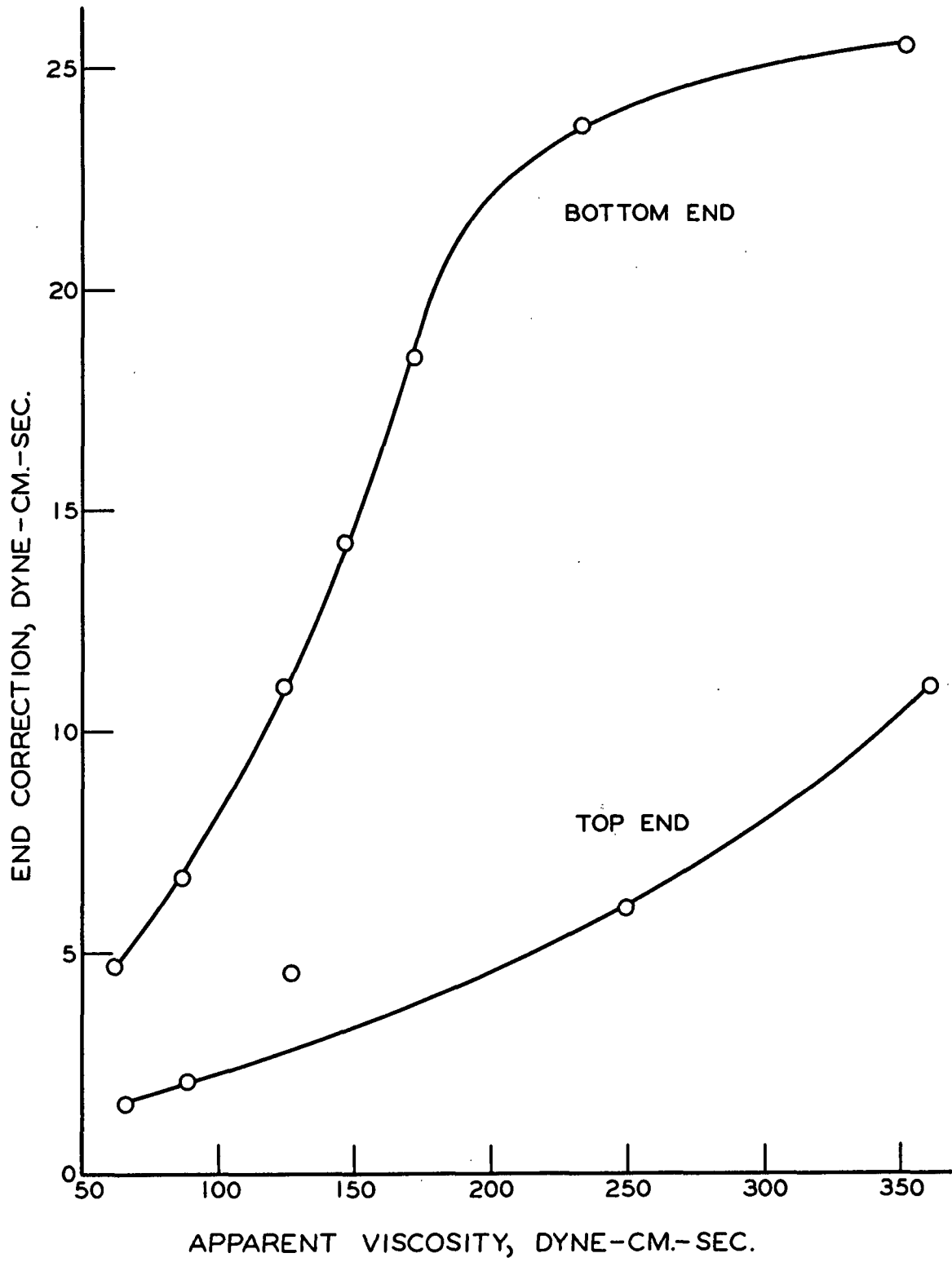


Figure 14. End Correction Curve

Preparation of Suspension

The quantity of fibers necessary to make the highest desired volume concentration to be studied was weighed and added to a TCE-PO solution. The suspension was stirred, deaerated for approximately 15 minutes and allowed to stand for two hours to determine whether or not the fibers would remain suspended. If the fibers floated or settled, either TCE (sp. gr. = 1.60) or PO (sp. gr. \approx 0.9) was added to adjust the solution density to that of the fibers.

The suspension was again deaerated, and transferred to the viscometer.

Determination of the Apparent Viscosity

Before each viscosity determination, the suspension was mechanically stirred while in the viscometer using a small teflon propeller connected to a stirrer by means of a long, thin spring.

The apparent viscosity was then determined in the manner outlined in the sections on Operation and Performance of the Viscometer.

Procedure for Changing Concentration

The concentration was changed by siphoning out of the viscometer annulus into a weighed bottle, a quantity of suspension which contained approximately the amount of fibers desired to be removed. The suspension remaining in the viscometer was then diluted to the original volume with pure solution, thus yielding the next lower concentration to be measured.

Determination of Volume Concentration

Since the solution and the fibers were of equal densities, the volume fraction was equal to the mass fraction and therefore the volume concentration could be determined by weighing the suspension and the fibers.

The weight of the fibers was determined after filtration from the suspension, washing with carbon tetrachloride, and drying at 50°C. in a vacuum oven overnight.

Determination of Changes in the Viscosity
of the Suspending Medium

Since a two-component solution was being used as the suspending medium, it was necessary to determine and correct for any changes in the viscosity of the suspending medium before relative viscosities were calculated.

Changes in the viscosity were determined by taking a sample of the filtrate from the concentration determinations and measuring the efflux time in a capillary viscometer. The densities of the suspending mediums were determined by weighing 25 ml. of solution in a specific gravity bottle.

The viscosities of the solutions were proportional to the efflux time times the density.

CALCULATION OF RELATIVE VISCOSITIES

The relative viscosities of the fiber suspensions were calculated in the following manner.

1. The apparent viscosities obtained for each concentration were corrected for the effect of the top end of the inner cylinder using the lower curve in Fig. 14.
2. The resulting apparent viscosities were corrected for the effect of the bottom end of the inner cylinder using the upper curve in Fig. 14.
3. The apparent viscosities corrected for end effects were then corrected for changes in the viscosity of the suspending medium by multiplying them by the

ratio of the density times the efflux time for the pure solution to the density times the efflux time for the suspending medium.

4. The corrected apparent viscosities for each concentration were then divided by the corrected apparent viscosity for the pure solution to obtain the relative viscosities.

An example of this procedure is given in Table V.

FIBER ORIENTATION DETERMINATIONS

In order to best evaluate Burgers' theory, it was necessary to determine the actual orientations of the fibers while under conditions of shear similar to those used in the viscosity measurements.

The orientation measurements were taken from photographs made of the suspensions under shear over the range of concentrations used in the viscosity studies.

The following is a description of the apparatus and techniques used in obtaining and analyzing these photographs.

APPARATUS

The design of the viscometer used in this study prevented photographing the suspensions under the actual conditions of flow used in the viscosity measurements. Therefore, it was necessary to find a similar apparatus on which a microscope and camera could be conveniently mounted. The concentric cylinder apparatus (40), designed at the Pulp and Paper Research Institute of Canada for the measurement of the flexibility of pulp fibers, fit the requirements very well. This apparatus produced conditions of flow which were essentially the same as that produced by Myers' viscometer except that the velocity gradient was slightly more linear due to the larger radii of the cylinders.

TABLE V
CALCULATION OF RELATIVE VISCOSITY

R ^a	AV ^a	TEC ^a	CTE ^a	BEC ^a	CT&B ^a	MVC ^a	CVC ^a	μ_r	$\underline{c} \times 10^2$
K	109.01	3.18	105.83	8.88	96.95	1.0000	96.95	1.0000	0.000
I	109.60	3.21	106.39	8.97	97.42	0.9971	97.13	1.0020	0.072
H	110.22	3.27	106.95	9.02	97.93	0.9953	97.47	1.0054	0.102
G	110.25	3.28	106.97	9.02	97.95	0.9958	97.54	1.0061	0.138
F	110.63	3.29	107.34	9.09	98.25	0.9951	97.77	1.0085	0.185
E	111.30	3.33	107.97	9.16	98.81	0.9953	98.35	1.0144	0.247
D	112.33	3.41	108.92	9.28	99.64	0.9981	99.45	1.0258	0.325
C	112.15	3.40	108.75	9.27	99.48	0.9976	99.24	1.0236	0.377
B	113.17	3.48	109.69	9.37	100.32	0.9973	100.05	1.0320	0.436
A	114.61	3.57	111.04	9.56	101.48	0.9994	101.42	1.0461	0.511

^aR = Run no.
 AV = Apparent viscosity
 TEC = Top end correction
 CTE = Corrected for top end effect
 BEC = Bottom end correction
 CT&B = Corrected for top and bottom ends
 MVC = Medium viscosity correction
 CVC = Corrected for medium viscosity change

The apparatus consists of two concentric cylinders of radii 10.14 and 12.70 cm. which rotate in opposite directions. The angular velocities of the cylinders could be independently varied. Due to the counterrotation of the cylinders, a plane of zero velocity existed in a suspension under shear between the two cylinders. A microscope could be mounted to the apparatus in such a way that the field of view could be moved vertically, radially, or through an arc of 120° concentric with the cylinders.

Since a detailed description of the apparatus itself is given in reference (40), only the camera and lighting arrangement will be discussed here.

Figure 15 is a diagram of this arrangement. The copper sulfate heat filter was placed between the light source and the lower cylinder to prevent convection in the annulus. The light was only used while focusing the microscope and exposing the film.

The angular velocities of the cylinders were adjusted to obtain a shear rate of 0.371 sec.^{-1} in the annulus. This shear rate was within the range covered by the viscosity measurements, and within the range of stable flow.

PHOTOGRAPHIC PROCEDURE

After each concentration change, the suspension in the annulus was thoroughly stirred and the cylinders were set into motion. Ten minutes were allowed for the system to come to equilibrium. Using the Microipso, the camera was focused 3 mm. below the surface of the suspension at the plane of zero velocity. This was approximately the maximum depth at which the microscope could be focused before the image became blurred. However, at this position, the particles at the surface of the suspension were out of focus.

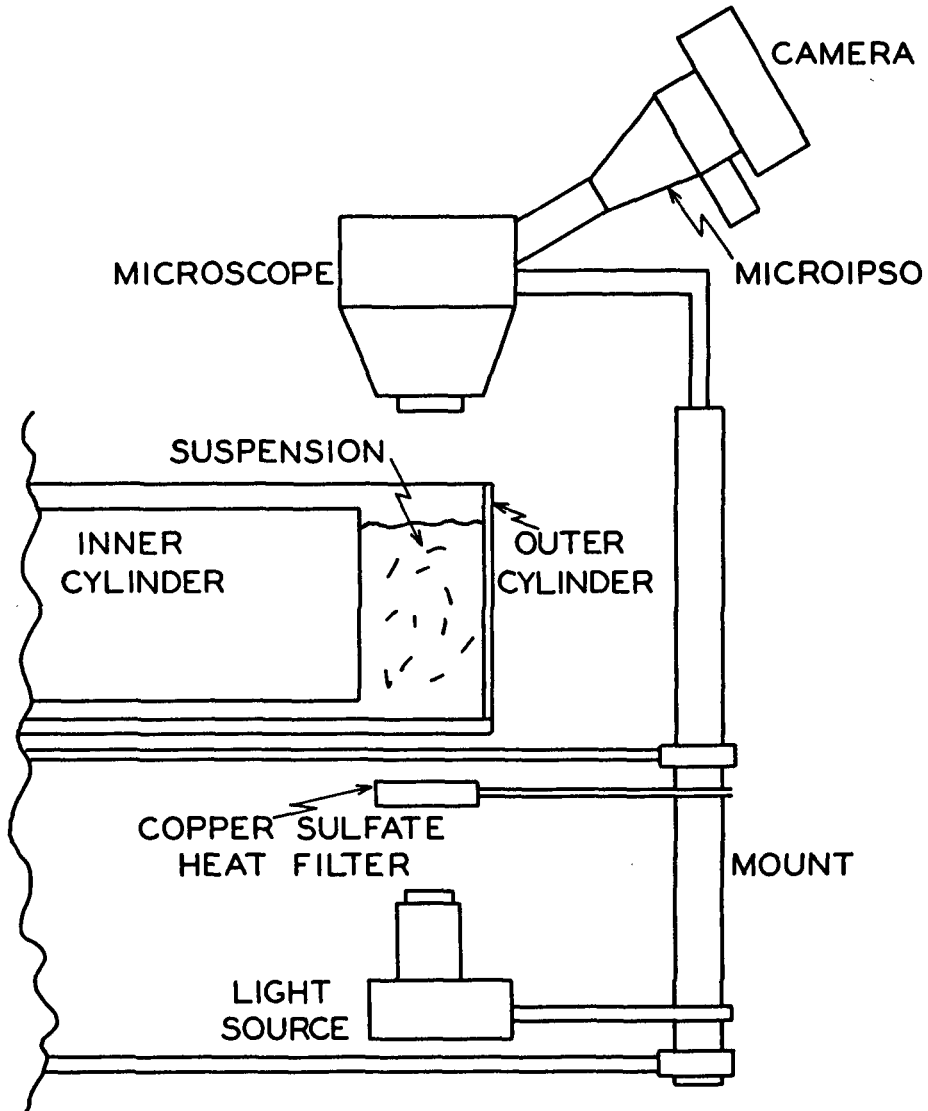


Figure 15. Camera and Lighting Arrangement

After the camera was focused, the room lights were turned off and four exposures were made. Shutter speeds, varying from 1/100 sec. at the lowest concentrations to 1/40 sec. at the highest concentrations, were used. This procedure was followed for each concentration.

The microscope, Microipso and camera resulted in a magnification of 6.67 times on the film. This was determined from photographs of a micrometer slide.

Positive prints, 3-1/8 by 4-1/2 in., were made from the negatives resulting in a total magnification of the fibers of 23.5 times.

ANALYSIS OF THE PHOTOGRAPHS

The purpose of making the photographs was to determine a value for the orientation factor $\frac{\sin^4 \theta \sin^2 2\phi}{\sin^4 \theta \sin^2 2\phi}$ in Burgers' theory which would represent the actual orientations of the fibers. Therefore, for each fiber, the angle ϕ (see Fig. 1) was measured to the nearest 5° using a protractor, and the projected length on the xy-plane (i.e., the length of the fiber in the photograph) was measured.

$\sin^4 \theta$ was determined by dividing the projected length of a fiber raised to the fourth power by the average of the true lengths of the fibers raised to the fourth power.

From the values for ϕ and $\sin^4 \theta$, $\frac{\sin^4 \theta \sin^2 2\phi}{\sin^4 \theta \sin^2 2\phi}$ was determined for each fiber. Fifty to 100 fibers were measured to determine $\frac{\sin^4 \theta \sin^2 2\phi}{\sin^4 \theta \sin^2 2\phi}$ at each concentration.

A more complete description of the analysis of the photographs is given in Appendix III.

RESULTS AND DISCUSSION

Throughout this study, nylon fibers of $L/d \approx 20$ were used. The data and discussions presented in the first five sections pertain to well-dispersed suspensions. A discussion of some data obtained using flocculated suspensions is given in the last section.

DISCUSSION OF THE TORQUE-ANGULAR VELOCITY RELATIONSHIP

Questions have often been raised as to the type of shear stress-shear rate, or torque-angular velocity relationship exhibited by suspensions of rigid rods. A brief discussion is given of this relationship, so that the reader will have a better understanding of the behavior of the suspensions discussed in later sections.

At the low concentrations used in this study, all of the data obtained using the well-dispersed suspensions indicated Newtonian behavior, i.e., the shear stress was directly proportional to the shear rate.

However, at volume concentrations of approximately 1/2 that necessary for the formation of a continuous fiber network, i.e., ~ 0.05 for fibers of $L/d = 37.5$ (32), Myers (16) found a torque-angular velocity relationship similar to the low shear rate behavior of Ostwald-Philippoff (OP) liquids (41).

Figure 16 gives an example of the behavior of an OP liquid.

Note that there is a first Newtonian regime followed by a non-Newtonian regime and a second Newtonian regime. The viscosity obtained from the first Newtonian regime is always greater than that obtained from the second Newtonian regime.

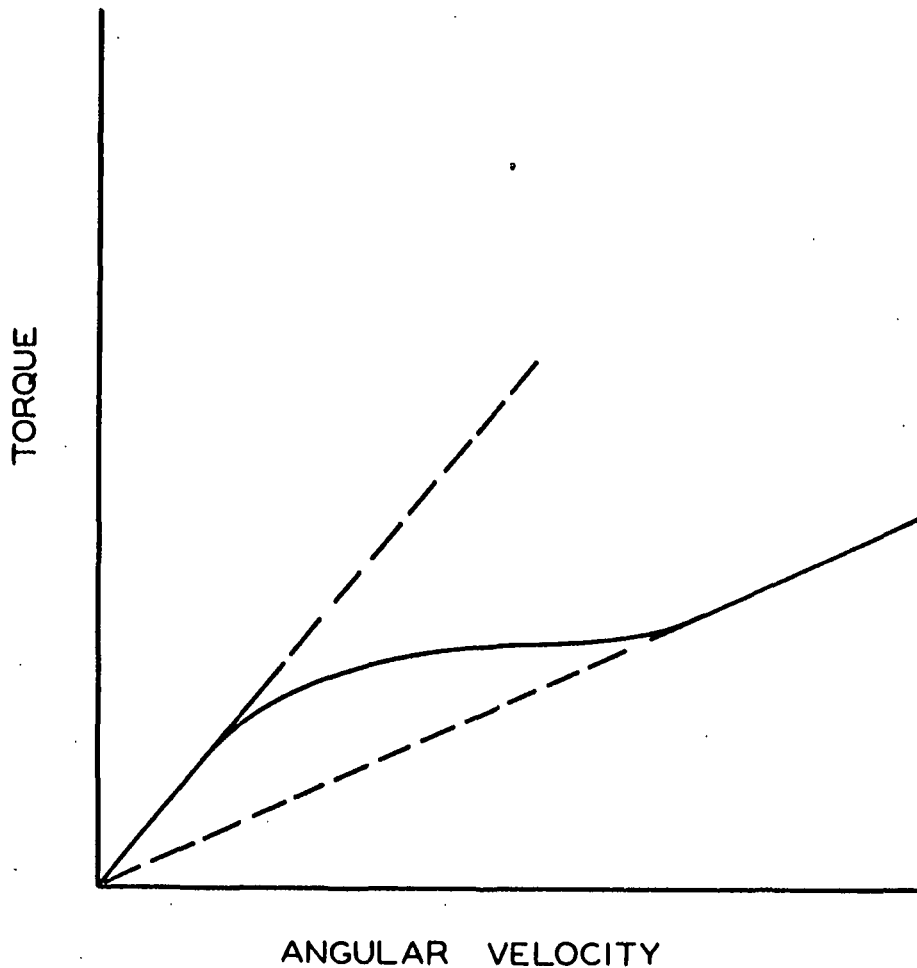


Figure 16. Behavior of an Ostwald-Philippoff Liquid

Merrill (41) has stated that suspensions of rigid rods or ellipsoids are of the OP type even at very low concentrations. It should be made clear that this is only true when the particles are so small that their orientations at low shear rates are governed by Brownian motion. In this case, the particles remain randomly oriented due to Brownian motion until the shear rate becomes large enough to overpower this effect. These two conditions would be found in the first Newtonian and second Newtonian regimes, respectively. The transition period would be in the non-Newtonian regime.

For suspensions of fibers large enough not to be affected by Brownian motion, it has been predicted theoretically by Jeffery (10) and confirmed experimentally by Trevelyan and Mason (22) that the period of rotation of the fibers times the velocity gradient is constant [see Equation (17)]. Thus, there would be no effect due to shear rate on the average orientation of the particles and Newtonian behavior would be obtained.

Unless otherwise noted, all of the viscosity data obtained or quoted in this study represent the behavior of suspensions of low enough concentration and large enough fibers so that the suspensions behaved in a Newtonian manner.

THE EFFECT OF CONCENTRATION ON THE ORIENTATIONS OF THE PARTICLES

From the results obtained by Mason and Manley (23) for the orientations of straight, rigid rods in a flowing suspension (see Analysis of the Problem), it was obvious that the actual orientations of the fibers in the suspensions studied had to be known before a logical comparison could be made between experimental results and Burgers' theory. It was also necessary to know whether or not the orientations of the fibers changed with the volume concentration so that a meaningful presentation of the experimental data could be made.

Therefore, the orientation factor, $\frac{\sin^4 \theta}{\sin^2 2\theta}$, of Equation (2) was determined by the method described in the Experimental Procedures at several volume concentrations over the range up to 0.007. The results of these determinations are presented in Table VI.

Note that the concentration range covered by these measurements included concentrations on either side of the previously discussed "critical concentration" of 0.0037 for these fibers. From examination of Table VI, it seems that

the data may be divided into two ranges. Below a concentration of 0.0042, which is close to the "critical concentration," the orientation factor remained essentially constant except for the value at $\underline{c} = 0.00212$. Also note that the values of the orientation factor in this concentration range were in good agreement with that found independently by Mason and Manley using different techniques for the measurements. However, in the higher concentration range above the "critical concentration," there were sharp changes in the orientation factor.

TABLE VI

VALUES OF THE ORIENTATION FACTOR AS A
FUNCTION OF CONCENTRATION

$$\underline{d} = 43.1 \text{ microns}, \lambda / \underline{d} = 20.3$$

Volume Concentration $\times 10^2$	$\frac{\sin^4 \theta \sin^2 2\theta}{\sin^4 \theta \sin^2 2\theta}$
0.0026 ^a	0.0510 ^a
0.106	0.0555
0.212	0.0687
0.318	0.0527
0.424	0.0535
0.504	0.0881
0.557	0.0665
0.663	0.0575

^aFrom the data of Mason and Manley (23).

Below the "critical concentration," the fiber centers are at least one fiber length apart. Therefore, it would not be expected that there should be sharp changes in the orientation factor such as that at $\underline{c} = 0.00212$. In support of this reasoning, consider the results of Trevelyan (42), and Mason and Manley (23).

Trevelyan found from observations of suspensions of straight glass fibers in a linear velocity gradient that there was no appreciable mechanical interaction between fibers until the concentration was in the range of the "critical concentration." In a study of the variation of $\lambda = f(K)$ (see Fig. 1), Mason and Manley showed that in the concentration range where mechanical interactions are not appreciable, hydrodynamic interactions sometimes increased and sometimes decreased λ and K . Thus, from the results given in Table VI, the changes in λ and K must compensate, causing the orientation factor to remain essentially constant.

Since, from the above discussion, sharp changes in the orientation factor below the "critical concentration" would not be expected, the data were tested to see if there was a real difference between the value obtained at $c = 0.00212$ and the remaining points at and below $c = 0.00424$. Using the t-test to determine the significance of the difference between means of each sample, it was found that the difference was not statistically significant. The 95% confidence level was used as the criterion for significance.

From the reasons discussed above, it was concluded that the orientation factor remains constant below the "critical concentration." Therefore, the arithmetic average of the first five values of the orientation factor in Table VI, i.e., 0.0563, will be used in subsequent discussions of the viscosity behavior in the concentration range below 0.0042.

On the other hand, at concentrations well above the "critical concentration," the fiber orbits overlap considerably. This would lead to increasing mechanical interactions between the fibers which might cause significant changes in the orientations of the particles. A statistical comparison of the value of the orientation factor obtained at $c = 0.00504$ showed that there was a significant difference between this value and the remaining values. In this range, the

viscosity data must be examined together with the variations in the orientation factor.

Before an explanation is given of the sudden rise in the orientation factor between concentrations of 0.0042 and 0.0050, consider the orbit of a freely rotating rod for different values of the orbit constant.

In a suspension where mechanical interaction is not appreciable, the orbit constants of fibers will be distributed between zero and infinity. However, using fibers of $L/d \approx 20$, Mason and Manley (23) found that approximately 60% of the fibers will have orbit constants below 0.4.

Table VII gives an example of how the relationship between ϕ and θ changes with the orbit constant, K , for fibers of $L/d = 20.3$.

TABLE VII

AN EXAMPLE OF THE CHANGES IN θ WITH ϕ FOR SEVERAL VALUES OF THE ORBIT CONSTANT

K	ϕ_1	θ_1	ϕ_2	θ_2
∞	0	90.0	90	90.0
10	0	89.6	90	84.3
1	0	86.1	90	45.0
0.5	0	82.2	90	26.6
0	0	0	90	0

The values of θ and ϕ were determined from Equation (9) after substituting $[1/(L/d)_e]^2$ for $(b/a)^2$. $(L/d)_e$ as determined from Equation (18) was 14.8.

As can be seen, for large values of K , θ changes very little as ϕ moves through 90° . However, for relatively small values of K , there is quite a large change in θ with ϕ .

Consider this behavior in terms of the orientation factor $\sin^4 \theta \sin^2 2\phi$. For fibers with relatively small orbit constants, large values of $\sin^4 \theta$ will fall at small values of $\sin^2 2\phi$ and vice versa. On the other hand, for large values of the orbit constant, large values of $\sin^4 \theta$ will fall at large values of $\sin^2 2\phi$.

In measuring the angles ϕ and θ from the photographs, it was found that at concentrations of 0 to 0.00424, small values of $\sin^4 \theta$ fell at large values of $\sin^2 2\phi$ indicating small values of the orbit constant, in agreement with the results of Mason and Manley (23). However, at a volume concentration of 0.00504 which is well above the "critical concentration," large values of $\sin^4 \theta$ fell at large values of $\sin^2 2\phi$ thus indicating a general shift of the fibers toward orientation in the xy-plane, or toward higher values of the orbit constant. Therefore, the fact that the orientation factor at a concentration of 0.00504 was higher than at lower concentrations was probably due to a shift in the orbits of the particles.

This same general behavior was also found by Arlov, et al. (43) using a suspension of pulp fibers of concentration, relative to the "critical concentration," approximately equal to that used in this study.

It seems that since hydrodynamic interactions between the fibers at low concentrations had no significant effect on the orientation factor, the shift in the orbits of the fibers between concentrations of 0.0042 and 0.0050 probably was due to a rapid increase in mechanical interactions. As the concentration of the fibers increased above 0.004, the formation of groups of two or three fibers increased rapidly. These groups generally formed when one fiber in the process of rotating through values of ϕ of 30-50° collided with another fiber which was essentially aligned in the direction of flow. These two fibers would then rotate

together for a short while, usually less than one-half rotation, and separate. It was not uncommon for a third fiber to be trapped in such a group at high concentrations. One would not expect these groups to rotate in any regular manner as do individual fibers and, therefore, the effect of such mechanical interactions on the orientation factor cannot be predicted a priori. However, the measured values of ϕ and θ indicated a gradual decrease in the orientation factor as the concentration increases beyond 0.005.

Although the measurements indicated the changes in the orientation factor discussed above, the author has been unable to determine the basic causes of this behavior.

However, with this background of the general behavior of the fibers with concentration changes, a more logical discussion of the effect of concentration on the relative viscosity can be made.

THE RELATIVE VISCOSITY-CONCENTRATION RELATIONSHIP

Two sets of fibers were used in this portion of the study. These sets were composed of straight, nylon fibers, 16.9 and 43.1 μ in diameter with L/d ratios of 19.2 and 20.3, respectively.

Viscosity measurements were made over a concentration range from 0 to 0.009 which included concentrations well above and well below the "critical concentration" of approximately 0.004 for these fibers.

The results of the viscosity measurements are given in Fig. 17.

Note that the total change in the relative viscosity over the concentration range covered was only approximately 5%. Thus, although the scatter in the data seems relatively large, actually it is quite small.

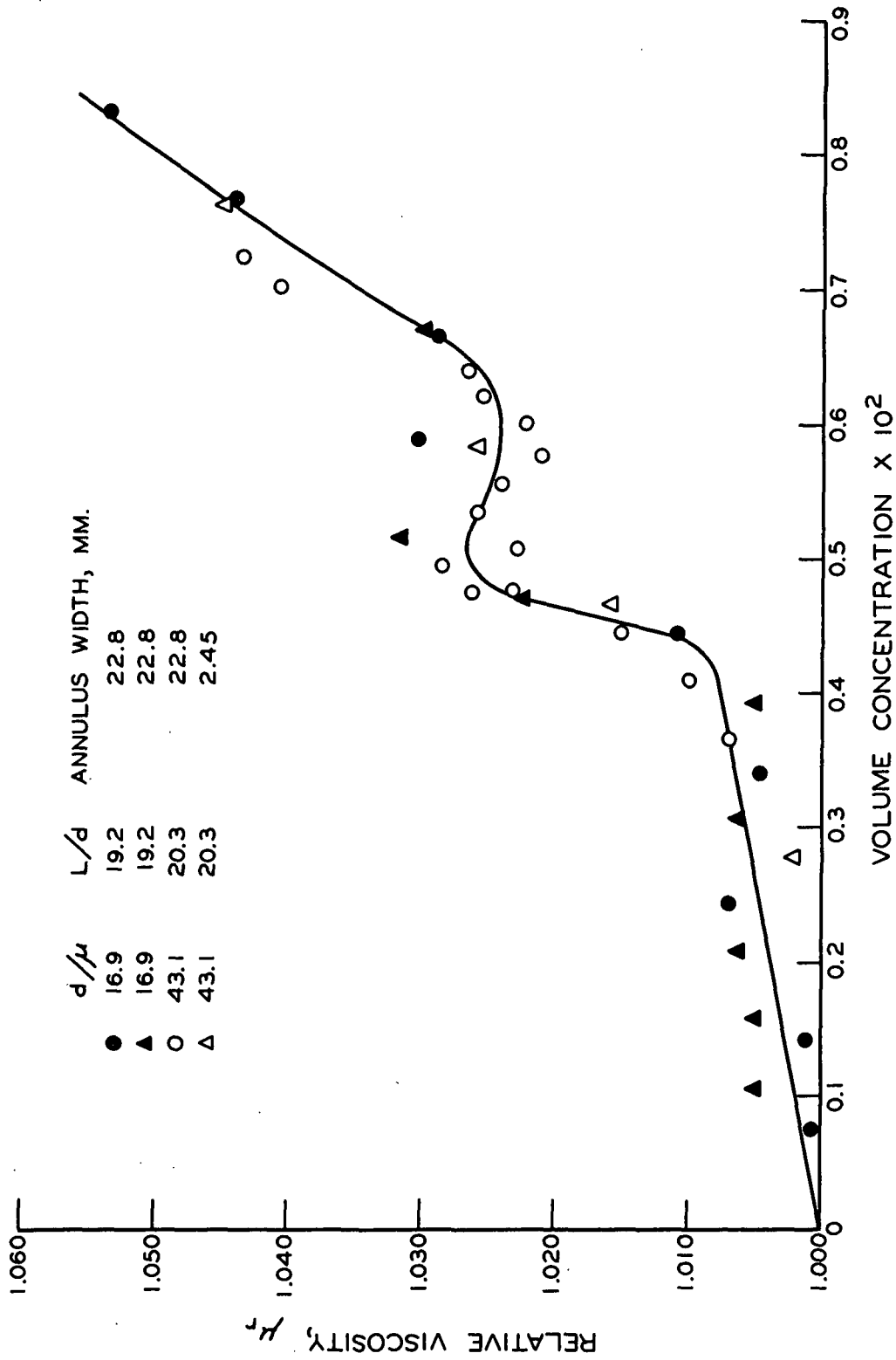


Figure 17. The Effect of Concentration on the Relative Viscosity

The viscosity-concentration relationship presented in Fig. 17 represents two new and significant findings.

First, there is a low slope at low concentrations which is much smaller than has been found previously.

Second, there is an abrupt increase in the viscosity in the concentration range from 0.0042 to 0.0050 followed by a slight decrease and a second increase.

A discussion of the viscosity-concentration relationship between concentrations of 0 and 0.0042 will be given first, followed by a discussion of the viscosity behavior at high concentrations.

DISCUSSION OF THE RELATIVE VISCOSITY-CONCENTRATION RELATIONSHIP AT LOW CONCENTRATIONS

One of the primary objectives of this study was to determine the effect of concentration on the relative viscosity at concentrations where fiber-fiber interactions are negligible.

From the behavior of the orientation factor (Table VI) and the relative viscosity (Fig. 17) over the concentration range from 0 to 0.0042, it seems that this has been accomplished.

The initial slope of the viscosity-concentration relationship in Fig. 17 which represents the intrinsic viscosity, α_0 , of the suspensions was found by least squares analysis to be 1.98. This value of α_0 is approximately 1/3 as large as the lowest α_0 value previously found (16) for suspensions of fibers of this L/d ratio.

The value for α_0 is also lower than predicted by Burgers' theory assuming random orientation of the fibers. This was expected since Equation (12),

corrected using Mason's β factor, predicts a value for $\overline{\sin^4 \theta \sin^2 2\theta}$ of 0.088 as compared to that of 0.0563 found from measured fiber orientations.

To compare the experimentally determined α_0 with Burgers' theory in the form obtained before attempts were made to predict $\overline{\sin^4 \theta \sin^2 2\theta}$, the experimentally determined value for the orientation factor (0.0563) was substituted into Equation (2) and α_0 was calculated. The α_0 value obtained was 1.95 as compared to 1.98 found experimentally. As can be seen, the agreement was very good. Using the value of 0.0510 for the orientation factor as found by Mason and Manley, Equation (2) gives a value of 1.78 for α_0 .

Therefore, it can be concluded that if the orientations of the fibers are known, Burgers' theory can be used to predict the viscosity of a well-dispersed suspension of straight, rigid rods within approximately 10% if the conditions assumed in the theory are met.

It can also be concluded that below a volume concentration of 0.004 for fibers with an L/d ratio ≈ 20 , fiber-fiber interactions do not contribute significantly to the viscosity of the suspension.

It is now possible to modify Burgers' theory to predict the intrinsic viscosity of suspensions of straight, rigid rods taking into account actual orientations of the fibers. This can be done, using the results of Mason, et al. (22-24), as follows:

From Equation (12) of Burgers' theory,

$$\overline{\sin^4 \theta \sin^2 2\theta} = 4d/L\pi \quad (28)$$

for random orientations of the fibers. Trevelyan and Mason (22) showed that L/d for an ellipsoid is equal to $1/(\underline{L/d})_e$ for a cylinder where $(\underline{L/d})_e$ is given by

Equation (18). Therefore, Equation (28) becomes:

$$\overline{\sin^4 \theta \sin^2 2\phi} = 4/[\pi(L/d)_e] \quad (29).$$

Now, from the results of Mason and Manley given in Table III,

$$\frac{\mu'_{sp}}{\mu_{sp}} = \frac{\overline{(\sin^4 \theta \sin^2 2\phi)_{actual}}}{\overline{(\sin^4 \theta \sin^2 2\phi)_{random}}} = 0.533 \quad (30).$$

Therefore,

$$\overline{(\sin^4 \theta \sin^2 2\phi)_{actual}} = (0.533)(4)/[\pi(L/d)_e] \quad (31).$$

By combining Equations (2), (18), and (31), the following expression is obtained for α_o :

$$\alpha_o = \left[\frac{(2)(0.533)(L/d)^2}{3\pi(\ln 2L/d - 1.80)} \right] \left[\frac{1}{3.72 + 0.547(L/d)} \right] \quad (32)$$

for $15 < \underline{L/d} < 140$ and $\underline{c} < \underline{c}_o = 1.5/(\underline{L/d})^2$.

This concentration limit is used since the "critical concentration" seems to agree very closely with the concentration at which fiber-fiber interactions become appreciable.

DISCUSSION OF THE RELATIVE VISCOSITY-CONCENTRATION RELATIONSHIP AT HIGH CONCENTRATIONS

Examination of Table VI and Fig. 17 reveals that the sudden increase followed by the slight dip in the relative viscosity came over the same concentration range as did the increase and decrease in the orientation factor. It is obvious, therefore, that changes in the orientations of the fibers were at least partially responsible for the changes in the relative viscosity. However, a comparison of the relative viscosities calculated using values of the orientation factor given

in Table VI with the experimentally determined relative viscosities shows that the change in the orientation factor is not nearly large enough to account for all of the change in the relative viscosity. This comparison is given in Fig. 18.

In order to obtain a better method of representing the experimental data, it will be beneficial to consider methods used in the past to explain the viscosity behavior of suspensions at relatively high concentration.

It has been found that, in general, experimental viscosity-concentration relationships for suspensions can be represented by equations of the form:

$$\mu_r = 1 + k_1 c + k_2 c^2 \quad (33).$$

Values for k_1 have been theoretically predicted for spheres (9), ellipsoids (10), and cylinders (6). The term $k_1 c$, as derived by Burgers, takes into account increases in the viscosity due to increases in the average shear rate caused by the suspended particles.

The term $k_2 c^2$ has been added to include the effect of particle interactions which can be either hydrodynamic or mechanical interactions, or both.

Both types of interaction would lead to additional disturbances of the suspending fluid and therefore to an increase in the dissipated energy which would be reflected by an increase in viscosity.

Frisch and Simha (44) state that the interaction term can also be written $k_3 (k_1 c)^2$. Simha (45) found from theoretical considerations that $k_3 = 0.73$ for purely hydrodynamic interactions between randomly oriented, rigid rods. For the system under consideration here, this would be $0.73(\alpha_0 c)^2$, which is negligible at the low concentrations used in this work. Thus, if Simha's prediction

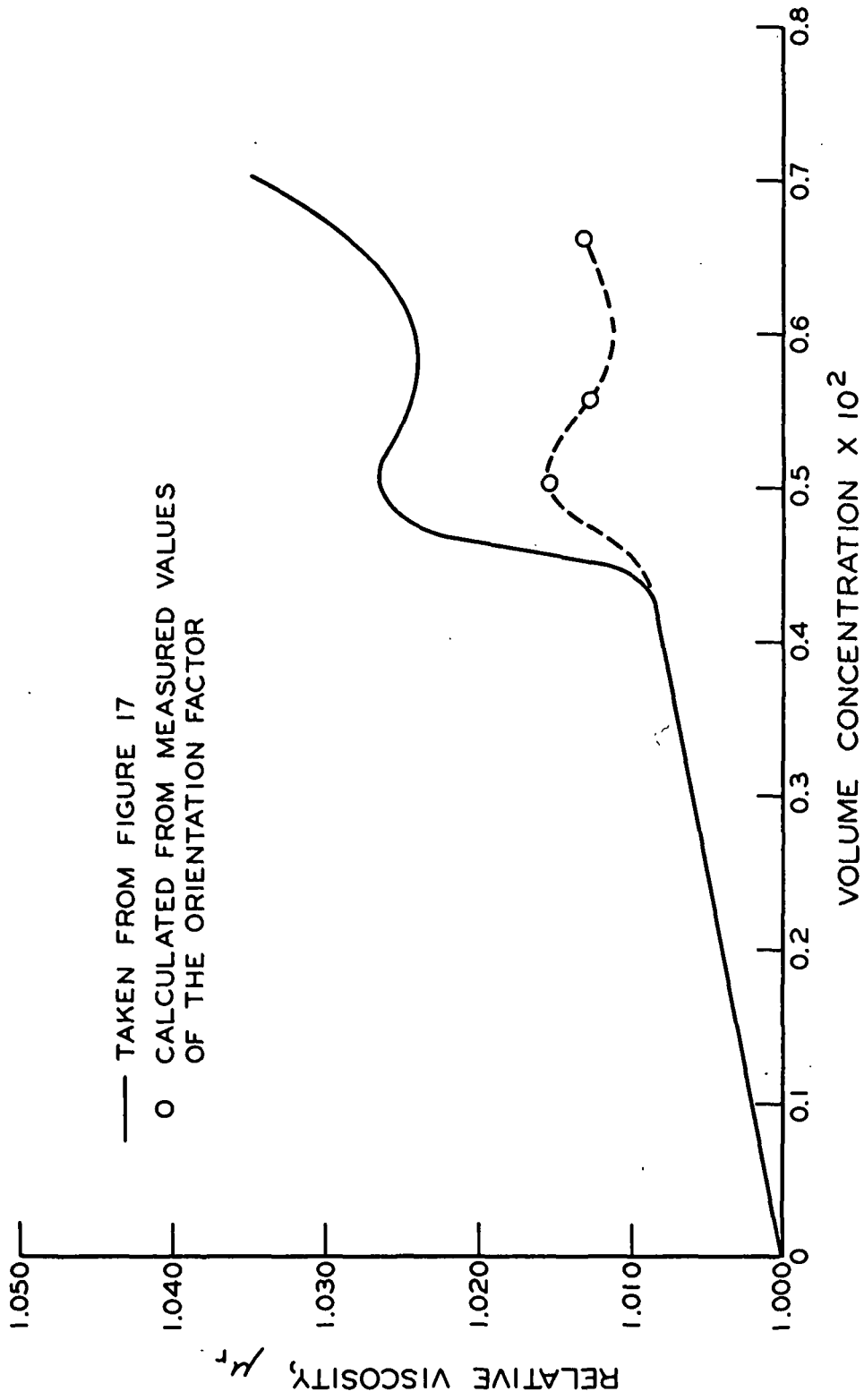


Figure 18. Comparison of Experimental and Calculated Relative Viscosities

of the effect of hydrodynamic interactions is correct, even to an order of magnitude, the results obtained in this study must have been due to some other effect. The most likely other effect is mechanical interactions. No theory has been proposed for rigid rods to account for this effect.

Since Burgers' theory was only intended to apply over a concentration range where fiber-fiber interactions can be neglected, a more general equation for larger ranges of concentration formed by addition of a second term to Equation (1) would not be appropriate. A better way to achieve the same purpose would be to write an equation intended to apply only over certain designated concentration ranges.

Equations (34) and (35) are relationships of this type.

$$\mu_r = 1 + \alpha_0 c + k''(c/c_0)^2 \quad (34)$$

$$\mu_r = 1 + \alpha_0 c + k'(\alpha_0 c)^2 \quad (35)$$

where, in each case, the second term is considered only when $c > c_0$.

Equation (34) ignores completely any effect which the orientations of the fibers would have on interaction. In Equation (35), it is assumed that the interaction term is of the same form as that applying to freely rotating fibers. It is probable that neither of these assumptions is exactly correct. However, since no better predictions of the effect of particle orientations on interaction have been made, attempts were made to correlate the data using these relationships.

The intrinsic viscosity, α_0 , was determined from Equation (2) using measured values of the orientation factor, and values of k'' and k' were determined by trial and error to give the best fit of the experimental data. A comparison

of the relative viscosities given by Equations (34) and (35) with those obtained experimentally is presented in Fig. 19.

As can be seen, Equation (34) seems to give the better fit over the whole range, whereas Equation (35) fits better in the region of the "bump" and dip. Therefore, it seems that the orientations of the fibers should be taken into account in the interaction term to predict the changes in the relative viscosity with concentration.

THE EFFECT OF THE WALL ON THE RELATIVE VISCOSITY

Before the experimental results obtained in this study are presented, a review of what these effects might be and how they might come about is in order.

Nawab and Mason (15) have suggested three ways in which the walls might affect the flow of suspensions. These are as follows:

1. When a suspension of spherical or nonspherical particles is sheared, "pseudo-slip" is predicted to occur as the result of hydrodynamic interaction between the particles and the wall. This effect is equivalent to interposing a particle-free liquid layer between the suspension and the wall.

2. Due to particle geometry, there is a minimum distance of approach of a particle center to the wall. For a rod, this distance depends on d , L/d and the orbit of the particle.

3. Phase separation, i.e., "plug flow," has been observed in suspensions of pulp fibers.

Vand (18) has calculated this first effect for spheres. In regard to this effect, Vand states that "in the region of high concentrations, considerable slip at the wall might develop" in both Couette and Poiseuille flow "due to the layers of low viscosity along the walls which might finally overshadow the effects

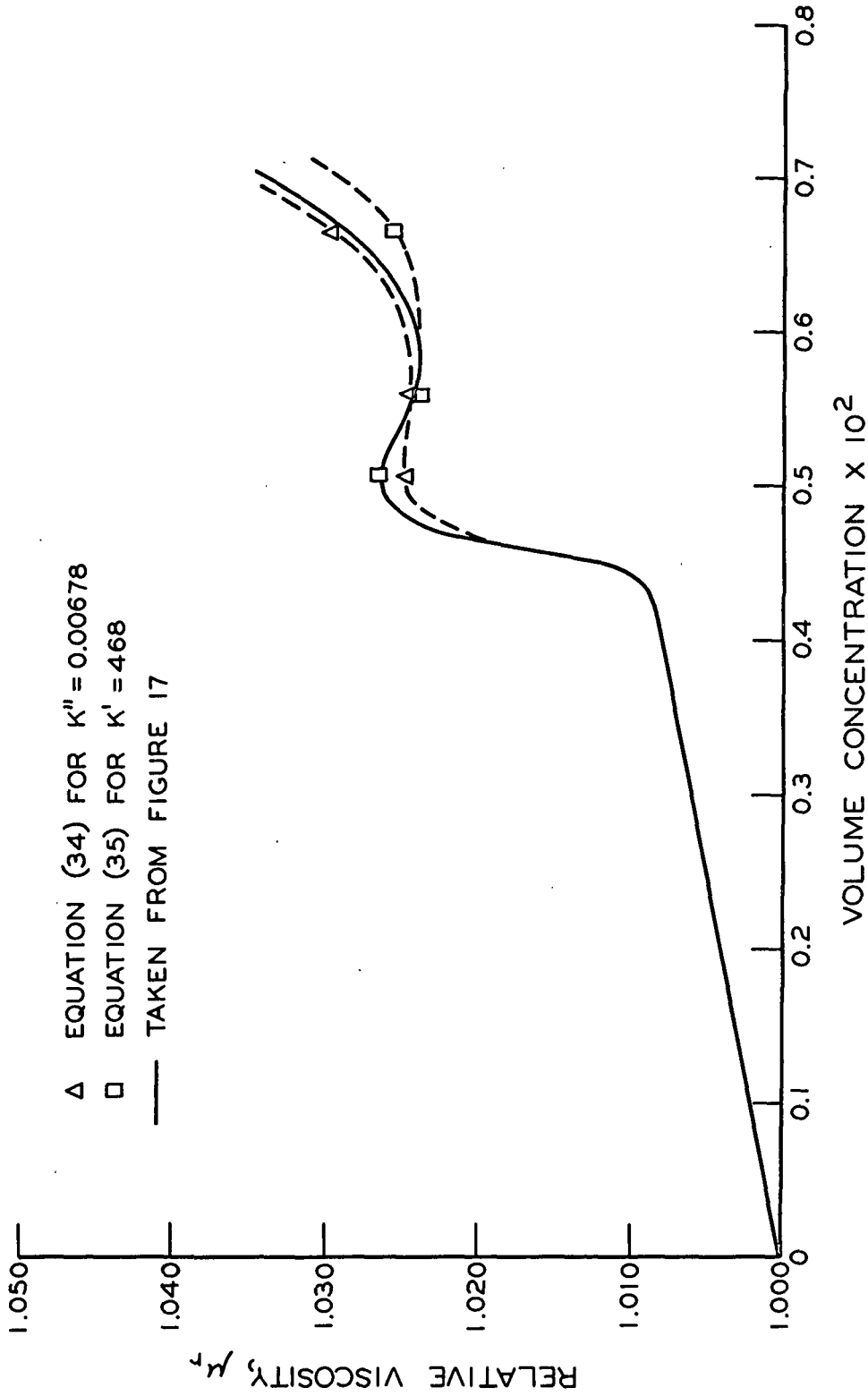


Figure 19. Comparison of Relative Viscosities Obtained Experimentally with Those Given By Equations (34) and (35)

of shear inside the suspension, making the measurements useless. It should be noted that this slip is quite distinct from the phenomenon of 'plug flow'----as it develops even in the region of concentrations where the suspensions behave in bulk as a true Newtonian liquid."

If pseudo-slip does occur as predicted by Vand, the measured apparent viscosities would be lower than would be obtained for a uniform suspension in contrast with the results of Myers, (16).

Mason (46) found that Vand's correction is necessary if viscosity measurements of suspensions of spheres are made in a capillary viscometer when the particle size is an appreciable fraction of the dimensions of the viscometer.

However, Sweeny and Geckler (47), and Eveson, et al. (48) did not find this effect when viscosity studies of suspensions of spheres were made in concentric cylinder viscometers. Eveson varied the annulus width-to-particle diameter ratio from 110:1 to 5:1 and found no evidence of wall "slip" or any other wall effect.

Goldsmith and Mason (49), in a study of the flow of suspensions of rigid rods [mean $(L/d)_e = 20.8$] through tubes, investigated the second effect listed above. They compared the period of rotation of rods whose centers were within a distance $L/2$ of the wall with the time the rods spent between $\phi = -4^\circ$ and $+4^\circ$. It was found that interaction with the wall was confined to these low values of ϕ where the particles spent 90% of their time. Measurements showed that when the rods were aligned at right angles to the flow, no contact with the wall occurred. As in Couette flow, it was found that the particles do not migrate away from the wall but hold their positions indefinitely. This is in agreement with the theoretical findings of Jeffery (10) that there would be no force normal

to the wall on a particle to cause it to move away from the wall. Therefore, there should be no time effect affecting the wall effects.

No wall effect of the third type, i.e., "plug flow," suggested by Nawab and Mason was found in the studies quoted or in this study.

A fourth type of wall effect which was not mentioned by Nawab and Mason is that due to purely hydrodynamic interactions between the particles and the wall. This effect has been predicted by Brenner (8) for a particle translating or rotating near a boundary. However, Brenner's theory was derived for the case of a particle moving with respect to the fluid and the wall. In the case of the motion of rigid cylinders in a linear velocity gradient, this criterion is met only for that component of the motion of the fluid directed along the axis of a cylinder as it rotates.

Brenner showed that the drag on a particle in finite boundaries as compared to that in an infinite medium could be expressed by Equation (36).

$$F/F_{\infty} = 1/[1 - K'(F_{\infty}/6\pi\mu UH)] \quad (36)$$

where

\underline{F} = actual drag on a particle

\underline{F}_{∞} = drag on a particle in an infinite medium

\underline{U} = velocity of the particle

\underline{H} = distance of the particle from the wall

K' = an experimentally determined constant

The constant, \underline{K}' , has been found to be of the order of magnitude of one to two for spheres in translation relative to various boundaries.

The effect of the wall on the rotation of a particle has been shown by Brenner to be:

$$L/L_{\infty} = 1/[1 - K''(L_{\infty}/8\pi\mu\Omega H^3)] \quad (37)$$

where

\underline{L} and \underline{L}_{∞} = the couple exerted on a particle in a bounded and unbounded medium, respectively

Ω = angular velocity of the particle

\underline{K}'' = an experimentally determined constant found to be one or less than one for spheres

Thus, the effect of the wall on rotation will be much less than the effect on translation.

Equations (36) and (37) can be used for any particle to determine \underline{F} or \underline{L} if \underline{F}_{∞} or \underline{L}_{∞} are known.

As was stated previously, the first part of this work was done using an annulus width of 22.8 mm. which resulted in maximum $\underline{d}/\underline{D}$ and $\underline{L}/\underline{D}$ values of 0.00189 and 0.0385. These values were in the range of $\underline{d}/\underline{D}$ and $\underline{L}/\underline{D}$ where Nawab and Mason found no wall effect. In order to determine the magnitude of the wall effects discussed above, the annulus width was decreased from 22.8 mm. to 2.45 mm. and viscosity measurements were made on suspensions of the 43.1 μ diameter fibers of $\underline{L}/\underline{d} = 20.3$. These fibers and this annulus width resulted in $\underline{L}/\underline{D}$ and $\underline{d}/\underline{D}$ values of 0.358 and 0.0176. The results of these measurements are represented by the triangles in Fig. 17. As can be seen, there was no detectable wall effect of any kind.

The following thoughts are presented as possible explanations for the absence of wall effects.

It was felt that the strength of the doublets formed due to the rotation of the fibers in a suspension might be affected to approximately the same degree as the drag force on a cylinder in translation between two walls.

Therefore, $\underline{F}/\underline{F}_\infty$ was calculated using Equation (36) for a fiber of the size used in this wall effect study. It was assumed that the fiber was translating perpendicular to its axis between two walls a distance \underline{H} apart. The value of \underline{H} was picked so that $\underline{L}/\underline{H} = \underline{L}/\underline{D} = 0.358$.

Equation (38) was used for \underline{F}_∞

$$F_\infty = \left(\frac{4}{3}\right) \frac{4 \pi \mu U}{\ln 2L/d + 0.5} \quad (38)$$

This equation was derived by Burgers (6) and corrected by Han (27). Han showed that the factor $4/3$ was necessary for agreement with experimental results.

$\underline{F}/\underline{F}_\infty$ was found to be 1.06. Thus, the effect of the wall resulted in an increased drag of only 6%.

If the strength of the doublet formed due to the rotation of the fibers is increased by this amount, there should be an increase in the relative viscosity at the highest concentration used in this study of only 0.3%. At lower concentrations, the effect would be even less. Therefore, if this estimation of the effect of hydrodynamic interaction between the fibers and the wall on the viscosity is correct even to an order of magnitude, it is likely that the effect would not have been detected.

Another possible explanation for the absence of wall effects can be obtained from the work of Goldsmith and Mason (49). Since it has been shown that interaction with the wall is confined to the part of the orbit between $\theta = -4^\circ$ to $+4^\circ$

where the disturbance to flow is at a minimum, even a large effect on rotation would have a very small effect on viscosity.

A third possible reason for the absence of wall effects is as follows.

Nelson (50) suggested that it is possible that the flow field produced by any one fiber is sufficiently masked by the flow fields of the other fibers that it is never "felt" by the wall.

Consider now the significance of the absence of wall effect in this study. In Myers' study (16), the most extreme cases of $\underline{L/D}$ and $\underline{d/D}$ were 0.268 and 0.00333 as compared to the most extreme case in this study of $\underline{L/D} = 0.358$ and $\underline{d/D} = 0.0176$. Thus, Myers' values of $\underline{L/D}$ and $\underline{d/D}$ fell into the range covered by this study where it has been shown that wall effects are negligible. It can be concluded, therefore, that wall effects were probably not important in Myers' study. If wall effects were not responsible for the increase in α_0 with \underline{d} at constant $\underline{L/d}$ (see Fig. 4) as found by Myers, then there must have been some other reason.

As was shown in the Analysis of the Problem, Nawab and Mason's, and Myers' work differed primarily in the amount of fiber-fiber interaction, the possibility of wall effects, and the degree of fiber curvature.

The effect of fiber-fiber interaction was probably one of the reasons why the work of Nawab and Mason, and Myers did not agree with theory. However, it does not explain why viscosity measurements made by Myers on suspensions of fibers with the same $\underline{L/d}$ ratio did not agree.

The absence of wall effects only eliminates one of the possible explanations of this behavior.

The effect of fiber curvature on viscosity is the only one of the three variables mentioned earlier which has not been considered.

THE EFFECT OF FIBER CURVATURE ON THE RELATIVE
VISCOSITY OF A FIBER SUSPENSION

As was stated previously, Forgacs and Mason (17) showed that a slight curvature of the fibers had a tremendous effect on the period of rotation of the fibers. They suggested that, due to the change in the rotational behavior, there would also be a significant effect on the contribution to viscosity. However, the magnitude of this effect in the absence of other effects such as fiber flexibility was not demonstrated.

In all cases where either photographs were available or the actual samples used could be obtained, it was found that the fibers used by Myers (16) in his viscosity studies were curved except for those 16.79μ in diameter with an L/d of 23.1 and the glass fibers. The most probable reason for this is that all of the fibers used by Myers, except those mentioned below, were cut by the parallel razor blade technique which has been found in this study to permanently deform nylon fibers. The 16.79μ diameter, $L/d = 23.1$ fibers were microtomed from wax, as was done to obtain the straight fibers used in this study.

In order to determine the magnitude of the effect of fiber curvature on viscosity, two viscosity-concentration studies were made using curved fibers. Again, Newtonian behavior was found.

The results of the viscosity measurements made using these curved fibers as compared to the results obtained with straight fibers are given in Fig. 20. The curvature of these fibers, as defined by the angle γ (see Fig. 3) was 176° . As can be seen, the effect of this slight curvature is quite large. If these

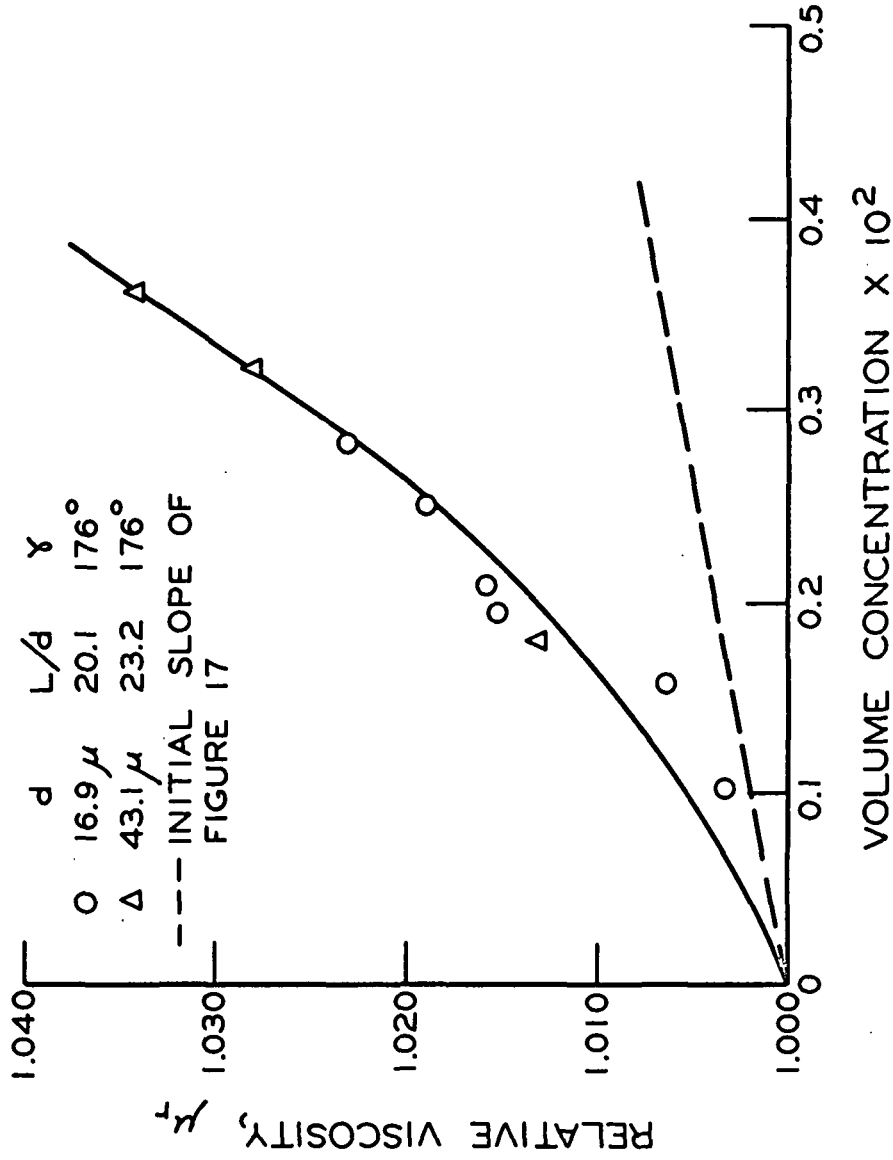


Figure 20. The Effect of Fiber Curvature on Viscosity

data are fitted to Equation (39) below, an α_0 value of 3.57 is obtained as compared to an α_0 of 1.98 obtained using straight fibers of comparable L/d .

$$\mu_r = 1 + \alpha_0 c + \alpha_1 c^2 \quad (39).$$

The most probable reasons for the effect of fiber curvature on viscosity are given below.

Consider the simplified system of a fiber rotating in the xy -plane of a linear velocity gradient (Fig. 21).

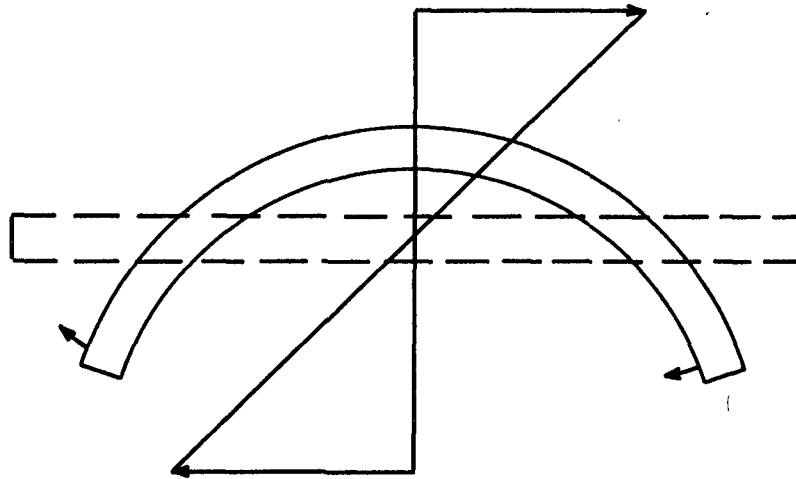


Figure 21. Curved Fiber in a Linear Velocity Gradient

As the fiber becomes curved, there will be a greater difference in the velocity of the fluid flowing past the two sides of the fiber than there would be for a straight fiber. This will result in more drag on the fiber, tending to make it rotate, and therefore the fiber will remain in the direction of flow for a shorter time. Since the fiber is also shortened due to the curvature, by the same reasoning, it will spend a longer time oriented perpendicular to the direction of flow. Thus, the result will be a shift from a preferred orientation

in the direction of flow toward a more random orientation with increasing fiber curvature.

This reasoning agrees with the qualitative observation by Myers (16) when a viscosity study was done using fibers with extreme curvature. Myers stated that the fibers seemed to have no preferred orientation.

It should be pointed out here that Equation (15) does not predict a maximum value for α_0 . Equation (15), taking into account Nawab and Mason's β factor, predicts the maximum value for α_0 which can be obtained using straight, rigid fibers in a suspension dilute enough so that the fibers follow the motion of the fluid. In the case of straight fibers, the fluid will cause the fibers to have a preferred orientation in the direction of flow. If there exists a situation, such as fiber curvature, which would cause the fibers to approach a more random orientation in the xy-plane, then a value for α_0 larger than that given by Equation (15) would be predicted.

The value of α_0 for random orientation in the xy-plane can be obtained from Equation (2). For this case, $\sin^4 \theta = 1$, and averaging $\sin^2 2\theta$ from 0 to π gives:

$$\alpha_0 = (L/d)^2 / [12(\ln 2L/d - 1.80)] \quad (40).$$

It is interesting to note that all of Myers' α_0 values fall well below those predicted by Equation (40).

Thus far, only the effect of fiber curvature on orientation has been considered. There will also probably be an effect on the strength of the doublet formed on the fiber. Tchen (7), has shown that the drag coefficient for a straight ellipsoid translating through a fluid in a direction parallel to its

axis can be expressed as follows:

$$D_s = 2\pi\mu/(\ln L/d + 0.19) \quad (41).$$

For an ellipsoid bent into a half-circle and translating as shown in Fig. 22, the drag coefficient is:

$$D_c = 3\pi\mu/(\ln L/d + 0.01) \quad (42).$$

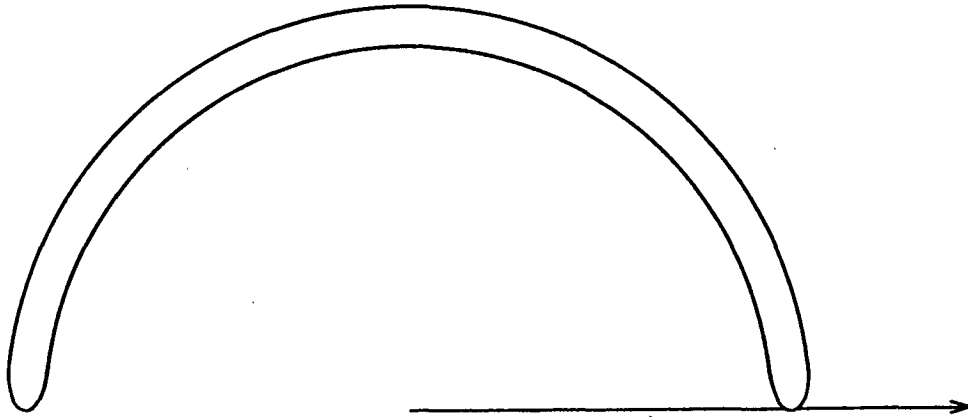


Figure 22. Curved Ellipsoid Translating Through a Fluid

Since the difference in the drag coefficients for these two extreme cases is only $\sim 30\%$, then the difference between the doublet strength formed by the presence of straight fibers, as compared to that formed with fibers of slight curvature, might be small.

An attempt has been made to correlate the values of α_o obtained by Myers (16) when using curved fibers by taking into account the effect of fiber curvature. Curvature measurements were made either from photographs presented by Myers or from the actual samples he used. Following Forgacs and Mason (17),

the angle γ was measured and attempts were made, without much success, to correlate the data based on γ only. It seemed more reasonable to base the correlation on the ratio of the length of the fiber to the maximum amount of the fiber which would lie across the velocity gradient when the fiber is aligned in the direction of flow. For a straight fiber, this would be, $\underline{L}/\underline{d}$. For a curved fiber, this would be $\underline{L}/(\underline{h} + \underline{d} \cos 1/2\epsilon)$, where \underline{h} and ϵ are defined by Fig. 23. The value of \underline{h} was obtained from γ and \underline{L} through the following relationships:

$$\epsilon = 180^\circ - \gamma \quad (43)$$

$$h = (180 \underline{L}/\pi\epsilon)(1 - \cos 1/2\epsilon) \quad (44)$$

Therefore, it can be seen that as $\gamma \rightarrow 180^\circ$, $\underline{h} \rightarrow 0$ and $\underline{L}/(\underline{h} + \underline{d} \cos 1/2\epsilon) \rightarrow \underline{L}/\underline{d}$.

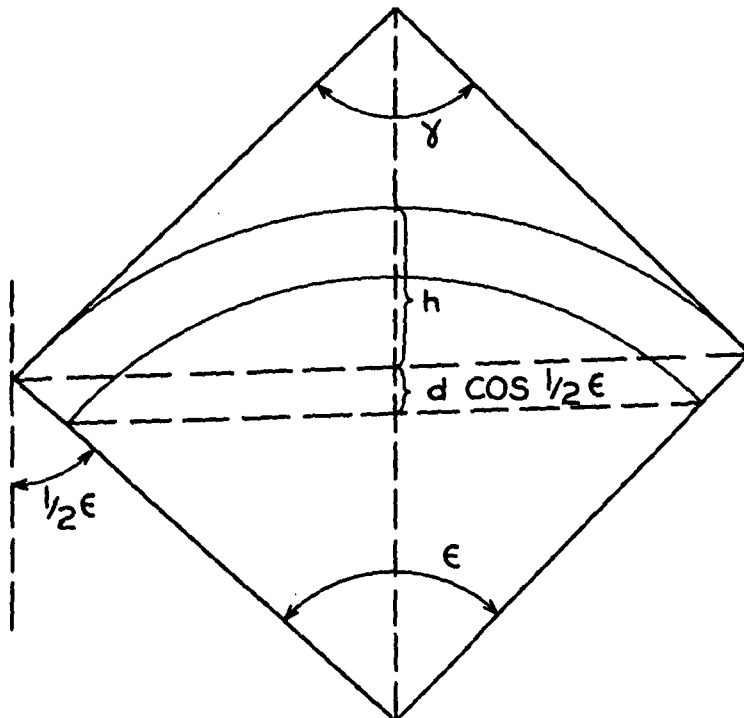


Figure 23. Definition of \underline{h} and ϵ

In order to eliminate from consideration the effect of $\underline{L}/\underline{d}$ on α_o , it was decided to use the ratio of the experimental values of intrinsic viscosity, α_{oE} , to the theoretical values, α_{oT} , as a basis of comparison.

If α_{oE}/α_{oT} is plotted versus $\underline{L}/(\underline{h} + \underline{d} \cos 1/2\epsilon)$, the relationship shown in Fig. 24 results. The values for the variables used to obtain this correlation are given in Table VIII. The values of α_{oT} used in this correlation were calculated using Equation (32).

TABLE VIII

VARIABLES USED IN THE CORRELATION INVOLVING FIBER CURVATURE

Sample No.	\underline{L} , mm.	\underline{d} , μ	$\underline{L}/\underline{d}$	α_{oE}	α_{oT}	α_{oE}/α_{oT}	γ	$\underline{L}/(\underline{h} + \underline{d} \cos 1/2\epsilon)$
680-.6 ^a	0.60	16.79	35.5	7.07	2.50	2.82	178	31.0
680-1.0 ^a	0.98	16.79	58.3	9.08	3.54	2.56	175	35.7
680-2.73 ^a	2.73	16.79	162.6	22.24	8.08	2.76	165	26.4
260-2.42 ^a	2.53	44.85	56.2	10.59	3.55	2.98	169	24.0
260-4.0 ^a	4.23	44.85	94.3	16.08	5.43	2.96	162	20.2
260-6.0 ^a	6.08	44.85	135.6	19.85	7.11	2.82	165	25.6
43.1 ^b	1.00	43.1	23.2	3.57	1.82	1.96	176	18.9
16.9 ^b	0.34	16.9	20.1	3.57	1.64	2.18	176	17.1

^aMyers' study.

^bThis study.

The primary point set forth in Fig. 24 is that as fiber curvature decreases, α_{oE}/α_{oT} approaches one, thus showing the importance of fiber curvature. Since $\underline{L}/(\underline{h} + \underline{d} \cos 1/2\epsilon)$ cannot be greater than $\underline{L}/\underline{d}$, there must be side curves breaking off the main curve and going down to the abscissa as shown. The steepness of the side curves leading up to the main curve shows the large effect which a slight curvature has on the viscosity.

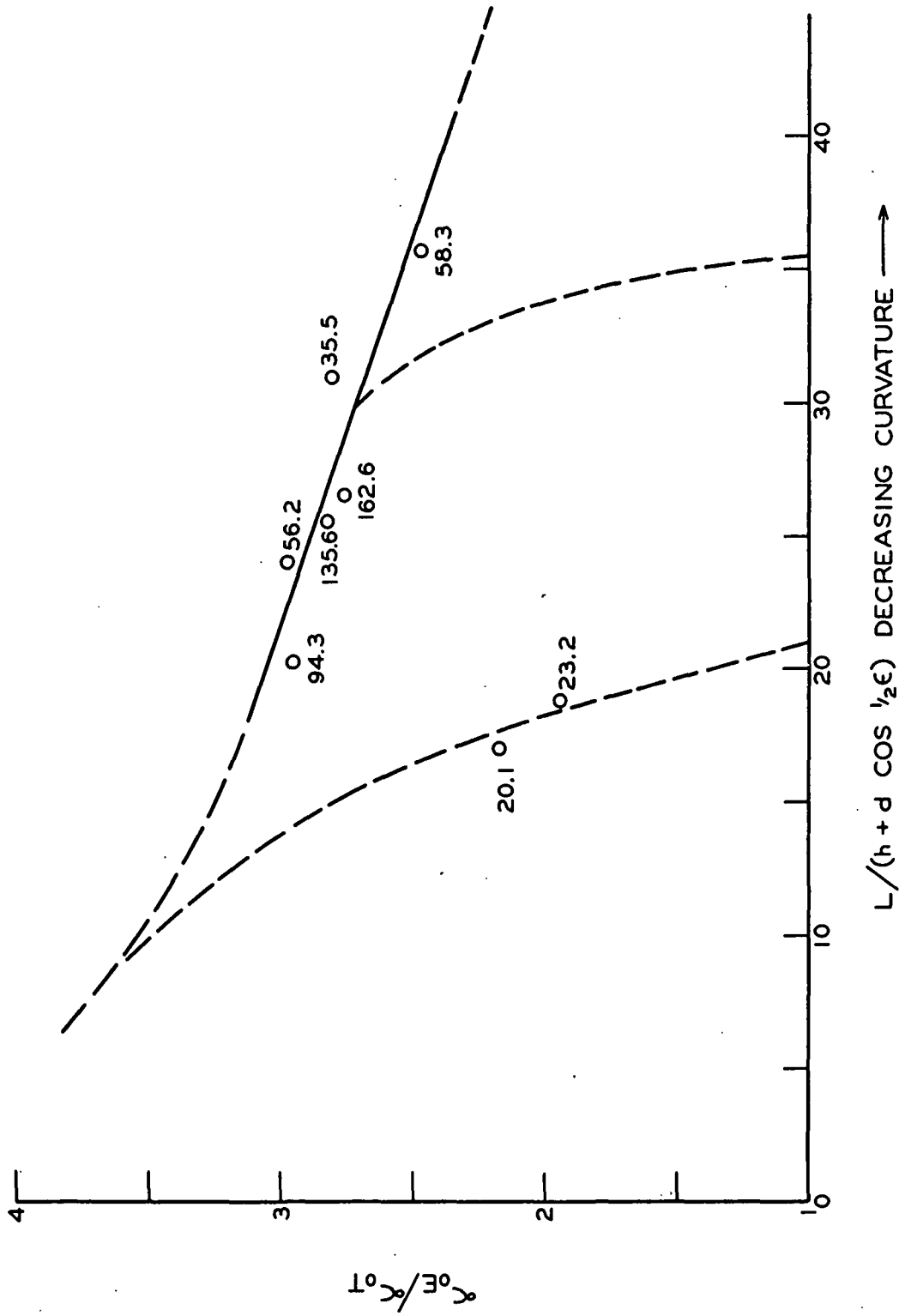


Figure 24. The Effect of Fiber Curvature on the Intrinsic Viscosity

The fact that the curve for any given L/d rises rapidly and then tends to level off agrees qualitatively with the results of Forgacs and Mason (17) for the effect of fiber curvature on the rotational behavior of fibers (see Fig. 3).

The number beside each point in Fig. 24 is the L/d ratio of the fibers used to obtain the point. Above a certain degree of curvature, the relationship presented depends only on $L/(\underline{h} + \underline{d} \cos 1/2\epsilon)$ and not on L/d . The amount of fiber curvature necessary to make α_{oE}/α_{oT} a function only of $L/(\underline{h} + \underline{d} \cos 1/2\epsilon)$ seems to depend on L/d , decreasing with increasing L/d . This can be seen from Table VIII and Fig. 24 by comparing the results obtained from Sample 43.1 in this study with Sample 680-.6 in Myers' study.

It is probable that as $L/(\underline{h} + \underline{d} \cos 1/2\epsilon)$ gets smaller, the main curve of Fig. 24 will begin to rise rapidly. This would be due to a closer approach to a random orientation as well as an increase in the fluid drag on the fibers due to increased curvature.

As $L/(\underline{h} + \underline{d} \cos 1/2\epsilon)$ increases, the main curve will probably approach the abscissa asymptotically. Thus, a slight curvature seems to have a much greater effect on the contribution to viscosity for fibers of small L/d than for those with a large L/d .

It can be seen from the discussion above that fiber curvature has a very significant effect on the contribution to viscosity of the fibers. Since the majority of the fibers used by Myers were curved, this is probably the primary reason why better agreement with Burgers' theory was not found.

DISCUSSION OF PAST EXPERIMENTAL WORK
IN RELATION TO THIS WORK

In the previous discussions, it has been demonstrated that two experimental conditions must be met which are of utmost importance if one is interested in obtaining the intrinsic viscosity of suspensions of rigid rods. These are: (1) It is necessary to work at concentrations below the "critical concentration" for the particular fibers used. (2) It is necessary to use straight, rigid rods.

The difficulty of meeting this first requirement with fibers of $L/d > 20$ can be readily seen from Table IX where the relative viscosity at the "critical concentration" is given for several values of L/d .

TABLE IX

PREDICTED VALUES OF THE RELATIVE VISCOSITY
AT THE "CRITICAL CONCENTRATION"

L/d	$c_o \times 10^2$	μ_r
10	1.500	1.0162
20	0.375	1.0063
35	0.123	1.0021
50	0.060	1.0013
100	0.015	1.0009
200	0.006	1.0006

Equations (1) and (32) were used to calculate μ_r at values of c_o determined from Equation (25).

All of the concentrations used by Nawab and Mason (15) were far above the "critical concentrations" for the fibers used. Also, in many cases (see Table I) the fibers used were either curved or flexible. Therefore, no agreement

between their study and this study or their study and theory would be expected, and none was found.

In Myers' study, the majority of the viscosity measurements were made on suspensions whose concentrations were above the "critical concentration." Also, as was pointed out, most of the fibers used by Myers were curved. However, three viscosity measurements were made on suspensions whose concentrations were near the "critical concentration." Two of the measurements were made using 16.79 μ diameter fibers of $L/\underline{d} = 23.1$ which have been shown to be straight. The other was made using 44.85 μ diameter fibers of $L/\underline{d} = 22.2$. It is not known whether these fibers were curved or straight.

A comparison of the results obtained by Myers using these fibers with the results obtained in this study is given in Fig. 25.

As can be seen, there is approximate agreement within the three sets of data at low concentrations. However, at higher concentrations the two curves obtained by Myers begin to separate rapidly with the results of this study falling between the two.

It should be noted that Myers did not present his data as shown in Fig. 25, but represented the data obtained using the 16.79 μ diameter fibers by a straight line and the data obtained with the 44.85 μ diameter fibers by a curved line. Myers questioned the results obtained with the 16.79 μ fibers (51). He felt that the relative viscosities at the high concentrations should have been larger and that a curved relationship should have been obtained with these fibers also. However, Myers could give no explanation for this difference in behavior.

It is doubtful that the 44.85 μ fibers were significantly curved since the data obtained with these fibers follows more closely the relationship found with straight fibers in this study than does the data obtained using the 16.79 μ fibers.

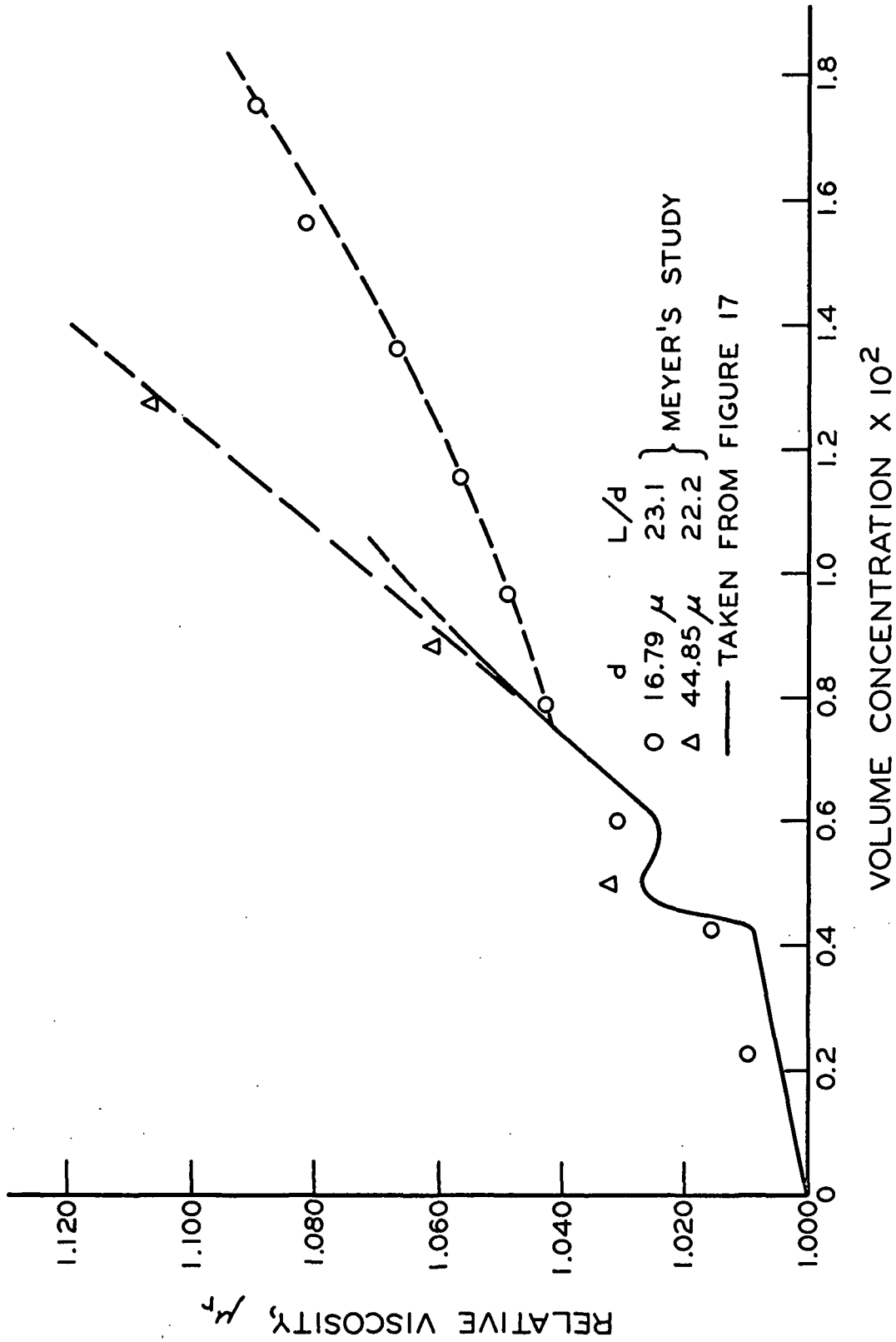


Figure 25. Comparison of the Results of This Study with Those of Myers'

One possible explanation for the difference in the two sets of data is as follows. Although Myers used a solution of tetrachloroethane and mineral oil as a suspending medium for his fibers, no corrections were made to account for changes in the viscosity of the suspending medium during a series of runs. Depending on the procedure used in handling the suspending medium in the dilution process between runs, appreciable changes could take place in the viscosity. Such changes in the viscosity of the suspending medium could have accounted for the differences in these runs.

It can be concluded from the above discussion that the primary reason for the lack of agreement within past experimental results, and between past experimental results and theory, was the failure of the experimenters to work with straight fibers and at low enough concentrations to prevent significant fiber-fiber interactions.

THE BEHAVIOR OF FLOCCULATED SUSPENSIONS

During the course of this study some viscosity measurements were made using flocculated suspensions. Although these measurements are of little value as far as the primary objectives of this study are concerned, i.e., for comparison with past work and theory, they are of interest themselves.

The term flocculation, as used in this discussion, means the formation of spherical aggregates of fibers, the aggregates being distributed throughout the suspensions. This is not to be confused with the formation of a continuous fiber network, such as that described by Wahren (32), since the concentration range covered in this part of the study is the same as that used in the first part of this study.

The flocculation that occurred in this study was not purposely caused. It was found that the flocculation which occurred in the TCE-PO was due to impurities, believed to be rust and/or water, in the TCE. In an effort to find a deflocculated system, a series of viscosity measurements was made using glycerol-water as a suspending medium. The glycerol-water solution was adjusted to a pH of ~ 10 since Myers stated that a minimum of flocculation would be obtained at this pH. However, the fibers flocculated more in the glycerol-water than in the contaminated TCE-PO.

No attempt was made to determine the mechanism of the flocculation. It was found that by purification of the TCE by fractional distillation, a well-dispersed suspension could be obtained.

GENERAL BEHAVIOR

At the start of each viscosity measurement, the suspension was stirred to disperse the fibers and a low torque was applied to the inner cylinder. The fibers immediately began to flocculate as the flow began and the flocs continued to grow until an equilibrium floc size was reached. The growth of the flocs caused the angular velocity of the inner cylinder to decrease (increasing viscosity) until an equilibrium floc size was reached. The angular velocity of the inner cylinder then remained constant. As the torque was increased, increasing the angular velocity, the flocs broke down slowly until another equilibrium floc size, smaller than before, was reached. This general behavior is the same as that found by Hubley, et al. (52) for suspensions of cellulose fibers.

A typical plot of torque versus angular velocity is given in Fig. 26.

The general shape of the curve in Fig. 26 is that of an Ostwald-Philippoff liquid. This non-Newtonian behavior was expected since the suspended particles (in this case the individual flocs) actually changed in size with increased shear.

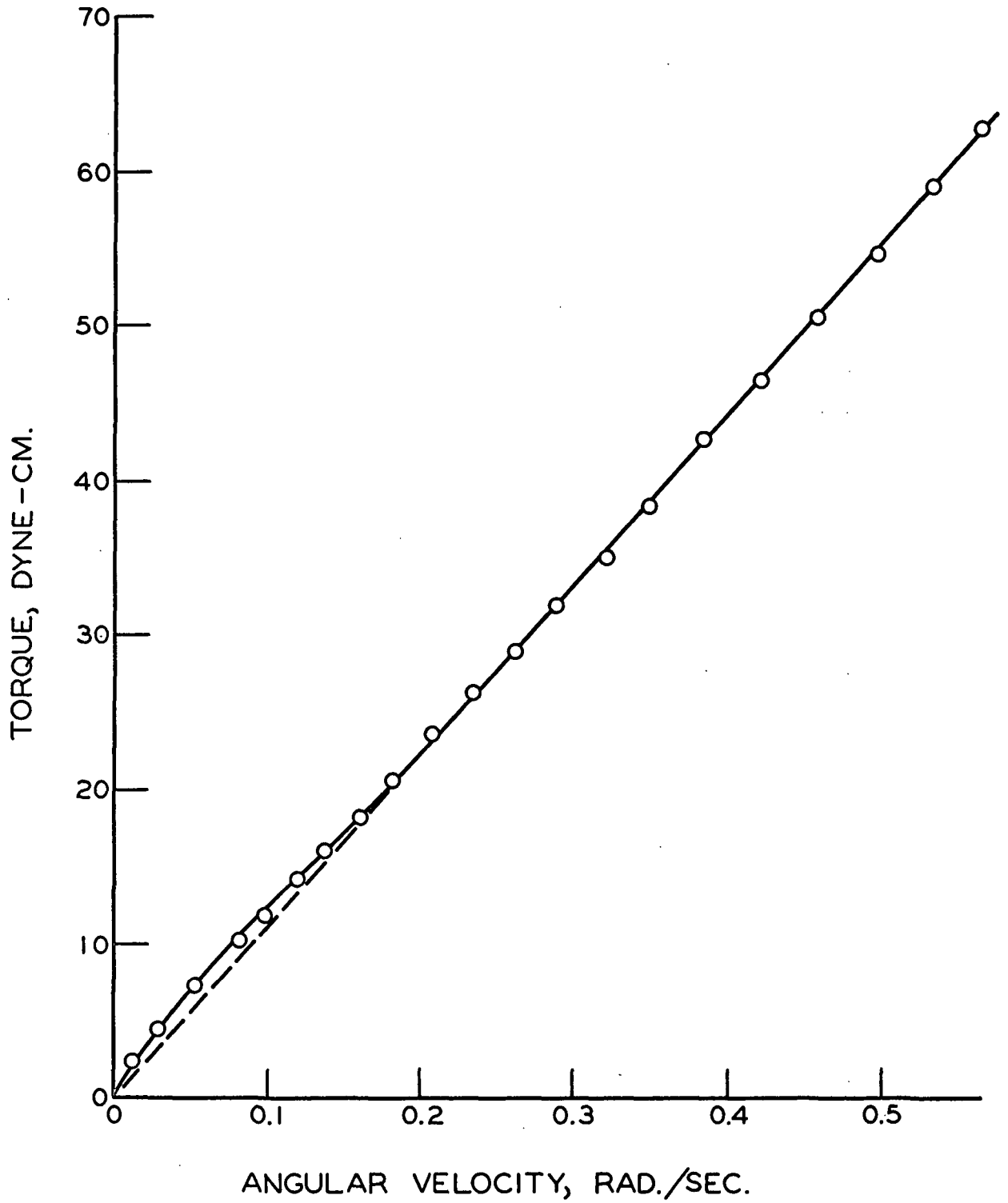


Figure 26. Torque-Angular Velocity Relationship for a Flocculated Suspension

This is to be contrasted with the Newtonian response found using the well-dispersed systems where the particle shape and contribution to viscosity are not affected by shear rate.

It is impossible to tell from the data taken on these flocculated suspensions whether or not there was a true first Newtonian regime. However, the non-Newtonian regime and the second Newtonian regime are well defined in Fig. 26.

Although the curve in Fig. 26 shows no indication of curvature in the second Newtonian regime, it is felt by the author that as the shear rate continues to increase, the flocs would continue to break down until a well-dispersed system is obtained. At this point, it seems that there should also be agreement with the viscosity of a well-dispersed suspension. To the author's knowledge, this behavior has never been found. If this type of behavior did take place, there would also be a second non-Newtonian regime and a third Newtonian regime.

All of the torque versus angular velocity curves obtained using flocculated suspensions were of the same general shape as Fig. 26. However, as the concentration decreased, the torque-angular velocity curves approached straight lines, i.e., became less non-Newtonian.

THE EFFECT OF CONCENTRATION ON THE RELATIVE VISCOSITY

Figure 27 shows the effect of fiber flocculation on the relative viscosity-concentration relationship. The slope in the second Newtonian regime was used in determining the relative viscosities. A comparison is made between the flocculated suspensions and the well-dispersed suspensions represented by the initial slope of Fig. 17 shown as a broken line.

As would be expected, the flocculated suspensions yielded higher viscosities at any given concentration than the well-dispersed suspensions.

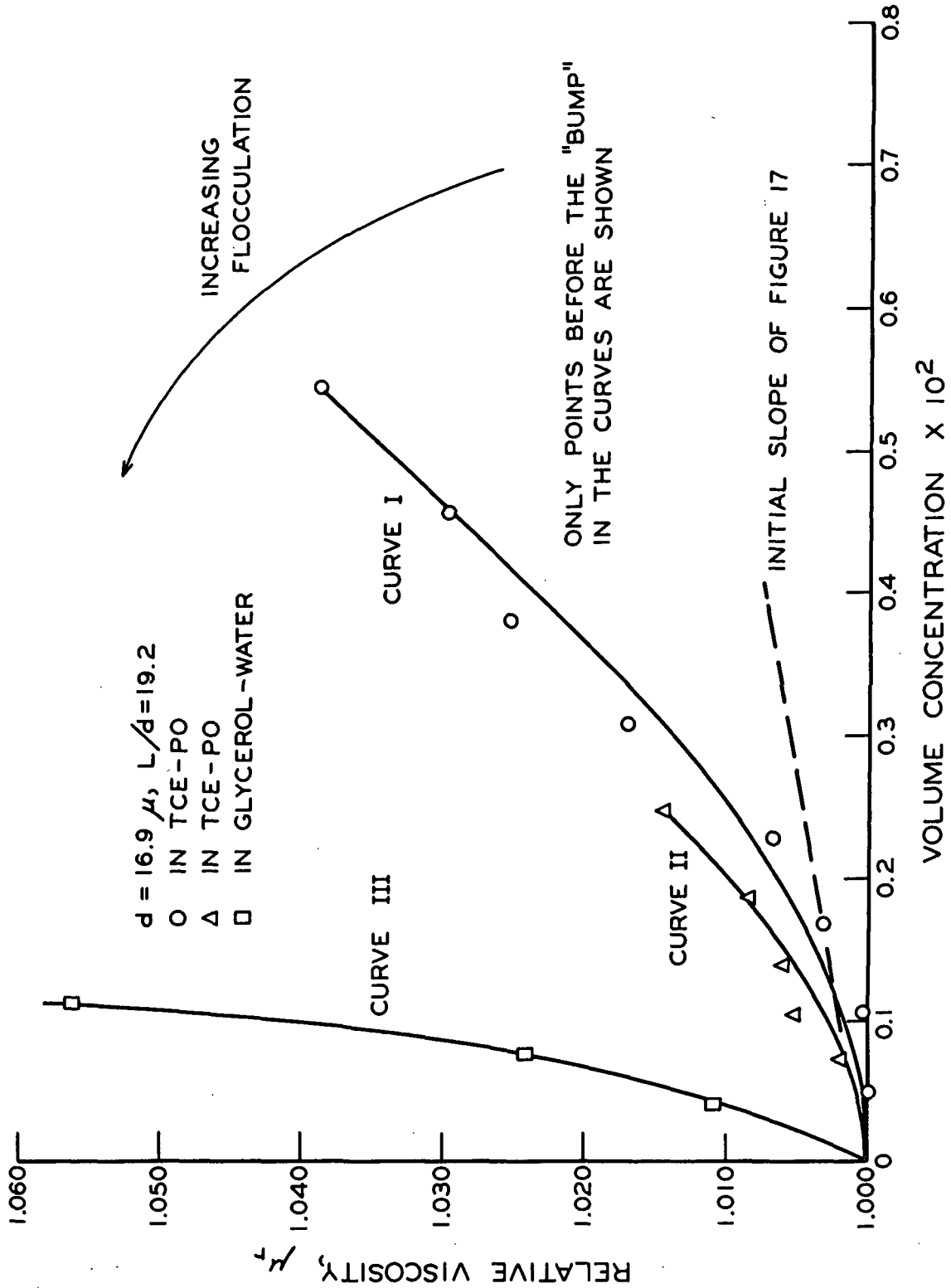


Figure 27. The Effect of Flocculation on the Relative Viscosity

Figures 28, 29, and 30 show separately the viscosity-concentration relationships found for each case shown in Fig. 27.

As can be seen, the "bump" in the viscosity-concentration curve was also found with the flocculated suspensions. However, there seems to be a tendency for the "bump" to shift toward lower concentrations with increasing flocculation. A possible reason for this shift is as follows.

In the flocculated suspensions, some of the fibers were bound in flocs while others were moving freely in the space between the flocs. From visual observation, the percentage of free fibers seemed to increase with decreasing concentration. Also, as the tendency to flocculate became stronger, lower and lower concentrations were necessary before any considerable percentage of the fibers became free.

Thus, if the "bump" in the viscosity-concentration relationship is a function of the orientation of the fibers as was suggested previously, then the position of the "bump" would depend on the percentages of the fibers in the suspension which are free to assume orientations and would move to lower concentrations with increasing tendency to flocculate.

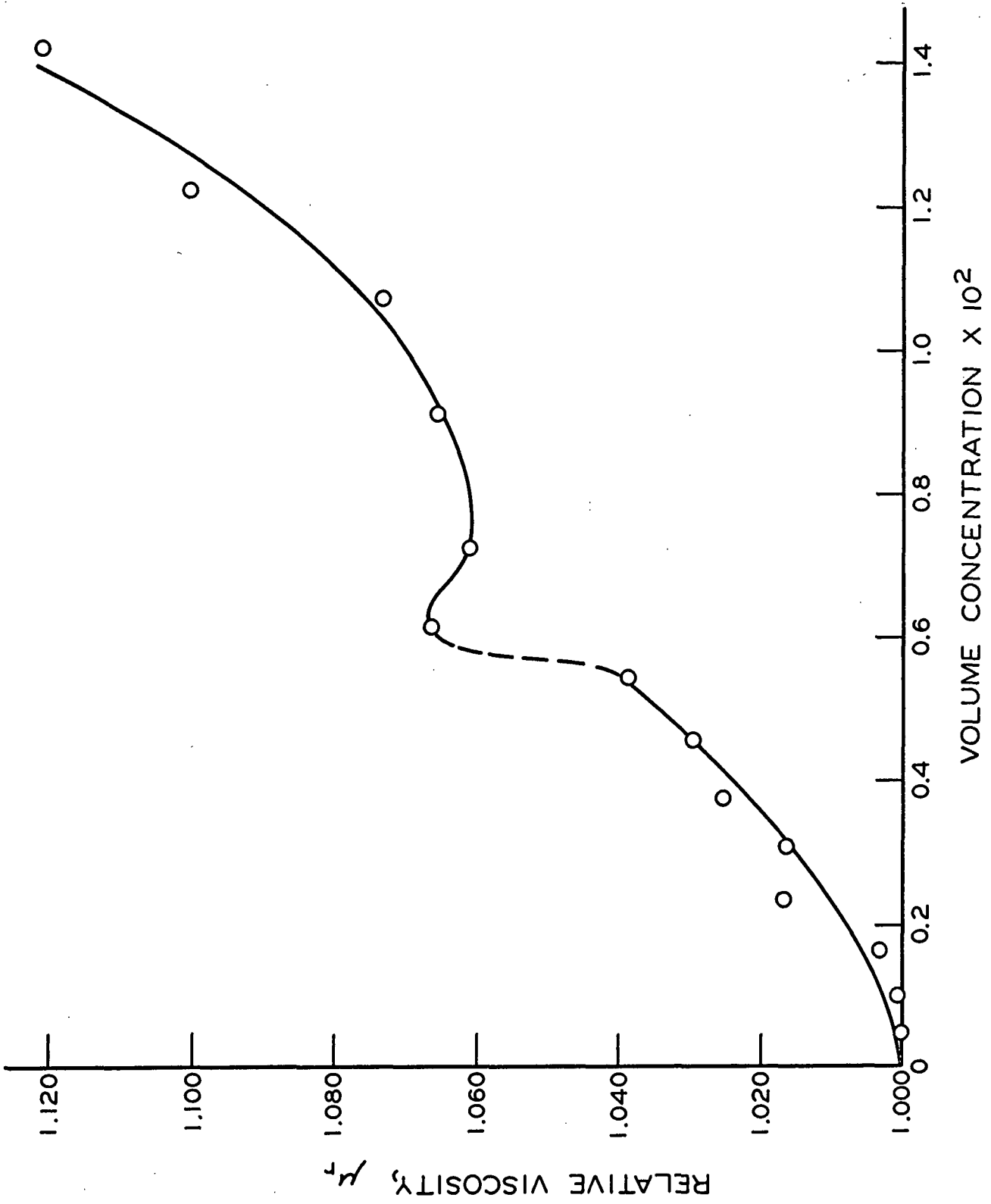


Figure 28. Curve I of Figure 27

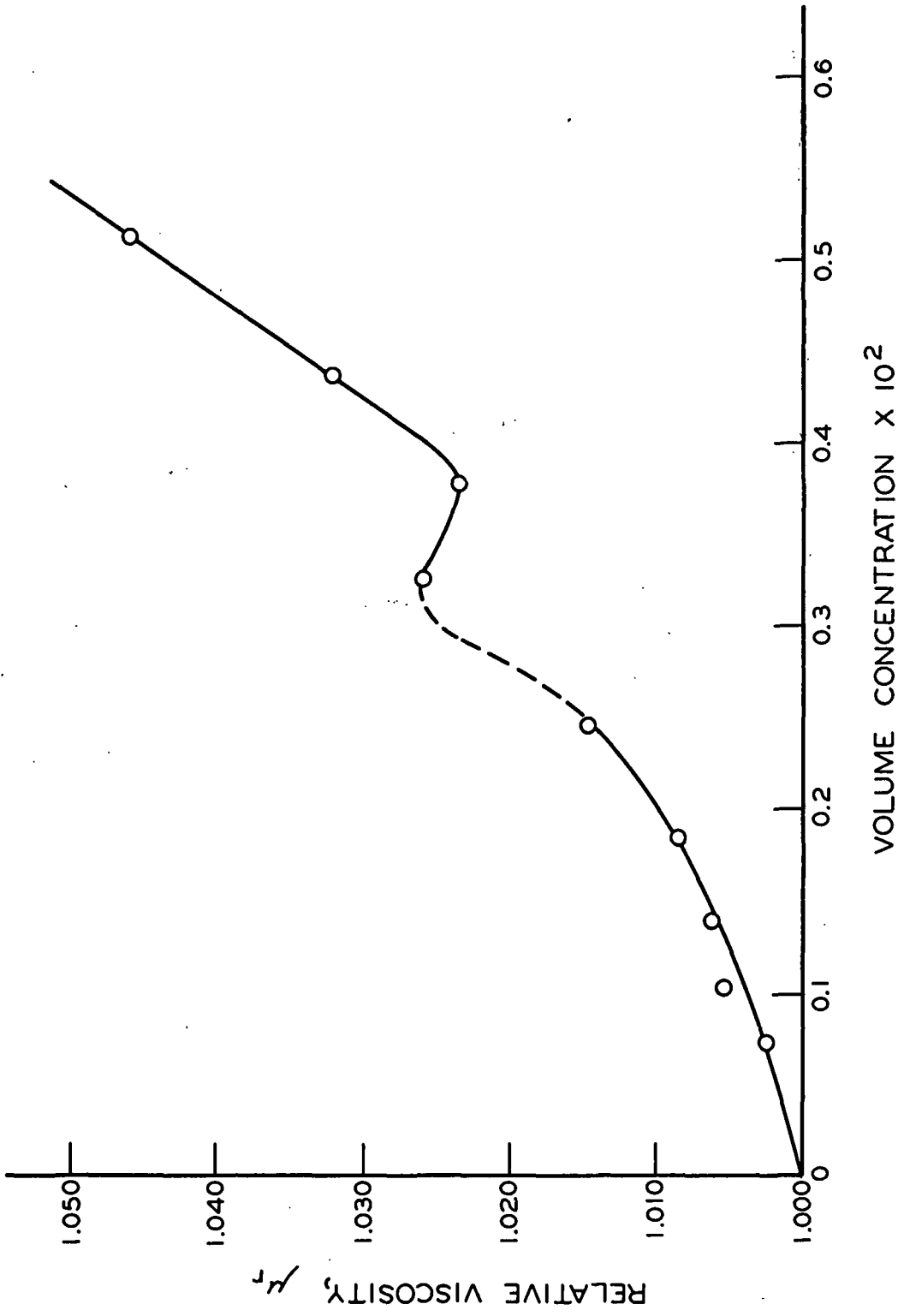


Figure 29. Curve II of Figure 27

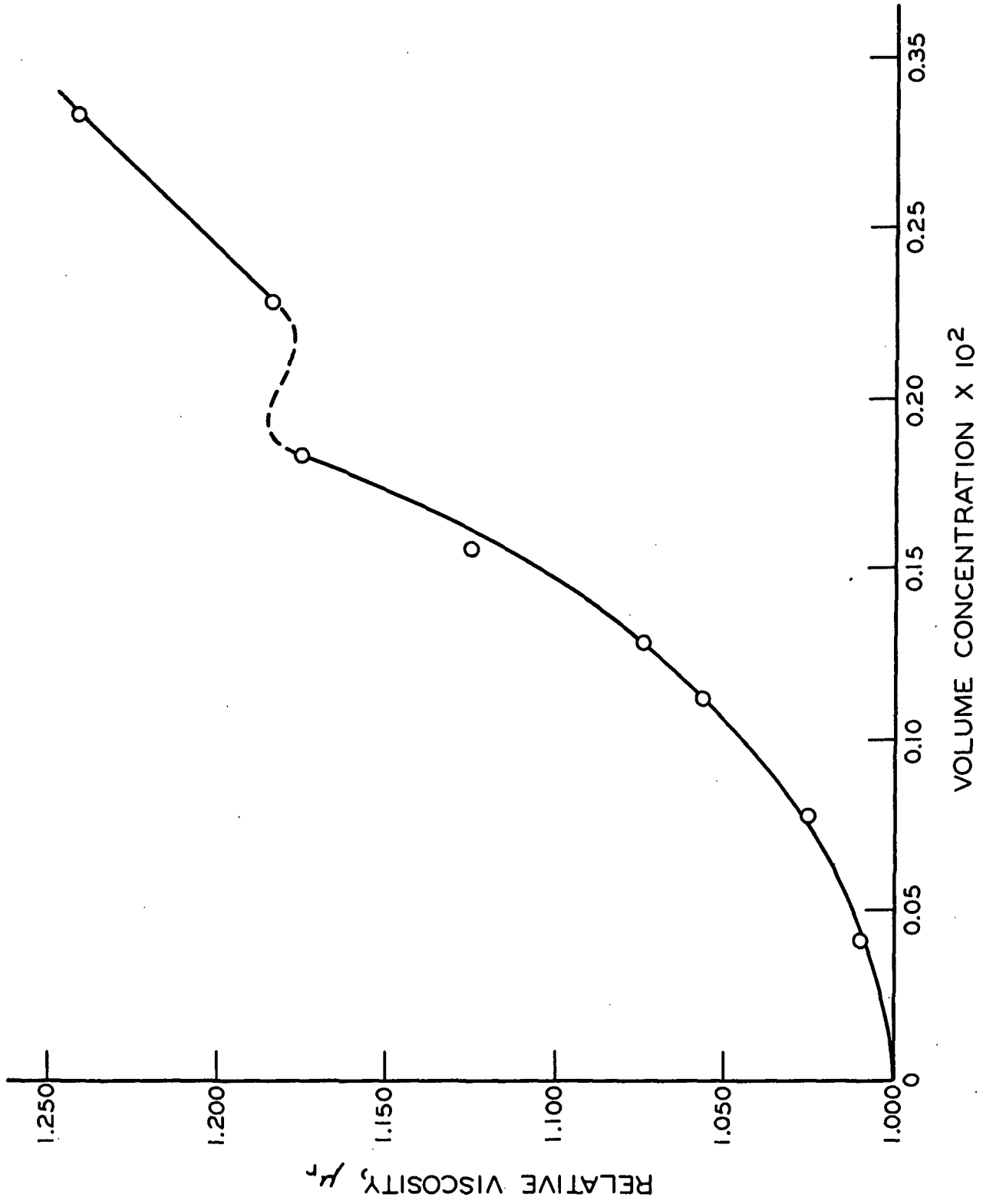


Figure 30. Curve III of Figure 27

CONCLUSIONS

The primary purpose of this study was to gain a general insight into the flow behavior of fiber suspensions so that a better evaluation of Burgers' theory and concepts could be made and to determine the effect of the wall and fiber curvature on the relative and intrinsic viscosities.

Measurements of relative viscosity and fiber orientations showed that at volume concentrations below approximately 0.0042, for straight, rigid nylon fibers of $L/d \approx 20$, fiber-fiber interactions were negligible. In this concentration range, intrinsic viscosities determined from the slope of the relative viscosity-concentration relationship agreed with Burgers' theory (6) within 10% when measured values of the orientations of the fibers were used in the calculations. This is the first time that Burgers' theory has been shown to be correct within the error of experimental measurements. Also, this result is to be contrasted with results of past workers (15, 16) where it was concluded the Burgers' theory was in error by a factor of at least three.

The study of the effect of concentration on the relative viscosity yielded two other new findings. First, there was a sudden increase in the relative viscosity as the concentration increased beyond 0.0042 followed by a slight decrease and a second increase. This behavior was found to be at least partially due to an increase and decrease in the orientation factor over the same concentration range. It was hypothesized that this viscosity behavior was also partially due to increasing fiber-fiber interactions. Second, it was found that the beginning of the rapid rise in the relative viscosity at a concentration of approximately 0.0042 agreed closely with the "critical concentration" for free rotation of the fibers as predicted by Mason (33).

The effect of the wall on the relative viscosity was found to be negligible even for fiber length and fiber diameter-to-annulus width ratios of 0.358 and 0.0176. This was of particular interest since $\underline{L/D}$ and $\underline{d/D}$ ratios several times smaller than these have been used to explain anomalous viscosity behavior.

Slight fiber curvatures ($\gamma = 162 - 178^\circ$) were found to have a large effect on the relative viscosity leading to increases in α_0 of 2 to 3 times that expected for straight fibers. For fibers of these small curvatures, this behavior was most probably due to the effect of curvature on the orientations of the particles.

A relationship between fiber curvature and the ratio of the experimental to the theoretical intrinsic viscosity was obtained. It was found that above a certain degree of curvature, the above ratio is dependent only on the degree of curvature and not on the length-to-diameter ratio of the particles.

From the above findings, it was concluded that the primary reasons for the inconsistencies in the results of the past experimental works were due to the fact that fibers of different degrees of curvature were used. The most probable reason for the lack of agreement between past experimental studies and theory was that curved fibers and too high concentrations were used.

Measurements on flocculated suspensions showed that the suspensions were non-Newtonian. The shear stress-shear rate relationships were similar to that of an Ostwald-Philippoff liquid. Also, the relative viscosity at any given concentration was higher for the flocculated suspensions than for the well-dispersed suspensions, the difference depending on the degree of flocculation.

SUGGESTIONS FOR FUTURE WORK

An investigation of the causes of the changes in the orientation factor found in this study would be of interest. Knowing the causes of these changes, one might obtain an explanation for the magnitude of the viscosity changes over the same concentration range.

This problem might be approached by observing individual fibers involved in interactions with other fibers. By prolonged observation, one might be able to determine whether or not there is any characteristic behavior of interacting particles as a function of concentration such as a tendency to cause changes in the average orientation in some preferred direction.

A significant contribution would be to predict theoretically the effect of fiber curvature on the rotational behavior in a linear velocity gradient and on the viscosity of suspensions of curved fibers. The mathematical procedure developed by Burgers (6) and Tchen (7) might be applied.

In the area of the flow of flocculated suspensions, a study of the shear stress-shear rate relationship over very large ranges of shear rate, including the very low range covered in this study, would be of help in the study of the flow of flocculated suspensions. Simultaneous measurements of the number of flocs per unit volume and floc size distribution, possibly using the method of Hubley (52), would be necessary for understanding of the system being studied. It would also be of interest to know if there is a third Newtonian regime at very high shear rates as was suggested in this study.

NOMENCLATURE

\underline{a}	= major semiaxis of an ellipsoid, or half length of a cylinder, cm.
$\underline{A}_1, \underline{A}_2$	= adjustable coefficients
\underline{b}	= minor semiaxis of an ellipsoid, or radius of a cylinder, cm.
\underline{c}	= volume concentration, cc./cc.
\underline{c}_0	= "critical concentration" for free rotation of the fibers
\underline{d}	= fiber diameter, cm.
\underline{D}	= annulus width, cm.
\underline{e}	= one half the distance between the origin of the forces in a doublet, cm.
\underline{E}_b	= modulus of elasticity in bending, dynes/sq. cm.
\underline{F}	= force, dynes
\underline{F}	= body force per unit volume of fluid, dynes/cc.
\underline{F}	= actual drag on a particle, dynes
\underline{F}_∞	= drag force on a particle in an infinite medium, dynes
$\underline{F}_x, \underline{F}_y, \underline{F}_z$	= components of body force \underline{F} .
\underline{g}	= body force per unit volume, dynes/cc.
\underline{G}_e	= effective shear rate in a suspension of rigid rods, sec. ⁻¹
\underline{G}_0	= shear rate or velocity gradient in a pure solution, sec. ⁻¹
\underline{h}	= length of inner cylinder, cm.
\underline{h}	= distance used in defining the curvature of a fiber, cm.
$\underline{h}_1, \underline{h}_2$	= distances from the center of a rod to the \underline{xz} -plane, cm.
\underline{H}	= distance from a wall of a particle in translation, cm.
\underline{k}	= velocity gradient, sec. ⁻¹
$\underline{k}', \underline{k}''$	= empirical constants
$\underline{k}_1, \underline{k}_2, \underline{k}_3$	= constants
\underline{K}	= constant of integration called the orbit constant

$\underline{K}', \underline{K}''$	= experimentally determined constants
$\underline{\ell}$	= distance along the axis of a rod from the center out, cm.
\underline{L}	= fiber length, cm.
\underline{L}	= couple exerted on a particle in a bounded medium, dyne-cm.
\underline{L}_∞	= couple exerted on a particle in an unbounded medium, dyne-cm.
$(\underline{L}/\underline{d})_e$	= "equivalent ellipsoidal" axis ratio
\underline{M}	= doublet strength, dyne-cm.
\underline{n}	= number of rods per unit volume
\underline{O}	= origin of a co-ordinate system
\underline{p}	= pressure, dynes/sq. cm.
\underline{P}	= point on a rod
\underline{r}	= $(\underline{x}^2 + \underline{y}^2 + \underline{z}^2)^{1/2}$
\underline{r}_1	= radius of inner cylinder, cm.
\underline{r}_2	= radius of outer cylinder, cm.
\underline{Re}	= Reynolds number, $\underline{dV}_x \rho / \mu$
\underline{t}	= time, sec.
\underline{T}	= period of rotation of a rod or ellipsoid, sec.
\underline{T}'	= torque delivered to the inner cylinder, dyne-cm.
\underline{U}	= translational velocity of a particle, cm./sec.
\underline{v}_P	= velocity of a point on a rotating fiber, cm./sec.
$\underline{v}_x, \underline{v}_y, \underline{v}_z$	= velocity components in the \underline{x} , \underline{y} , and \underline{z} directions, cm./sec.
$\underline{v}_{x'}, \underline{v}_{y'}, \underline{v}_{z'}$	= velocity components in the \underline{x}' , \underline{y}' , and \underline{z}' directions, cm./sec.
$\underline{v}_\theta, \underline{v}_\phi, \underline{v}_\ell$	= components of \underline{v}_P
\underline{V}_A	= volume of a fiber, cc.
\underline{V}_E	= effective volume occupied by a fiber while rotating, cc.
$\underline{V}_x \hat{i}$	= uniform velocity of the fluid in the \underline{x} -direction, cm./sec.
$\underline{x}, \underline{y}, \underline{z}$	= rectangular co-ordinates, cm.

$\underline{x}', \underline{y}', \underline{z}'$	= rectangular co-ordinates, cm.
α_0	= intrinsic viscosity of a fiber suspension
α_1	= empirical constant
α_{0E}	= experimentally determined intrinsic viscosity
α_{0R}	= intrinsic viscosity of a suspension of randomly oriented rods
α_{0T}	= theoretically predicted intrinsic viscosity
α_{oxy}	= intrinsic viscosity of a suspension of rods oriented in the <u>xy</u> -plane
β	= ratio of actual to "equivalent ellipsoidal" axis ratio
γ, ϵ	= angles used in defining the curvature of a fiber
θ, ϕ, λ	= angles defining the orientation of a rod in a linear velocity gradient
μ	= microns
μ	= viscosity, dyne-sec./sq. cm.
μ_e	= effective viscosity of a suspension of rods
μ_r	= relative viscosity
μ_{sp}	= specific viscosity determined from theory
μ_{sp}'	= specific viscosity calculated using measured values of \underline{K}
ρ	= fluid density, g./cc.
τ	= shear stress, dynes/sq. cm.
ω, ω_b	= angular velocity of the inner cylinder, rad./sec.
ω_c	= critical angular velocity for stable flow in the viscometer annulus, rad./sec.
Ω	= angular velocity of a suspended particle, rad./sec.

ACKNOWLEDGMENTS

The author sincerely appreciates the guidance contributed by the thesis advisory committee during the course of this study. Members of the committee were Mr. S. T. Han, chairman, Mr. H. Meyer, and Dr. J. A. Van den Akker. Special thanks are extended to Mr. Han for the many hours of fruitful discussion throughout this study.

The aid of the following people is also gratefully acknowledged:

Dr. H. D. Wilder who served on the thesis advisory committee during the early part of this work.

Dr. R. W. Nelson for his help in understanding the theory and interpretation of results.

Mr. K. W. Hardacker for his advice and suggestions concerning various experimental techniques.

Mr. H. W. Marx for his help in building and modifying parts of the viscometer.

Mr. F. Sweeney for his assistance during the photographic work.

The author also expresses his deep appreciation to his wife, Beth, for her continued encouragement throughout this study and for typing the original manuscript.

Other members of the Institute staff made lesser but valuable contributions to the success of this work and their help is sincerely appreciated.

LITERATURE CITED

1. Stokes, G. G. In Lamb's Hydrodynamics. 6th ed. p. 602-3. New York, Dover, 1945.
2. Navier, C. L. M. H. In Lamb's Hydrodynamics. 6th ed. p. 577. New York, Dover, 1945.
3. Oseen, C. W. In Lamb's Hydrodynamics. 6th ed. p. 609-17. New York, Dover, 1945.
4. Overbeck, A. In Lamb's Hydrodynamics. 6th ed. p. 604-5. New York, Dover, 1945.
5. Lamb, H. Hydrodynamics. 6th ed. p. 615-16. New York, Dover, 1945.
6. Burgers, J. M. In Second report on viscosity and plasticity. p. 113-84. New York, Nordemann, 1938.
7. Tchen, C. M., J. Appl. Phys. 25:463(1954).
8. Brenner, H., J. Fluid Mech. 12:35(1962).
9. Einstein, A. Investigations on the theory of Brownian movement. p. 49-54. New York, E. P. Dutton, 1926.
10. Jeffery, G. B., Proc. Roy. Soc. (London) A102:161-79(1923).
11. Eirich, F., and Goldschmid, O., Kolloid Z. 81:7(1937).
12. Smith, H. F., Rubber Chem. and Tech. 15:301(1942).
13. Taylor, G. I., Proc. Roy. Soc. (London) 103:58(1923).
14. Eirich, F., Margaretha, H., and Bunzul, M., Kolloid Z. 75:20(1936).
15. Nawab, M. A., and Mason, S. G., J. Phys. Chem. 62:1248(1958).
16. Myers, W. T., Jr. The rheology of synthetic fiber suspensions. Doctor's Dissertation. Appleton, Wis., The Institute of Paper Chemistry, 1962. 189 p.
17. Forgacs, O. L., and Mason, S. G., J. Colloid Sci. 14:473(1959).
18. Vand, V., J. Phys. and Colloid Chem. 52:300(1948).
19. Myers, W. T., Jr., J. Appl. Poly. Sci. 8:863(1964).
20. Lamb, H. Hydrodynamics. 6th ed. p. 576. New York, Dover, 1945.
21. Oseen, C. W. In Second report on viscosity and plasticity. p. 115. New York, Nordemann, 1938.

22. Trevelyan, B. J., and Mason, S. G., J. Colloid Sci. 6:354(1951).
23. Mason, S. G., and Manley, R. St. J., Proc. Roy. Soc. (London) A238:117(1956).
24. Bartok, W., and Mason, S. G., J. Colloid Sci. 12:243(1957).
25. Eisenschitz, R., Z. Phys. Chem. A158:85(1932).
26. Goldsmith, H. L., and Mason, S. G., J. Fluid Mech. 12:88(1962).
27. Han, S. T. Personal communication, 1962.
28. Happel, J. Unpublished work, 1964.
29. Taylor, G. I., Proc. Roy. Soc. (London) A157:546(1936).
30. White, C. M., Proc. Roy. Soc. (London) A186:472(1946).
31. Forgacs, O. L., and Mason, S. G., J. Colloid Sci. 14:457(1959).
32. Wahren, D., Svensk Papperstid. 67:536(1964).
33. Mason, S. G., Pulp Paper Mag. Can. 51, no. 5:93(1950).
34. Bulletin X-48, E. I. du Pont de Nemours and Co., Wilmington, Delaware, 1956.
35. Ilvessalo-Pfäffli, M-S., and Alfthan, G., Paperi Puu 39:509(1957).
36. Dyson, J., J. Opt. Soc. Am. 50:754(1960).
37. Bates, F. J. Polarimetry, saccharimetry and the sugars. p. 671. Washington, U. S. Government Printing Office, 1942.
38. Oka, S. In Eirich's Rheology. Vol. 3, p. 37. New York, Academic Press, 1960.
39. Lindsley, C. H., and Fischer, E. K., J. Appl. Phys. 18:988(1947).
40. Robertson, A. A., Meindersma, E., and Mason, S. G., Pulp Paper Mag. Can. 62:T3(1961).
41. Merrill, E. W. In Acrivos' Modern chemical engineering. Vol I. p. 141. New York, Reinhold, 1963.
42. Trevelyan, B. J. as quoted by Mason (33).
43. Arlov, A. P., Forgacs, O. L., and Mason, S. G., Svensk Papperstid. 61:61 (1958).
44. Frisch, H. L., and Simha, R. In Eirich's Rheology. Vol. I. p. 576. New York, Academic Press, 1956.
45. Simha, R., J. Res. Natl. Bur. Stds. 42:409(1949).

46. Mason, S. G. In Mills' Rheology of disperse systems. p. 81. New York, Pergamon Press, 1959.
47. Sweeny, K. H., and Geckler, R. D., J. Appl. Phys. 25:1135(1954).
48. Eveson, G. F., Whitmore, R. L., and Ward, S. G., Nature 166:1074(1950).
49. Goldsmith, H. L., and Mason, S. G., J. Colloid Sci. 17:448(1962).
50. Nelson, R. W. Personal communication, 1964.
51. Myers, W. T., Jr. Personal communication, 1964.
52. Hubley, C. E., Robertson, A. A., and Mason, S. G., Can. J. Res. B28:770 (1950).

APPENDIX I

BURGERS' DERIVATION OF AN EQUATION FOR THE VISCOSITY
OF A SUSPENSION OF RIGID RODS

Burgers (6) was concerned with the effect of rigid rods suspended in a liquid on the apparent viscosity of the liquid. The following is a discussion of how Burgers arrived at an equation to describe this effect.

The assumptions made by Burgers at the start of his derivation are given on page 7 in the Theoretical section.

If a rigid rod is placed in a liquid in flow described by the equations:

$$\begin{aligned}v_x &= G_o y \\v_y &= 0 \\v_z &= 0\end{aligned}\tag{45}$$

the rod will translate, rotate, and spin about its axis.

Burgers assumed that there would be no slip of the liquid at the surface of the rod and also that there would be no inertial effects connected with the rod or the liquid. Therefore, the center of the rod would move at the same velocity as the fluid. By taking the origin of a co-ordinate system at the center of the rod, the velocity imparted to a point, P, on the rod in the liquid can be expressed by:

$$v_P = G_o \ell \sin \theta \sin \phi\tag{46}$$

where θ and ϕ are defined by Fig. 1, and ℓ is the distance between the center of the fiber O and P.

Using the relationships for spherical co-ordinates, Equation (46) can be broken down into three components, one tending to decrease ϕ , one tending to increase θ , and one along the axis of the particle, as follows:

$$v_{\phi} = G_o \ell \sin \theta \sin^2 \phi \quad (47)$$

$$v_{\theta} = G_o \ell \sin \theta \cos \theta \sin \phi \cos \phi \quad (48)$$

$$v_{\ell} = G_o \ell \sin^2 \theta \sin \phi \cos \phi \quad (49).$$

Since the rod follows the motion of the fluid as described by Equations (47) and (48), it will not disturb this motion. Therefore, there will be no effect upon the viscosity of the liquid which is directly connected with these rotational components. However, as Burgers stated, "actually there is a small effect, connected with the fact that the thickness of the rod is not infinitely small."

On the other hand, the component of velocity along the axis of the rod does have a pronounced effect on the suspension viscosity. As assumed, the fluid adheres to the rod, and since the rod cannot follow the motion of the fluid directed along its axis, a disturbance of the fluid motion will result.

In order to determine the disturbance of the liquid, Burgers considered the case of a rod immersed in a field of flow with the velocity:

$$v_{x'} = k x' \quad (50)$$

\underline{x}' , \underline{y}' , and \underline{z}' being rectangular co-ordinates with the \underline{x}' axis along the axis of the rod. The equation of continuity requires that there will also be components $\underline{v}_{y'}$, and $\underline{v}_{z'}$. However, since the rod has been assumed to have a very small diameter and since $\underline{v}_{y'}$, and $\underline{v}_{z'}$, are proportional to the diameter, these components will be practically zero at the surface of the rod and therefore will be neglected.

In order to obtain an expression for \underline{v}_x , Burgers turned to Oseen's (3) solution of the Navier-Stokes equation for the effect of an arbitrary force on the velocity of a fluid. The form of the Navier-Stokes equation used in this case was that pertaining to a fluid of constant density, ρ , and constant viscosity, μ , and can be expressed as follows:

$$\rho \frac{D\vec{v}}{Dt} = -\nabla p + \mu \nabla^2 \vec{v} + \rho \vec{g} \quad (51)*$$

where

\vec{g} = any body force per unit volume

ρ = fluid density

p = pressure

μ = Newtonian viscosity coefficient

t = time

$$* \frac{D\vec{v}}{Dt} = \frac{\partial \vec{v}}{\partial t} + (\vec{v} \cdot \nabla) \vec{v}$$

$$(\vec{v} \cdot \nabla) v_x = v_x \frac{\partial v_x}{\partial x} + v_y \frac{\partial v_x}{\partial y} + v_z \frac{\partial v_x}{\partial z}$$

There will be similar expressions for the y and z directions.

$$\nabla p = \vec{i} \frac{\partial p}{\partial x} + \vec{j} \frac{\partial p}{\partial y} + \vec{k} \frac{\partial p}{\partial z}$$

$$\nabla^2 v_x = \left(\frac{\partial^2 v_x}{\partial x^2} + \frac{\partial^2 v_x}{\partial y^2} + \frac{\partial^2 v_x}{\partial z^2} \right)$$

with similar expressions for the y and z directions.

The unique point about Oseen's solution of the Navier-Stokes equation is that he took inertial effects into consideration to some extent by linearizing the inertial terms, $(\vec{v} \cdot \nabla) \vec{v}$. This was done by using $\frac{V_x \vec{i}}{x} + \underline{v}_x$ for \underline{v}_x and neglecting terms of second order in \underline{v}_x , \underline{v}_y , and \underline{v}_z . Here, $\frac{V_x \vec{i}}{x}$ is the undisturbed velocity of the fluid in the x -direction.

In vector form, the result of this simplification of Equation (51) can be written:

$$\rho(V_x \vec{i} \cdot \nabla) \vec{v} = -\nabla p + \mu \nabla^2 \vec{v} + \vec{F} \quad (52)$$

where \vec{F} = some body force per unit volume.

Consider the case of the action of a single force of given constant magnitude acting at a point Q , taking the origin of the co-ordinate system x , y , z at Q . Suppose that the fluid originally had a constant uniform velocity $\frac{V_x \vec{i}}{x}$. The force then produces a disturbance of this motion by superimposing upon it a field of motion with the components \underline{v}_x , \underline{v}_y , and \underline{v}_z . For the case where the force is small, Oseen, using Equation (52), arrived at the following expressions for the velocity components:

$$v_x = \frac{1}{8\pi\mu} \left[F_x \nabla^2 \psi - F_x \frac{\partial^2 \psi}{\partial x^2} - F_y \frac{\partial^2 \psi}{\partial x \partial y} - F_z \frac{\partial^2 \psi}{\partial x \partial z} \right] \quad (53)$$

$$v_y = \frac{1}{8\pi\mu} \left[F_y \nabla^2 \psi - F_x \frac{\partial^2 \psi}{\partial x \partial y} - F_y \frac{\partial^2 \psi}{\partial y^2} - F_z \frac{\partial^2 \psi}{\partial y \partial z} \right] \quad (54)$$

$$v_z = \frac{1}{8\pi\mu} \left[F_z \nabla^2 \psi - F_x \frac{\partial^2 \psi}{\partial x \partial z} - F_y \frac{\partial^2 \psi}{\partial y \partial z} - F_z \frac{\partial^2 \psi}{\partial z^2} \right] \quad (55)$$

where $\frac{F_x}{x}$, $\frac{F_y}{y}$, and $\frac{F_z}{z}$ are the components of the applied force taken per unit volume and ψ is given by Equation (56).

$$\psi = \frac{2\mu}{\rho V_x} \int_0^{\rho} \frac{V_x(r-x)/2\mu}{\lambda} \frac{1 - e^{-\lambda}}{\lambda} d\lambda \quad (56)$$

where $\underline{r}^2 = \underline{x}^2 + \underline{y}^2 + \underline{z}^2$.

By integration of Equation (56), for small values of $\rho \underline{V_x} \underline{r}/\mu$, ψ becomes:

$$\psi = (r - x) - \rho V_x / 8\mu (r^2 - 2rx + x^2) \quad (57)$$

or for $\underline{V_x} \underline{r}/\mu \ll \underline{r}$,

$$\psi = r - x \quad (58)$$

However, since ψ appears in derivatives of the second order, the term $-x$ drops out completely and Equation (58) becomes:

$$\psi = r \quad (59).$$

Note that by assuming $\rho \underline{V_x} \underline{r}/\mu$ to be negligibly small compared to \underline{r} , Burgers returned to the case of creeping motion. This explains his assumption of no inertial effects.

For the case of a force acting in the \underline{x} -direction, $\underline{F_y} = \underline{F_z} = 0$, and by substitution of \underline{r} for ψ in Equations (53)-(55) and performing the necessary differentiations the components of velocity become:

$$v_x = (F_x / 8\pi\mu)(1/r + x^2/r^3) \quad (60)$$

$$v_y = (F_x / 8\pi\mu)(xy/r^3) \quad (61)$$

$$v_z = (F_x / 8\pi\mu)(xz/r^3) \quad (62).$$

In connection with the assumptions made by Burgers in deriving Equations (57) and (58), Nelson (50) has shown that Equations (60)-(62) are a limiting

case of Stokes' problem [see Lamb (5) p. 598]. To show this, it is only necessary to let the radius of the sphere approach zero while the product of the radius times the translational velocity of the sphere is kept constant. Nelson stated that "this procedure, while physically unrealistic is nevertheless mathematically correct."

Thus, Burgers could have used Stokes' method (complete elimination of inertial effects) and arrived at his same result.

Now that expressions have been obtained for the velocity components, consider again the case of a rigid rod in a velocity gradient.

Burgers stated that a system of forces $\underline{f}(\underline{l}) \underline{d}l$ distributed along the axis of the rod must be found, which will produce a velocity $-\underline{k} \underline{x}' = -\underline{v}_{\underline{x}}$, along the surface of the cylinder in order to satisfy the condition of absence of slip at the surface of the rod. Here, \underline{l} is the distance along the axis of the rod.

Since it has been assumed that $\underline{v}_{\underline{y}}$, and $\underline{v}_{\underline{z}}$, are negligible, only the component $\underline{v}_{\underline{x}}$, will be considered.

Now by replacing $\underline{F}_{\underline{x}}$ with $\int \underline{f}(\underline{l}) \underline{d}l$, \underline{r} with $[(\underline{x}' - \underline{l})^2 + \underline{b}^2]^{1/2}$ and \underline{x} with $(\underline{x}' - \underline{l})$, then Equation (60) becomes:

$$\int_{-a}^{+a} \frac{\underline{f}(\underline{l}) \underline{d}l}{8\pi\mu} \left\{ \frac{-1}{[(\underline{x}' - \underline{l})^2 + \underline{b}^2]^{1/2}} + \frac{(\underline{x}' - \underline{l})^2}{[(\underline{x}' - \underline{l})^2 + \underline{b}^2]^{3/2}} \right\} = -\underline{k}\underline{x}' \quad (63)$$

where $\underline{a} = \underline{L}/2$, and $\underline{b} = \underline{d}/2$.

To solve Equation (63), Burgers assumed that $\underline{f}(\underline{l})$ could be expressed as follows:

$$\underline{f}(\underline{l}) = -8\pi\mu\underline{k}\underline{a} [A_1(\underline{l}/\underline{a}) + A_2(\underline{l}/\underline{a})^3] \quad (64)$$

where \underline{A}_1 and \underline{A}_2 are adjustable coefficients.

By substitution of Equation (64) into Equation (63) and integrating, values for A_1 and A_2 can be obtained.

The system of forces obtained in this manner can be compared to the formation of a doublet of magnitude given by Equation (65).

$$M = \int_{-a}^{+a} f(\ell) \ell \, d\ell \quad (65)$$

Substitution of $f(\ell)$ from Equation (64) into Equation (65) and integrating yields:

$$M = -16\pi\mu ka^3(1/3 A_1 + 1/5 A_2) \quad (66).$$

Now by substitution of the values found for A_1 and A_2 , Equation (66) becomes:

$$M \approx - (4\pi\mu ka^3) / [3(\ln 2L/d - 1.80)] \quad (67).$$

From Equation (49), it can be seen that k has the value $G_0 \sin^2 \theta \sin \phi \cos \phi$.

Therefore, the strength of the doublet M , becomes:

$$M \approx - \frac{4\pi\mu G_0 a^3}{3(\ln 2L/d - 1.80)} \sin^2 \theta \sin \phi \cos \phi \quad (68).$$

To determine the effect of a doublet of the magnitude given by Equation (68) on the velocity gradient, Burgers again used Equations (53)-(55).

For this case, Burgers wrote the doublet strength as $M = 2F_z$; and F_x , F_y , and F_z as $F \sin \theta \cos \phi$, $F \sin \theta \sin \phi$ and $F \cos \theta$.

Also, Burgers stated that for this case, ψ must be written as follows:

$$\psi = -2e (\partial r / \partial x) \sin \theta \cos \phi + (\partial r / \partial y) \sin \theta \sin \phi + (\partial r / \partial z) \cos \theta \quad (69).$$

Again by substitution for ψ into Equations (53)-(55) and integration, the following results are obtained:

$$v_x = -(M/8\pi\mu)(x/r^3)(1 - 3R^2/r^2) \quad (70)$$

$$v_y = -(M/8\pi\mu)(y/r^3)(1 - 3R^2/r^2) \quad (71)$$

$$v_z = -(M/8\pi\mu)(z/r^3)(1 - 3R^2/r^2) \quad (72)$$

where $R = \underline{x} \sin \theta \cos \phi + \underline{y} \sin \theta \sin \phi + \underline{z} \cos \theta$.

As before, the expression for $\underline{v_x}$ will be the only one of interest. To determine the disturbance of the motion produced by the rod, $\underline{v_x}$ is integrated over a plane $\underline{y} = + \underline{h_2}$ (where $\underline{h_2}$ may be arbitrarily great) as follows:

$$\int_{-\infty}^{+\infty} \int v_x \, dx \, dz = (M/2\mu) \sin^2 \theta \sin \phi \cos \phi \quad (73)$$

where $\underline{v_x}$ is given by Equation (70).

The particle also produces changes in the velocity gradient $\partial \underline{v_x} / \partial \underline{y}$, but these changes are partly positive, and partly negative so that the integral over $\underline{y} = + \underline{h_2}$ is zero as shown below:

$$\int_{-\infty}^{+\infty} \int \partial \underline{v_x} / \partial \underline{y} \, dx \, dy = 0 \quad (74)$$

Again, $\underline{v_x}$ is given by Equation (70).

Since the shear stress, τ , over a plane parallel to the \underline{xz} -plane is given by $\tau = \mu(\partial \underline{v_x} / \partial \underline{y} + \partial \underline{v_y} / \partial \underline{x})$, it is obvious that the disturbance of the motion produced by the rod does not change the total value of the frictional force, $\int \int \tau \, \underline{dx} \, \underline{dz}$ transmitted across the plane $\underline{y} = \underline{h_2}$.

If these same calculations are made for a plane $\underline{y} = - \underline{h}_1$, it will again be found that the total value of the shear stress transmitted across the plane does not change, but that there is a decrease of velocity, the integral of which has the value, $- (\underline{M}/2\mu) \sin^2 \theta \sin \phi \cos \phi$.

The difference between the velocities at the two planes will therefore be increased by an amount, the integral of which has the value $(\underline{M}/\mu) \sin^2 \theta \sin \phi \cos \phi$. Now, for \underline{n} rods per unit volume, the difference between the mean velocities at the two planes, found from integrating $(\underline{Mn}/\mu) \sin^2 \theta \sin \phi \cos \phi$ from $\underline{y} = + \underline{h}_2$ to $\underline{y} = - \underline{h}_1$ is $(\underline{Mn}/\mu) \sin^2 \theta \sin \phi \cos \phi (\underline{h}_1 + \underline{h}_2)$. Therefore, the mean shear rate between the two planes increases from the original value \underline{G}_0 , to the value:

$$\underline{G}_e = \underline{G}_0 + (\underline{Mn}/\mu) \sin^2 \theta \sin \phi \cos \phi \quad (75)$$

where \underline{G}_e = effective shear rate.

Now since the tangential stress across $\underline{y} = \text{constant}$ is constant, then:

$$\tau = \mu \underline{G}_0 = \mu_e \underline{G}_e \quad (76)$$

where μ_e = effective viscosity of the suspension.

Rearrangement of Equations (75) and (76) gives:

$$\mu/\mu_e = 1 + (\underline{Mn}/\mu \underline{G}_0) \sin^2 \theta \sin \phi \cos \phi \quad (77).$$

By taking the reciprocal of Equation (77), multiplying numerator and denominator by $[1 - (\underline{Mn}/\mu \underline{G}_0) \sin^2 \theta \sin \phi \cos \phi]$, and assuming the resulting squared term is small compared to one, the following expression for the relative viscosity, μ_r , is obtained:

$$\mu_r = \mu_e/\mu = 1 - (\underline{Mn}/\mu \underline{G}_0) \sin^2 \theta \sin \phi \cos \phi \quad (78).$$

Substitution of \underline{M} from Equation (68), and $\underline{L}/2$ for \underline{a} and $\underline{d}/2$ for \underline{b} gives:

$$\mu_r = 1 + \frac{\pi \underline{L}^3 n}{6(\ln 2\underline{L}/\underline{d} - 1.80)} \sin^4 \theta \sin^2 \phi \cos^2 \phi \quad (79)$$

or,

$$\mu_r = 1 + \alpha_o c \quad (80)$$

where

$$\alpha_o = \frac{(\underline{L}/\underline{d})^2}{6(\ln 2\underline{L}/\underline{d} - 1.80)} \sin^4 \theta \sin^2 2\phi \quad (81)$$

and \underline{c} = volume concentration = $\underline{n}\pi(\underline{d}^2/4)\underline{L}$.

In order to obtain an average value for the expression $\sin^4 \theta \sin^2 2\phi$, Burgers considered the motion of the particles in the suspension.

The velocity components given by Equations (47) and (48) will cause a rotation of the cylinder as follows:

$$d\phi/dt = G_o \sin^2 \phi \quad (82)$$

$$d\theta/dt = G_o \sin \theta \cos \theta \sin \phi \cos \phi \quad (83)$$

If Equation (82) is integrated, the result is:

$$-\cot \phi = G_o(t - t_o) \quad (84)$$

where

\underline{t} = time the cylinder has been in motion

\underline{t}_o = initial time.

If Equation (84) is correct, at $\underline{t} = \text{infinity}$, ϕ would be 0° , i.e., all the particles would be aligned in the direction of flow and remain there. Of course, this is not the case, as Burgers realized. The reason for this result is that

throughout his derivation, Burgers assumed that the cylinders were infinitely thin. For any real situation, the cylinders would not be infinitely thin and, therefore, when they come into a position parallel to the direction of flow, they would continue to move because of the difference in the drag force on the two sides of the fiber.

Due to this result, Burgers turned to Jeffery's (10) equations for the motion of ellipsoids in order to obtain an expression for $\frac{\sin^4 \theta \sin^2 2\theta}{\sin^2 2\theta}$.

The remaining parts of this derivation have been presented on pages 8 through 11 of the Theoretical section.

APPENDIX II

EXPERIMENTAL DATA

TABLE X

REPRODUCIBILITY MEASUREMENTS ON A TCE-PO SOLUTION
(See Fig. 11)

Run 1		Run 2		Run 3	
Torque, dyne-cm.	Angular Velocity, rad./sec.	Torque, dyne-cm.	Angular Velocity, rad./sec.	Torque, dyne-cm.	Angular Velocity, rad./sec.
4.3	0.0447	4.1	0.0423	4.5	0.0457
7.7	0.0760	7.0	0.0687	7.7	0.0760
11.4	0.112	10.6	0.104	11.0	0.108
15.3	0.150	14.5	0.142	14.7	0.144
20.2	0.197	18.7	0.184	20.0	0.193
25.6	0.251	23.8	0.233	24.6	0.240
31.9	0.314	29.8	0.292	30.3	0.298
38.1	0.369	36.8	0.362	36.8	0.358
44.4	0.433	44.3	0.436	45.6	0.444
52.1	0.511	52.0	0.509	52.0	0.511
59.8	0.584	61.6	0.598	61.5	0.596
71.1	0.667	67.8	0.661	69.9	0.661
81.4	0.725	77.5	0.706	79.4	0.708
91.7	0.760	89.8	0.776		
99.1	0.792				

TABLE XI

REPRODUCIBILITY MEASUREMENTS ON FIBER SUSPENSIONS
(See Fig. 12)

Run 4A		Run 4B	
Torque, Dyne-cm.	Angular Velocity, rad./sec.	Torque, dyne-cm.	Angular Velocity, rad./sec.
10.6	0.110	10.5	0.110
14.7	0.159	14.5	0.150
19.0	0.198	19.0	0.198
24.3	0.250	24.4	0.250
30.0	0.311	30.5	0.315
36.3	0.374	36.8	0.377
44.1	0.452	44.5	0.455
52.1	0.524	52.2	0.530
59.8	0.571	59.9	0.573

TABLE XI (Continued)

REPRODUCIBILITY MEASUREMENTS ON FIBER SUSPENSIONS
(See Fig. 12)

Run 5A		Run 5B	
Torque, dyne-cm.	Angular Velocity, rad./sec.	Torque, dyne-cm.	Angular Velocity, rad./sec.
10.7	0.102	10.9	0.103
14.5	0.135	14.7	0.137
18.7	0.177	19.2	0.180
24.4	0.227	24.3	0.224
30.2	0.284	30.2	0.282
36.0	0.336	36.8	0.339
43.8	0.402	44.3	0.409
51.4	0.471	52.0	0.479
60.7	0.548	60.8	0.564
69.4	0.607	68.0	0.595

TABLE XII

RELATIVE VISCOSITIES AS A FUNCTION OF CONCENTRATION
 FOR SUSPENSIONS OF STRAIGHT, NYLON FIBERS
 (See Fig. 18)

$$\underline{d} = 16.9 \mu, \underline{L}/\underline{d} = 19.2$$

Volume Concentration $\times 10^2$	Relative Viscosity	Volume Concentration $\times 10^2$	Relative Viscosity
0.000	1.0000	0.000	1.0000
0.074	1.0009	0.104	1.0052
0.143	1.0014	0.164	1.0051
0.242	1.0072	0.209	1.0065
0.338	1.0048	0.307	1.0067
0.444	1.0107	0.392	1.0052
0.587	1.0307	0.472	1.0228
0.664	1.0295	0.514	1.0319
0.770	1.0440	0.671	1.0300
0.834	1.0533		

$$\underline{d} = 43.1 \mu, \underline{L}/\underline{d} = 20.3$$

0.000	1.0000	0.513	1.0260
0.363	1.0072	0.552	1.0242
0.410	1.0101	0.575	1.0208
0.443	1.0151	0.602	1.0221
0.473	1.0230	0.618	1.0253
0.493	1.0284	0.642	1.0266
0.473	1.0264	0.701	1.0408
0.508	1.0228	0.723	1.0436

TABLE XIII

WALL EFFECT DETERMINATION
 (See Fig. 18)

$$\underline{d} = 43.1 \mu, \underline{L}/\underline{d} = 20.3$$

0.000	1.000	0.578	1.026
0.276	1.002	0.761	1.045
0.467	1.016		

TABLE XIV

DETERMINATION OF THE EFFECT OF FIBER CURVATURE
(See Fig. 21)

$\underline{d} = 16.9 \mu, \underline{L}/\underline{d} = 20.1$		$\underline{d} = 43.1 \mu, \underline{L}/\underline{d} = 23.2$	
Volume Concentration $\times 10^2$	Relative Viscosity	Volume Concentration $\times 10^2$	Relative Viscosity
0.000	1.000	0.000	1.000
0.105	1.003	0.181	1.013
0.159	1.007	0.322	1.028
0.184	1.015	0.360	1.034
0.213	1.016		
0.250	1.019		
0.278	1.023		

TABLE XV

EXAMPLE OF THE TORQUE-ANGULAR VELOCITY RELATIONSHIPS
OBTAINED WITH FLOCCULATED SUSPENSIONS
(See Fig. 27)

Torque, dyne-cm.	Angular Velocity, rad./sec.	Torque, dyne-cm.	Angular Velocity, rad./sec.
2.33	0.012	28.9	0.261
4.26	0.028	31.8	0.288
7.11	0.052	35.0	0.321
10.2	0.081	38.3	0.349
11.8	0.098	42.5	0.384
14.2	0.119	46.5	0.423
15.8	0.137	50.5	0.459
18.2	0.161	54.6	0.498
20.4	0.181	58.8	0.533
23.7	0.209	62.2	0.567
26.2	0.234		

TABLE XVI

RELATIVE VISCOSITY-CONCENTRATION DATA FOR
FLOCCULATED SUSPENSIONS
(See Fig. 28-31)

$$\underline{d} = 16.9 \mu, \underline{L}/\underline{d} = 19.2$$

Suspending medium was TCE-PO

Volume Concentration $\times 10^2$	Relative Viscosity	Volume Concentration $\times 10^2$	Relative Viscosity
Curve I		Curve II	
0.000	1.000	0.000	1.000
0.051	1.000	0.072	1.002
0.107	1.001	0.102	1.005
0.166	1.003	0.138	1.006
0.227	1.007	0.185	1.009
0.306	1.017	0.245	1.014
0.378	1.025	0.325	1.026
0.445	1.030	0.377	1.024
0.544	1.039	0.436	1.032
0.619	1.067	0.511	1.046
0.729	1.061		
0.913	1.065		
1.072	1.073		
1.226	1.100		
1.428	1.121		

Curve III

Suspending medium was
glycerol-water

0.000	1.000
0.041	1.011
0.077	1.024
0.111	1.056
0.128	1.074
0.155	1.125
0.182	1.175
0.228	1.184
0.283	1.241

APPENDIX III

DETERMINATION OF THE ORIENTATIONS OF THE FIBERS
IN A FLOWING SUSPENSION FROM PHOTOGRAPHS

The major complication which arose in analyzing the photographs came about due to the relatively large depth of focus of the microscope being used. Because of this feature, there was no sharp contrast between fibers in focus and a little out of focus. Of course, in measuring the angles ϕ and θ , it was necessary to measure only those fibers in some predetermined degree of focus. This was almost impossible to do objectively, particularly for those fibers aligned in the direction of flow.

In order to overcome the subjectivity of this type of measurement, the orientations of all clearly distinguishable fibers were measured if ϕ was 5° or greater.

The number of fibers between $\phi = 0$ and 5° was determined by the following method.

Using Equation (3) derived by Jeffery (10), Mason and Manley (23) solved for the distribution of ϕ and showed that the fraction of particles having orientations between 0 and ϕ can be expressed as:

$$P(\phi) = 2/\pi \tan^{-1} [(L/d)_e \tan \phi] \quad (85).$$

From Equation (85), the fraction of the fibers having values of ϕ between 0 and 5° was determined. Knowing this fraction and the number of fibers having values of $\phi = 5^\circ$ or larger, the total number of fibers to be used in the average was determined.

Using this method of determining the total number fibers to be considered, the subjectivity of the measurements was removed. However, this method was

based on the assumption that the distribution of ϕ is not influenced by concentration. It was felt that this was a good assumption since Mason and Manley showed that interactions between fibers sometimes increased and sometimes decreased the period of rotation. Therefore, for a large number of rotations of a single fiber, or for a large number of fibers, the net result would be no change in the distribution of ϕ .

The average value of $\sin^4 \theta \sin^2 2\phi$ was determined by the following method. The angle ϕ was measured to the nearest 5° using a protractor.

It can be seen from Fig. 1 that $\sin \theta$ is equal to the projected length of the fiber on the xy-plane divided by the actual length of the fiber. Therefore, to determine $\sin^4 \theta$, the projected length of the fiber was measured, raised to the fourth power, and divided by the average of the actual fiber lengths raised to the fourth power.

From the values determined for ϕ and $\sin^4 \theta$, $\sin^4 \theta \sin^2 2\phi$ was determined for each fiber.

The average value of $\sin^4 \theta \sin^2 2\phi$ for each concentration was then determined by summing the individual values and dividing by the number of fibers measured plus the number between $\phi = 0$ and 5° .

APPENDIX IV

THE VISCOSITY OF SUCROSE AND GLYCEROL SOLUTIONS

It was reported by Myers (16) that 33% sucrose and 55% glycerol solutions increased in viscosity by approximately 17% after being left undisturbed in the viscometer for 2 hours. Larger increases were found after longer times. Myers found that the viscosity could be returned to approximately its original value by vigorous stirring.

A study of this effect showed that the apparent viscosity of these solutions could be reproduced within 1% after the solutions had been standing for 2, 12, and 24 hours. Determinations were made with the inner cylinder both submerged and exposed, and also both submerged and exposed with a film of mineral oil over the surface to prevent evaporation and surface effects.

No explanation can be given for the results of Myers.

APPENDIX V

GENERAL COMMENTS CONCERNING THE USE OF MYERS' VISCOMETER

The following comments are presented for the benefit of those who might use Myers' concentric cylinder viscometer.

It is suggested that the viscometer be mounted on a very rigid base, preferably a large concrete block, and that the magnetic drive be given more support than it now has to eliminate changes in the spacing between the drive and the air bearing.

A six-volt storage battery such as the one used as the current supply to the magnetic drive has, from full charge, a current versus time relationship as shown in Fig. 31.

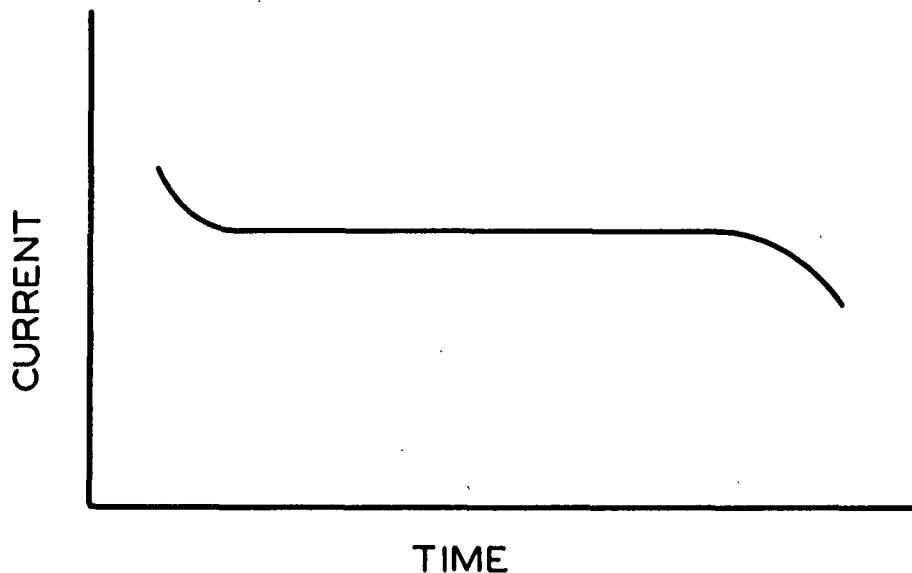


Figure 31. Current versus Time for a Six-Volt Storage Battery

Therefore, after charging, the battery should be allowed to deliver a small current (0.2 ampere) for approximately 15 minutes so that the current will be essentially constant with time during operation of the viscometer.

At times, a piece of lint may become lodged between the male portion of the air bearing and the Plexiglas shield, the air bearing mount or the cover of the outer cylinder causing erratic behavior of the viscometer.

Once, oil from the bearings of the magnetic drive got between the brushes and the slip rings causing large fluctuations in the current to the drive.

For proper performance, the d.c. ammeter should not be mounted in the instrument panel of the viscometer but should be mounted horizontally.

It was found that a leather belt between the magnetic drive and the motor was much more satisfactory than a rubber one. Rubber belts (large O-rings) sometimes slipped and often cracked and broke.

The air bearing should be thoroughly cleaned and polished about every 8-10 months. It was found that "Brasso," an ammonia-base metal polish, worked well. After polishing, the bearing was washed with acetone to remove lint and particles left from the polish.